Alma Mater Studiorum – Università di Bologna

DOTTORATO DI RICERCA IN

SCIENZE E TECNOLOGIE AGRARIE, AMBIENTALI E ALIMENTARI

Ciclo XXXV

Settore Concorsuale: 05/A1

Settore Scientifico Disciplinare: BIO/01

INTEGRATION OF BY-PRODUCTS AND WASTE FROM AGRI-FOOD SUPPLY CHAINS INTO THE «WATER-ENERGY-FOOD» NEXUS (RECOW-ER): THE ROLE OF FUNGI

Presentata da: Federico Puliga

Coordinatore Dottorato
Prof. Massimiliano Petracci

Supervisore
Prof.ssa Alessandra Zambonelli

Co-supervisore
Prof.ssa Ornella Francioso

Esame finale anno 2023

Abstract

Water, energy, and food are the vital resources that sustain life as well as global, regional, and national economies and the world's demand for these resources is set to grow. The agricultural sector is undoubtedly one of the sectors that has the greatest impact on the use of water and energy to produce food. The circular economy allows to reduce waste, obtaining maximum value from products and materials, through the extraction of all possible by-products from resources. Consequently, circular economy, reduce energy consumption and carbon dioxide emissions, minimizing water-energy-food nexus. Circular economy principles for agriculture include recycling, processing, and reusing agricultural waste in order to produce bioenergy, nutrients, and biofertilizers.

Approximately 1.3 billion tonnes of agro-industrial food waste are produced yearly. These wastes are usually destined to landfills or uncontrolled disposal, resulting in damage to the environment and financial loss. Agricultural and industrial waste materials can be used to produce high-value products such as biogas, biofuels, fine chemicals, and enzymes. Moreover, since agro-industrial wastes are principally composed of lignin, cellulose, and hemicellulose they can represent a suitable substrate for mushroom growth and cultivation.

Mushrooms play the fundamental ecological role of decomposers of organic matter, particularly lignin, and are also considered healthy foods with several medicinal properties. Nowadays more than 50 species of saprotrophic fungi are

cultivated in the world and their cultivation is usually carried out on different agro-wastes.

The thesis is structured in seven chapters. In the first chapter an introduction on the water, energy, food nexus, on agro-industrial wastes and on how they can be used for mushrooms cultivation is given. Chapter 2 details the aims of this dissertation thesis: The role of fungi in the recovery or degradation of agro-industrial wastes and the evaluation of their production and/or degradation capacity through the application of vibrational spectroscopy was studied. Emphasis is given to 3 different types of agro-industrial waste: the solid fraction of corn digestate resulting from the anaerobic digestion of agricultural biomass for biogas production; hazelnut shells produced during the cracking process and finally the polyethylene mulching films used in agriculture.

In chapters three and four, corn digestate and hazelnut shells were tested for mushrooms cultivation and their lignocellulosic degradation capacity were assessed by using ATR-FTIR spectroscopy. The results obtained shown that it is possible to use the solid fraction of the corn digestate and the hazelnut shells as substrates for the cultivation of different species of edible and medicinal mushrooms. Through Attenuated Total Reflectance–Fourier Transform Infrared (ATR-FTIR) spectroscopy, the degradation of the lignocellulosic component present in the cultivation substrate was assessed. Moreover, the ATR-FTIR spectroscopy carried out to study the chemical composition of fruit bodies obtained during the cultivation trials showed differences between mushrooms grown on the different substrates studied. In particular, in chapter three, *Pleurotus ostreatus* showed the highest biological efficiency and fruiting body production in the presence of corn digestate; moreover, *P. ostreatus* and *Pleurotus cornucopiae* were able to degrade the lignin. Likewise, in chapter four *Ganoderma lucidum*, *L. edodes*, and *P. cornucopiae* were able to grow and decay

the lignocellulosic fraction of hazelnut shells. Cultivation trials showed a similar biological efficiency but a different fruiting body production in the presence of hazelnut shells with respect to the control. ATR-FTIR analysis provided a chemical insight for the examined fruiting bodies, and differences were found among the substrates studied.

In chapter five, through the use of the Surface-enhanced Raman Scattering (SERS) spectroscopy was possible to set-up a new method for study mushrooms composition and for identify different mushroom species based on their spectrum. Six edible and/or medicinal mushrooms: *L. edodes*, *G. lucidum*, *P.cornucopiae*, *P. ostreatus*, *Tuber aestivum* and *Tuber magnatum* were studied. Results obtained showed characteristic spectra for each species. One group of mushrooms (*L. edodes*, *G. lucidum*, *T. aestivum* and *T. magnatum*) was dominated by the bands of nucleic acids; and the other one (*P. cornucopiae* and *P. ostreatus*), by the bands of pigments such as melanins; carotenoids; azafilones; polyketides; and flavonoids located in the cell wall.

In chapter six, the isolation of different strains of fungi from plastic residues collected in the fields and the ability of these strains to growth and colonizing the Low-density Polyethylene (LDPE) were explored. The structural modifications of the LDPE, as consequence of their growth were monitored by using the Scanning Electron Microscope (SEM) and ATR-FTIR spectroscopy. Results showed that *Cladosporium cladosporioides* Clc/1 strain was able to grow and degrade the LDPE substrate after 90 days trial and further studies will be necessary in order to investigate the enzymes involved in the degradation.

Finally, chapter seven outlines the conclusions and some hints for future works and applications are provided.

To my family…

Table of content

List of figures

List of tables

List of abbreviations

A	Adenine
ABTS	2,20-azinobis- 3-ethylbenzthiazoline-6-sulfonate
AD	Anaerobic digestion
AGR	Area growth rate
ANOVA	Analysis of variance
AS	Ash
ATR	Attenuated total reflectance
ATR-FTIR	Attenuated total reflectance – fourier transform infrared
BC	Beech chips
BE	Biological efficiency
C	Carbohydrates
CD	Corn digestate
CP	Crude proteins
DISTAL	Department of Agricultural and Food Sciences
FBP	Fruiting body production
FR	Fibers
FT	Fats
FTIR	Fourier transform infrared
G	Guanine
GHGs	Greenhouse gases
GHs	Glycoside hydrolases

Glu	*Ganoderma lucidum*
HS	Hazelnut shells
HTR	Hydraulic retention time
IR	Infrared
ITS	Internal transcribed spacer
Lac	Laccases
LDPE	Low-density Polyethylene
Led	*Lentinula edodes*
LiPs	Lignin peroxidases
LMCO	Laccase-like multicopper oxidase
LSPR	Localized surface plasmonic resonance
M	Melanins
MDF	Medium density fiberboard
MnPs	Manganese-dependent peroxidases
NPs	Nanoparticles
P	Phosphate groups
PC	Poplar chips
PCA	Principal components analysis
Pco	*Pleurotus cornucopiae*
PCRs	Polymerase chain reactions
PDA	Potato dextrose agar
PE	Polyethylene
PODs	Peroxidases
Pos	*Pleurotus ostreatus*
PP	Polypropylene
rGR	Radial daily growth rate
SD	Solid digestate

SDGs	Sustainable development goals
SE	Standard error
SEM	Scanning electron microscope
SERS	Surface-enhanced Raman Scattering
T	Thymine
Tae	*Tuber aestivum*
Tmg	*Tuber magnatum*
VPs	Versatile peroxidases
WB	Wheat bran
WS	Wheat straw

CHAPTER 1

INTRODUCTION

Water, energy, and food are the vital resources that sustain life as well as global, regional, and national economies. The world's demand for water, energy and food due to increasing world population, urbanization, sustainable development, international trade, changing lifestyles, cultural and technological, and climate change is set to grow between 30 and 50% by 2050 (Ferroukhi et al., 2015; Gupta, 2017). The growing demand for these resources combined with environmental and climate change concerns presents a set of scientific, policy, and management issues that are critical for achieving the 2030 agenda of the United Nations: "Sustainable Development Goals" (SDGs) (United Nations, 2015). However, it is possible to slow down this growing demand by reducing the waste and losses of water, food, and energy, saving resources during production, and reducing environmental impact. Water, energy, and food are interconnected resources, and actions in a sector adversely or positively affect one or both other resources. The water, energy, food nexus concept was conceived to study the global management of resources (Rasul, 2016; Smajgl et al., 2016; Yillia, 2016), gaining increasing attention in the scientific and political community (Garcia and You, 2016; Weitz et al., 2017). The term "nexus" means "to connect" (De Laurentiis et

al., 2016) and this word underlies the interaction between two or more dependent or interdependent elements.

The water, energy, food nexus is the study of the connections that exist between these resources and their management strategies for example, water to produce food, water to produce energy, food for energy, and energy to produce food.

Considering the individual factors, the planet has enough water to support global demand, but in some areas of the world, due to the unevenness in the distribution of water reserves, water is very scarce. The United Nations estimates show that 1.2 billion people live in areas where water is scarce and another 1.6 billion live in areas where water scarcity is due to economic reasons (Walsh et al., 2015). Regarding water quality, 748 million people do not have access to a source of drinking water (UNESCO, 2015).

According to the projections of the 2030 Water resources group (2030 Water resources group, 2021), by 2030, global demand for fresh water will exceed supply by 40 percent and in many areas, water has already run out. In addition, the United Nations water report predicts an increase in world water demand of about 55% in 2050 (UNESCO, 2015).

Regarding the demand for energy, this is growing due to the increase in global population and gross domestic product. Fossil fuels are expected to remain dominant and account for about 80% of energy sources in 2035, while among renewables, gas will account for 10% of the total (Salam et al., 2017).

Finally, great attention is paid to food production to support the growing world population. Arable fields as well as the water resources allocated to them are also decreasing due to increasing urbanization and industrialization and it has been estimated that by 2050 global production must increase of 60% (UNESCO, 2015).

1.1. Nexus and circular economy in agriculture

Following the increase in the world population, estimated at 9.7 billion in 2050 (United Nations, 2019) the consumption of natural resources (water, energy, and raw materials) is growing quickly. The agricultural sector is undoubtedly one of the sectors that has the greatest impact on the use of water and energy to produce food. In fact, agriculture is the largest user of water in the world, and more than a quarter of global energy is used in food production and supply (Del Borghi et al., 2020).

The circular economy allows to reduce waste, obtain maximum value from products and materials, extract all possible by-products from resources, and consequently reduce energy consumption and carbon dioxide emissions, minimizing water-energy-food nexus. It is therefore evident that the circular economy and the nexus are related (Reinhard et al., 2017).

The circular economy is based on nature, because of waste does not exist in nature. The waste of one organism is the food of another organism and the energy and nutrients flow in a closed cycle of growth, decay and reuse. This model is in contrast to the current linear model of the food and agriculture system which does not contemplate any mechanism for the recovery of waste and its reuse in the production cycle (Jones et al., 2021) (Figure 1.1).

Figure 1.1. Linear (left) and circular (right) systems. From Jones et al. (2021).

The circular economy model base economic development on the protection of the environment and resources (Del Borghi et al., 2020). At European level, circular economy has gained importance since the introduction of the Circular economy action plan in 2015 and subsequently modified in 2020 (European Commission, 2020). This plan is one of the main pillars of the European green deal for sustainable growth (European Commission, 2019).

Circular economy principles for agriculture include recycling, processing, and reusing agricultural waste in order to produce bioenergy, nutrients, and biofertilizers (Ellen MacArthur Foundation, 2018). With reference to the management of agro-industrial waste, the bioeconomy refers to the production of renewable biological resources and their transformation into nutrients, energy, and bio-based products (European Commission, 2012). To this end, the development and implementation of circular economy models are necessary to create value-added products and improve resource use efficiency (Donner et al., 2020).

1.2. Agro-industrial waste

Approximately 1.3 billion tonnes of agro-industrial food waste are produced yearly. Fruits, vegetables, roots, and tubers represent 40–50% of them, with a volume ranging from 520 to 650 million tonnes (Ravindran et al., 2018). These wastes are usually destined to landfills or uncontrolled disposal, resulting in damage to the environment and financial loss. Moreover, the mismanagement of agro-wastes can lead to high greenhouse gases production, mainly CO_2 and CH_4.

Agro-wastes can be classified into two main groups: i) field residues and ii) process residues. i) Field residues are represented by seed pods, stems, leaves, and stalks present in the field during the harvesting process. ii) Process residues

consist in husks, nuts, straw, leaves, shells, peel, pulp, roots, molasses, bagasse, and other waste biomass which became a waste when the crop has been turned into a profitable replacement commodity (Kumar et al., 2021; Kumla et al., 2020). They are generally used as soil amendments, fertilizers, animal feed and for food production (Sadh et al., 2018). In the latter group we can also include the anaerobic digestate which is the final product of the anaerobic digestion process that allows the production of renewable energy from plant biomass, livestock by-products, and municipal organic waste (Figure 1.2b, c).

A particular type of agro-waste is represented by plastic. In fact, although they are not considered crop wastes, polyethylene (PE) mulching films become part of the production cycle representing a problem at its end. In fact, PE mulching films are widely used in agriculture, and once their function is finished, they were abandoned in the field due to the excessive amount of work that concerns its removal, creating accumulations of plastic waste even greater (Abe et al., 2010). Moreover, over time and due to the agricultural mechanization operations, PE films abandoned in the field can undergo fragmentation, gradually reaching the size of microplastics (Figure 1.2a).

Figure 1.2. (a) Residues of PE mulching film in an agricultural field; (b) solid digestate storage trench; (c) particular of solid digestate fraction.

Agricultural and industrial waste materials can be used for high-value products such as biogas, biofuels, fine chemicals, and enzymes (da Silva, 2016). Moreover, agro-industrial wastes are principally composed of lignin, cellulose, and hemicellulose (Kumla et al., 2020) (Figure 1.3), in different percentages depending on the plant species and the environment (Table 1.1).

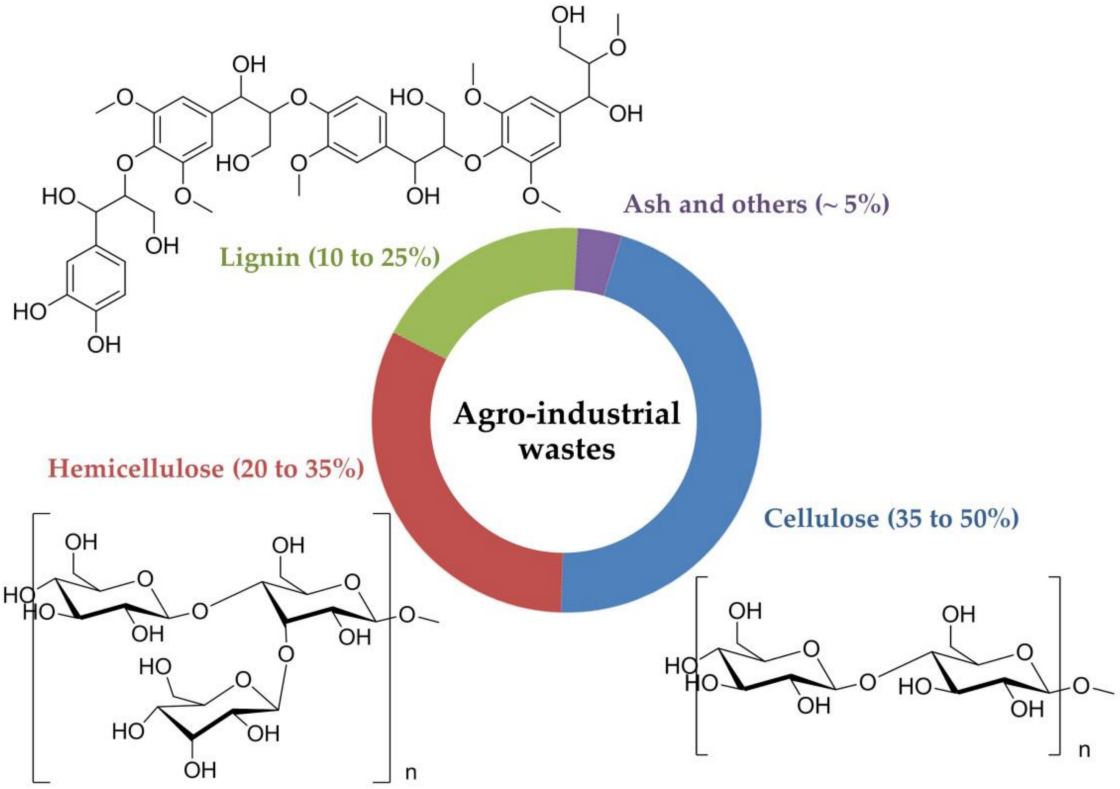

Figure 1.3. Main composition of agro-wastes. From Kumla et al. (2020).

Lignin is a rigid three-dimensional, aromatic, hydrophobic and amorphous highly branched polymer with different aliphatic, phenolic hydroxyls, methoxyl, carbonyl, and carboxylic groups that give lignin a very complex and unique structure (Davin and Lewis, 2005; Geneau-Sbartaï et al., 2008; Rico-García et al., 2020).

Table 1.1. Agro-wastes composition and their C/N ratio. Modified from Kumla et al. (2020) and references therein.

	Composition (% dry weight basis)			
Agro-industrial wastes	**Cellulose**	**Hemicellulose**	**Lignin**	**C/N ratio**
Almond shell	38	29	30	61/1
Apple pomace	43	24	20	48/1
Banana leaves	55	20	25	38/1
Banana peel	12	10	3	18-29/1
Banana straw	53	29	15	40/1
Barley straw	23-33	21-22	14-19	82-120/1
Beech sawdust	41	33	22	100-331/1
Birch sawdust	40	36	20	700/1
Canola straw	22	17	18	33-45/1
Chestnut shell	21	16	36	8/1
Coconut husk	24-43	3-12	25-45	75-186/1
Coffee husk	43	7	9	40/1
Corn bran	34	39	49	ND
Corn cob	35-45	35-44	11-15	50-123/1
Corn digestate*	35	25	28	ND
Corn stalk	34-61	19-24	7-9	57-80/1
Corn straw	30	25	8	50/1
Cotton seed hull	31	20	18	59-67/1
Cotton stalk	58	14	22	70-78/1
Grasses	25-41	25-50	7-30	16-42/1
Hardwoods	40-55	24-40	18-25	150-450/1
Hazelnut shell	55	34	35	50-58/1
Lemon peel	12	5	2	ND
Oak sawdust	25-38	18-29	18-25	162-200/1
Oat bran	49	25	18	12/1
Oat straw	25-40	21-27	17-18	48-83/1
Oil palm cake	64	15	5	ND
Oil palm empty fruit bunch	45-51	28-29	12-15	77/1
Olive oil cake	31	21	26	14-17/1
Orange peel	9-14	6-11	1-2	102/1
Pine sawdust	42	25	28	724-1070/1
Pineapple leaf	36	23	27	49/1

Pineapple peel	22	75	3	77/1
Pistachio shell	43	25	16	43/1
Poplar sawdust	44	32	21	46-71/1
Potato peel	35	5	4	25/1
Rice bran	35	25	17	12-48/1
Rice husk	35	25	20	30-80/1
Rice straw	32-39	23-24	18-36	35-72/1
Rubber tree sawdust	38	25	15	177/1
Rye straw	38	31	19	82/1
Softwood	45-50	25-35	25-35	310-520/1
Sorghum stalk	17	25	11	45/1
Sorghum straw	36	26	8	20-46/1
Soya stalk	35	25	20	20-40/1
Spruce sawdust	42	26	28	763-1000/1
Sugarcane bagasse	30-45	26-36	11-23	50/1
Sugarcane straw	36-41	21-31	16-26	70-120/1
Sunflower oil cake	25	12	8	ND
Sunflower stalk	42	30	13	97/1
Tomato pomace	9	5	5	ND
Walnut shell	36	28	43	175/1
Water yacinth	21	34	7	11/1
Wheat bran	30	50	15	19/1
Wheat straw	27-38	21-29	18-21	50-80/1

"ND" = not determined; * from Santi et al. (2015b)

Cellulose is a homopolymer composed of several hundred to many thousands of linear chains of β-anhydroglucose units (β-1,4 linked d-glucose units). Each of these units consists of three hydroxyl groups (OH), one primary (C6 position) and two secondary (C2 and C3 positions) hydroxyl groups, each of which exhibits different polarities and is capable of being involved in the intra- and intermolecular hydrogen bonds (Heinze, 2015; Zhou et al., 2016).

Hemicellulose is a heteropolymer composed of a polysaccharide matrix. Its structure depends on the sugar units (*i. e.* pentoses like arabinose and xylose,

hexoses like mannose, glucose, and galactose) hexuronic acids such as 4-*O*-methyl-d-glucuronic acid, galacturonic acid, and glucuronic acid, small amounts of rhamnose and fucose, and an acetyl group (Zhou et al., 2016). These binding sugars can assemble into a range of various hemicellulose polysaccharides, such as galactan mannans, xylans, xyloglucan, and β-1,3/1,4-glucans (Ebringerová et al., 2005; Zhou et al., 2016).

1.3. Recycling agro-wastes for mushrooms cultivation

Fungi are a kingdom of unicellular or multicellular eukaryotic organisms whose diversity is far to be determined. Hawksworth and Lücking (2017) recently revised the number of fungal species from 2.2 to 3.8 million, however, the new culture-independent approaches, such as new high-throughput amplicon sequencing, are dramatically increasing the number of estimated fungal species up to 12 million (Wu et al., 2019). Fungi are ubiquitous components of almost all ecosystems on Earth, most of them are free-living in soil or water as saprotrophs; others establish parasitic or symbiotic relationships with plants or animals and several of them can combine different lifestyles (saprophytic, pathogenic, or symbiotic) and therefore their boundaries are not well defined (Grigoriev, 2013). Fungal plant pathogens exhibit distinct feeding strategies: those that feed off living tissue are known as biotrophs, those that kill and feed off dead tissue are known as necrotrophs, and those that exhibit a biphasic feeding strategy, initial colonizing as a biotrophic pathogen then switching to necrotrophy once the infection is established, are known as hemibiotrophs (Newman and Derbyshire, 2020).

Many saprotrophs that affect weak hosts, at the beginning or at the end of their life cycle (*e.g.*, at seedling or senescent stages) are considered necrotrophs (Jarosz and Davelos, 1995; Thomma, 2003). Moreover, some necrotrophic fungi

can cause disease in a few specific hosts but can infect other host plant species asymptomatically as endophytes.

Saprotrophic fungi are known to have the ability to degrade lignin and other phenolic compounds of forests (Baldrian, 2008). These fungi can be divided into three main groups: white-rot fungi which have a unique ability to degrade all wood cell wall polymers, brown-rot fungi which hydrolyze cellulose and hemicelluloses, leaving modified, mainly demethoxylated, lignin behind, and soft-rot fungi to a large extent ascomycetes, able to degrade polysaccharides and in this case the degradation involves a browning and softening of the wood following the production of laccases and peroxidases which are less specific of those isolated from white-rot and brown-rot fungi. (Andlar et al., 2018; Sugano et al., 2021).

White-rot mushrooms such as *Ganoderma* spp., *Lentinula* spp., and *Pleurotus* spp., carry out delignification through two main patterns: nonselective delignification and selective delignification (Martínez et al., 2005). In nonselective delignification, the degradation of lignin, cellulose and hemicellulose occurs simultaneously. Selective delignification involves the degradation of lignin and hemicellulose before the attack of cellulose (Boddy et al., 2008; C. P. Kubicek, 2012; Martínez et al., 2005). The ligninolytic system of white-rot fungi depends on extracellular oxidative enzymes, particularly class II peroxidases (class II PODs). These fungi also secrete various glycoside hydrolases (GHs) that break down crystalline cellulose.

Brown-rot fungi such as *Fistulina* spp., *Fomitopsis* spp., and *Laetiporus* spp., are deficient in most oxidative enzymes and cellulases possessed by white rot fungi (Floudas et al., 2012) and decompose lignocellulose through an initial nonenzymatic step: generation of reactive oxygen species, including hydroxyl

radicals generated by the Fenton reaction ($H_2O_2 + Fe^{2+} + H^+ \rightarrow H_2O + Fe^{3+} + \bullet OH$) (Hatakka and Hammel, 2011; Martinez et al., 2009).

Although the mechanisms are not yet clear, during the litter decomposition process, a fungal succession pattern was observed in which specific taxa dominate the different stages of this process (Vivelo and Bhatnagar, 2019). Even mycorrhizal fungi can also act as decomposers, producing extracellular lytic enzymes and metabolizing C (Talbot et al., 2008). Most of the evidence that mycorrhizal fungi can act as decomposers comes from studies of ericoid and ectomycorrhizal fungi (Read et al., 2005, 2004; Read and Perez-Moreno, 2003), although there is increasing experimental evidence for a role of arbuscular mycorrhizal fungi in soil C decomposition (Hodge et al., 2001; Tu et al., 2006). Ectomycorrhizal fungi have the capacity to oxidize organic matter, either by Fenton chemistry, typical of brown-rot fungi, or by using white-rot peroxidases (Lindahl and Tunlid, 2015), and the oxidation is triggered by the addition of glucose, which suggests that the mechanism can be regulated by the host C supply (Rineau et al., 2013).

In addition to playing the fundamental ecological role of decomposers of organic matter and particularly of lignin, mushrooms are also considered healthy foods. In fact, edible mushrooms are rich in protein (15-35%), carbohydrates (35-70%), fiber, vitamins, and minerals, and low in fat (< 5%) (Kalač, 2013; Valverde et al., 2015). Moreover, several species such as *Ganoderma lucidum* (Curtis) P. Karst., *Lentinula edodes* (Berk.) Pegler, *Grifola frondosa* (Dicks.) Gray, *Hericium erinaceus* (Bull.) Pers., *Agaricus blazei* Murrill, and some *Pleurotus* species, have importance due to their antimicrobial, anti-inflammatory, immunomodulatory, antidiabetic, cytotoxic, antioxidant, hepatoprotective, anticancer, antioxidant, antiallergic, antihyperlipidemic, and prebiotic properties (Venturella et al., 2021).

Nowadays more than 50 species of saprotrophic fungi are cultivated in the world. The main cultivated edible mushrooms belong to the genera *Agaricus*, *Agrocybe*, *Auricularia*, *Flammulina*, *Ganoderma*, *Hericium*, *Lentinula*, *Lentinus*, *Pleurotus*, *Tremella*, and *Volvariella*. However, the principal worldwide cultivated genera are *Lentinula*, *Pleurotus*, *Auricularia*, and *Agaricus* (Ma et al., 2018).

Mushroom cultivation is widespread all over the world, with a global volume production around to 40 million tons, and China is the largest producer (Thakur, 2020). The indoor cultivation of lignocellulolytic mushrooms is usually carried out in bags or bottles filled with sterilized or pasteurized substrates (Oei, 2016). Since agro-industrial wastes are rich in lignin, cellulose, and hemicellulose, they can represent a suitable substrate for mushroom growth and cultivation and several studies were carried out in order to assess the suitability of different agro-wastes (alone or in mixture). In particular, the production and Biological Efficiency (BE) calculated as percentage ratio of fresh weight of mushrooms over the dry weight of substrate (Chang et al., 1981), were evaluated on different agro-wastes such as: wheat straw, barley straw, oat straw, rice straw, corn straw, corn cob, banana leaves, sawdust, sugarcane bagasse, soya and sunflower stalk for edible and medicinal mushrooms cultivation (Kumla et al., 2020) (Table 1.2).

The anaerobic digestate, presents significant management and environmental problems due to the large quantities produced daily (more than 30 tons per day) and to the release of ammonia (NH_3) and greenhouse gases such as CO_2, N_2O because of the presence of undigested organic matter that determines a residual biomethanation power of the digestate itself (Gioelli et al., 2011; Menardo et al., 2011; Monlau et al., 2015). Among the different type of anaerobic digestates, corn digestate (CD) is a promising substrate for mushrooms cultivation due to its high lignocellulose content.

Table 1.2. Biological efficiency and chemical composition of some mushrooms grown on different agro-industrial wastes (From Kumla et al., 2020 and reference therein).

Agro-indstrial waste	Mushroom species	BE (%)	Chemical composition (% dry weight)				
			CP	C	FT	FR	AS
Wheat straw	*Agaricus bisporus*	47.2–51.1	21.0–27.0	38.0–48.0	3.0–4.0	17.0–23.3	8.0–11.0
	Agaricus subrufescens	53.7	28.4	63.2	1.6	6.2	6.8
	Agrocybe cylindracea	61.4	1.5	89.6	0.3	40.4	8.6
	Hericium erinaceus	39.4–43.5	26.8	58.9	3.7	ND	10.5
	Lentinula edodes	66.0–93.1	15.2–15.4	63.7–65.7	1.1–1.5	ND	3.8–4.4
	Lentinus sajor-caju	74.9	22.9	56	2.6	7.1	6.6
	Pleurotus citrinopileatus	98.3–105.6	25.3	64	2.7	ND	8.1
	Pleurotus colombinus	69.2	2.9	25.9	0.42	5.4	8.5
	Pleurotus eous	75.1	19.5	50.2	2.6	7.8	6
	Pleurotus eryngii	48.2	21.5	56	2.4	13.5	7.6
	Pleurotus florida	66.4	27.9	51.2	2.4	12.2	8.7
	Pleurotus ostreatus	22.6–52.6	11.6–14.6	47.5–74.4	1.8–2.5	19.1–27.1	8.6–12.0
	Pleurotus sapidus	62.2	14.9	48.5	2	7.3	6.2
Barley straw	*Lentinula edodes*	64.1–88.6	15.1–16.8	75.1–77.7	1.9–2.2	ND	5.2–5.8
	Pleurotus ostreatus	21.3	12.8	54.7	29.9	0.9	1.2
Oat straw	*Agaricus bisporus*	47.2–52.9	26.8–36.2	ND	2.3–3.1	6.6–10.3	9.8–11.3
	Ganoderma lucidum	2.3	9.9	ND	ND	ND	1
Rice straw	*Lentinula edodes*	48.7	16.2	78	6	1.5	3.4
	Lentinus sajor-caju	78.3	23.4	55	2.4	7.9	6.8
	Hericium erinaceus	33.9	24.1	60.5	4.2	ND	11.3
	Pleurotus citrinopileatus	76.5–89.2	22.8	64.9	3.2	ND	91
	Pleurotus colombinus	71.4	4.8	27.3	0.3	5	7.7
	Pleurotus eous	79.8	29.3	48	2.4	8	6.2
	Pleurotus eryngii	45.9	21.8	53	1.9	13.8	8.7
	Pleurotus pulmonarius	23.5	21.1	ND	5.2	7	6.9
	Pleurotus ostreatus	25.6–84.6	12.5–23.4	55.3–57.4	2.8–16	7.7–0.7	6.3–13.6
	Pleurotus sapidus	64.7	23.4	45.6	1.6	8	6.4
	Pleurotus djmor	82.7	24.8	37.7	3.1	22	8.3
	Volvariella volvacea	10.2–15.0	36.9–38.1	42.8–42.3	0.8–1.0	4.4–6.0	9.0–10.3
	Coprinus comatus	18	10.9	76.6	1.9	ND	20.5
Corn straw	*Pleurotus florida*	31.6	26.3	31.3	0.5	19.6	5.2
	Volvariella volvacea	ND	23	13.9	1.4	36.6	11.9
Corn cob	*Agrocybe cylindracea*	33.5	14.8	72.4	2.9	17	10.1
	Pleurotus colombinus	79.1	1.9	28.5	0.2	4.12	9.3
	Pleurotus cystidiosus	50.1	24.5	40.6	3	24.3	7.57

	Pleurotus eryngii	51.8	23.8	54.8	1.9	9.7	7
	Pleurotus florida	55	29.1	38.2	0.9	22.8	3.5
	Pleurotus ostreatus	31.7–66.1	15.4–29.7	30.8–73.4	2.7–3.4	13.8–29.8	7.1—8.0
Banana leaves	*Pleurotus ostreatus*	ND	15	24.9	2.2	5.1	11.2
	Pleurotus pulmonarius	17.9	16.9–23.5	26.2	1.9–5.5	5.8–7.2	6.4–10.3
	Volvariella volvacea	15.2	23.9	ND	ND	8.1	6.1
Soya stalk	*Lentinus sajor-caju*	83	25.8	52.2	2.8	6.7	7.3
	Pleurotus eous	82.3	30.5	50.5	2.6	9	6.5
	Pleurotus ostreatus	85.2	24.7	53.2	2.8	7.2	6.7
	Pleurotus colominus	90.6	7.4	33.3	0.4	5.1	9.2
	Pleurotus florida	87.6	23.5	57.8	2.5	8	8
	Pleurotus sapidus	72.7	26.8	24.9	2.1	7.5	7
Sunflower stalk	*Lentinus sajor-caju*	63.1	21	50.7	2.8	7.7	6.9
	Pleurotus eous	61.5	27.4	52	2.2	7.9	5.2
	Pleurotus sapidus	45.9	20.1	48.5	2.4	7.3	6.2
Oil palm empty fruit bunch	*Schizopyllum commune*	3.7	6.1	37.4	4.5	0.01	1.94
	Volvariella volvacea	3.6–6.5	33.5–41.0	27.9–45.7	3.7–5.1	7.7–16.0	9.4–9.9
Cotton stalk	*Pleurotus florida*	25.1	29.8	37.3	2.2	19.4	8.7
	Pleurotus pulmonarius	42.3	29.3	44.5	3.1	11.3	9.2
	Pleurotus ostreatus	44.3	30.1	40.2	2.1	17.2	8.4
Rice husk	*Pleurotus ostreatus*	9.5	5.9	48.5	30.9	0.3	14.3
Sugarcane bagasse	*Lentinula edodes*	130.0–133.0	13.1–13.8	73.0–78.9	0.9–1.0	ND	6.2–7.1
	Pleurotus cystidiosus	49.5	22.1	45.2	2.3	22.8	7.5
	Pleurotus djmor	101.7	25.1	45.2	2.1	9.1	4.1
	Pleurotus eryngii	41.3	20.5	49	3.1	8	7.8
	Pleurotus florida	75.6	8.7	ND	4	2.5	0.3
	Pleurotus ostreatus	65.7	27.1	34.9	2	29.3	6.7
Sugarcane straw	*Lentinula edodes*	83.0–98.0	14.4	72.5–78.2	0.7–0.9	NR	6.4–6.5
Cotton hull	*Pleurotus florida*	13.6	20	61.2	11.9	11.9	5.5
	Pleurotus ostreatus	8.9	17.5	65.9	1.2	10.2	5.2
Cassava peel	*Pleurotus ostreatus*	24.0–26.1	10.5–10.7	73.0–74.6	2.1–2.2	8.5–8.9	7.5–7.7
	Volvariella volvacea	0.6-2.3	11.5–14.3	51.4–53.4	2.4–2.6	0.4–0.5	5.0–6.2
Hardwood sawdust	*Hericium erinaceus*	47.5–50.3	24.8	60.9	3.6	ND	10.6
Acacia sawdust	*Pleurotus cystidiosus*	36.3	15.7	55.9	2.1	20.1	6.3
	Pleurotus ostreatus	46.4	19.5	51.3	1.3	22	5.9
Beech sawdust	*Agrocybe cylindracea*	38.3	18.4	70.3	3.4	15	8.2
	Ganoderma lucidum	61.2	16.8	77.9	2.2	47.9	3.1
	Pleurotus ostreatus	46.8	16.1	73.6	3.5	15.8	6.2

Sawdust	*Auricolaria polytricha*	13.9–44.6	10.2	78.4	0.9	ND	4.2
	Pleurotus colombinus	89.1	1.7	25	0.2	4.6	9.1
	Pleurotus citrinopileatus	38.4–51.6	24.1	65.6	2.6	ND	7.8
	Pleurotus eryngii	35.5	19.5	52.5	2.4	7.8	7.5

"BE" biologial efficiency, "CP" crude proteins, "C" carbohydrates, "FT" fats, "FR" fibers, "AS" ash

1.4. Lignocellulosic fraction degradation by fungi

As mentioned above, the lignocellulosic material is composed of three main biomacromolecules: cellulose, hemicellulose and lignin, which linked together, make it difficult to degrade requiring the synergistic action of more carbohydrate-active and lignin enzymes. These enzymes are responsible for the assembly and breakdown of the glycosidic bond (Andlar et al., 2018; Eichorst and Kuske, 2012; Lombard et al., 2014) and in particular, oxidative enzymes that participate in the degradation of lignin, and hydrolytic enzymes, responsible for the degradation of cellulose and hemicellulose, are involved (Lombard et al., 2014; López-Mondéjar et al., 2016; Madeira et al., 2017) (Figure 1.4).

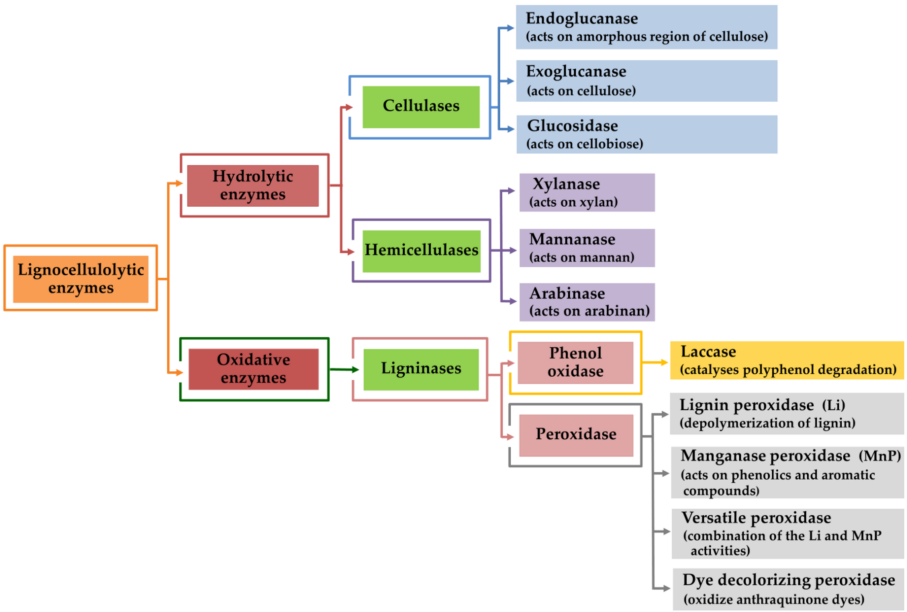

Figure 1.2. Main enzymes involved in lignin, cellulose, and hemicellulose degradation. From Kumla et al. (2020).

1.4.1. Lignin degradation

The degradation of lignin is the initial step that then allows hydrolytic enzymes to attack cellulose and hemicellulose (Anderson and Akin, 2008; Jurak et al., 2015). Lignin degradation can be mainly attributed to basidiomycetes white-rot fungi since they are capable to degrade lignin more quickly and extensively than other microorganisms (Woiciechowski et al., 2013).

Lignin attack is mainly accomplished by four major groups of several ligninases produced by the white-rot fungi: laccases (Lac), manganese-dependent peroxidases (MnPs), lignin peroxidases (LiPs), versatile peroxidases (VPs) (Kracher and Ludwig, 2016) (Figure 1.5).

Lac are blue multicopper enzymes capable to oxidize a variety of phenolic and non-phenolic compounds. Phenolic compounds, including lignin and polyphenols, are oxidized by one-electron abstraction that leads to an associated reduction of oxygen to water as a by-product (Coconi-Linares et al., 2014; Dwivedi et al., 2011; Gochev and Krastanov, 2007). In the presence of a mediator [2,20-azinobis- 3-ethylbenzthiazoline-6-sulfonate (ABTS)], that behaves as an electron shuttle, these enzymes can oxidize also non-phenolic compounds (Cragg et al., 2015).

Other important enzymes are peroxidases. Peroxidases by themselves are too large to penetrate the dense lignocellulosic matrix and they act by generating small molecular radical species capable to catalyse the oxidation of the lignin (Cullen and Kersten, 2004). LiPs, which belong to the oxidoreductases family are able to reduce O_2 to H_2O_2 and superoxides (Wong, 2009). LiPs are strong oxidants and can degrade phenolic and non-phenolic aromatic compounds.

MnPs is an oxidoreductase that can not directly react with the lignin structure (Ardon et al., 1998). This enzyme requires H_2O_2 for lignin oxidation and Mn^{2+} as a co-factor. Mn^{2+} is an electron donor and MnP is oxidized under H_2O_2 action in

an unstable MnP and accepts an electron from Mn^{2+} to Mn^{3+}. The product Mn^{3+} is released from the active site in the presence of a chelator such as oxalate, malate, and lactate, that stabilizes it against disproportionation to Mn^{2+} and insoluble Mn^{4+}. The chelated Mn^{3+} ion can diffuse into the lignified cell wall, where it oxidizes simple phenols, amines, phenolic and non-phenolic lignin components (Burlacu et al., 2018; Cragg et al., 2015).

VPs, are also known as polyvalent peroxidases because combine the substrate specificity characteristics of LiPs and MnPs. Unlike these two enzymes, it is able to degrade a wide range of phenolic and non-phenolic substrates (Wong, 2009). It requires hydrogen peroxide as an electron acceptor to catalyse the oxidative reaction at the home centre with the release of H_2O (Ardon et al., 1998).

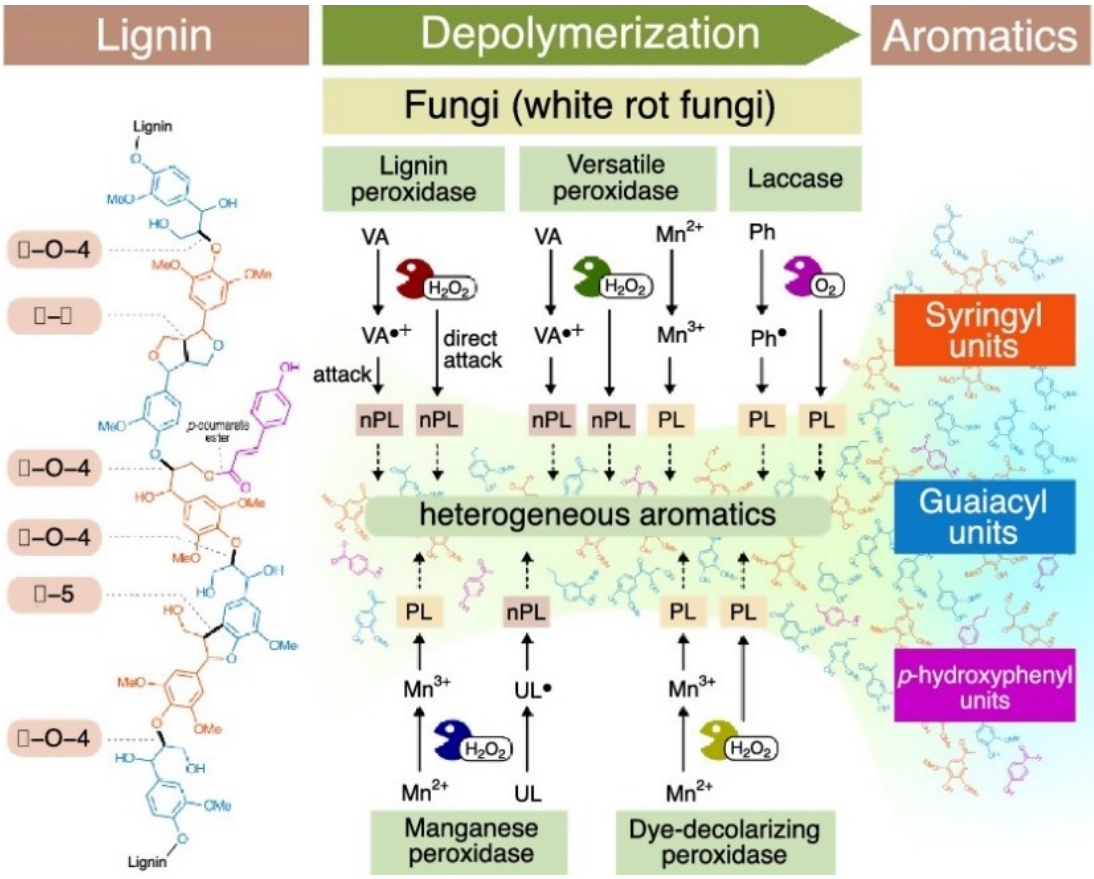

Figure 1.3. Lignin degradation by white-rot fungi enzymes. Modified from Kamimura et al. (2019).

1.4.2. Hemicellulose degradation

Due to its complex structure, hemicellulose hydrolysis requires the synergistic action of different enzymes (Figure 1.6). Hemicellulases are carbohydrate esterases or glycoside hydrolases involved in polysaccharide degradation. Xylanase, β-xylosidase, *α*-arabinofuranosidase, *α*-glucuronidase, and β-mannosidases are the enzymes involved in hemicellulose degradation (Horn et al., 2012; Lombard et al., 2014). However, xylanases and mannanases are the two most important enzymes for hemicellulose hydrolysis.

The endo-1,4-β-xylanase and the exo-1,4-β-xylosidase are two xylanases predominantly involved in hemicellulose degradation (Sánchez, 2009). They act by degrading the linear polysaccharide xylan into xylose by catalyzing the hydrolysis of the glycosidic linkage (β-1,4) of xylosides. Endo-1,4-β-xylanases hydrolyse β-1,4-xylan chains, and generate xylo-oligosaccharides whereas β-1,4-xylosidases cleave xylobiose and xylo-oligosaccharides releasing xylose (Sánchez, 2009) (Figure 1.6).

Mannans degradation is accomplished with β-Mannanases (endo-β-1,4-mannanase) that are endohydrolases that randomly attacks mannan fibers by cleaving β-1,4 bonds and producing new reducing and non-reducing ends. Depending on the active site organization most β-mannanases are active on oligosaccharides consisting of three or four monomeric units. β-mannosidase enzymes (exo-β-1,4-mannosidase) support the hydrolytic action of β-mannanases by carrying out the hydrolysis of terminal, non-reducing β-d-mannose residues. In case of glucomannan degradation, β-glucosidases can cleave the bond between one mannose and one glucose residue (Moreira and Filho, 2008) (Figure 1.6).

The degradation of wood xylans and mannans hemicellulose is supported by arabinases that work synergistically to generate L-arabinose through the

hydrolysis of arabinan (Maijala et al., 2012; Olaniyi et al., 2015; Pinho et al., 2014; Saeed et al., 2019; Titapoka et al., 2008) (Figure 1.6).

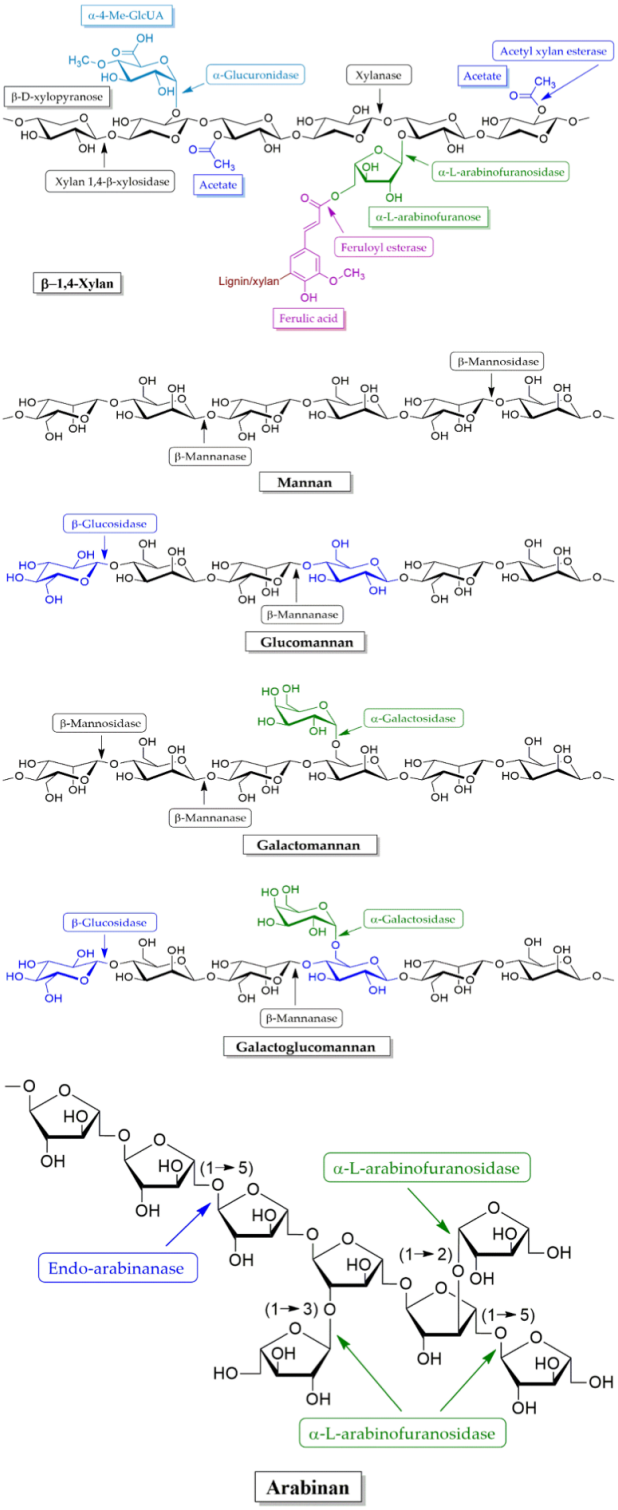

Figure 1.4. Enzymes involved in hemicellulose xylan, mannan, and arabinan degradation. Modified from Kumla et al. (2020).

1.4.3. Cellulose degradation

Cellulose hydrolysis can be achieved thanks to a combination of three major classes of cellulases (endo-1,4-β-d-glucanase, exo-1,4-β-d-glucanase or cellobiohydrolases and β-glucosidase) which convert cellulose into oligosaccharide, cellobiose, and glucose (Horn et al., 2012; Ritota and Manzi, 2019) (Figure 1.7).

Endoglucanases internally cleave β-1,4-glycosidic bonds in the amorphous regions of cellulose generating several reducing and non-reducing ends (Horn et al., 2012; Ritota and Manzi, 2019). Endoglucanases also act on the intermediate product of cellulose hydrolysis (cellodextrins), converting them into cellobiose and glucose.

Exoglucanases also known as cellobiohydrolases, release cellobiose from the reducing end or the nonreducing end of the cellulose chain, allowing the production of cellobiose which can easily be transformed into glucose by β-glucosidases (Madeira et al., 2017; Yeoman et al., 2010; Zhang et al., 2006). These enzymes may also act on cellodextrins and in this case, they are commonly named cellodextrinases (Saini et al., 2015). The oligosaccharides produced from these enzyme activities are converted to glucose through the action of cellodextrinases, while the cellobiose released by the action of cellobiohydrolases is converted to glucose by β-glucosidases (Sajith et al., 2016).

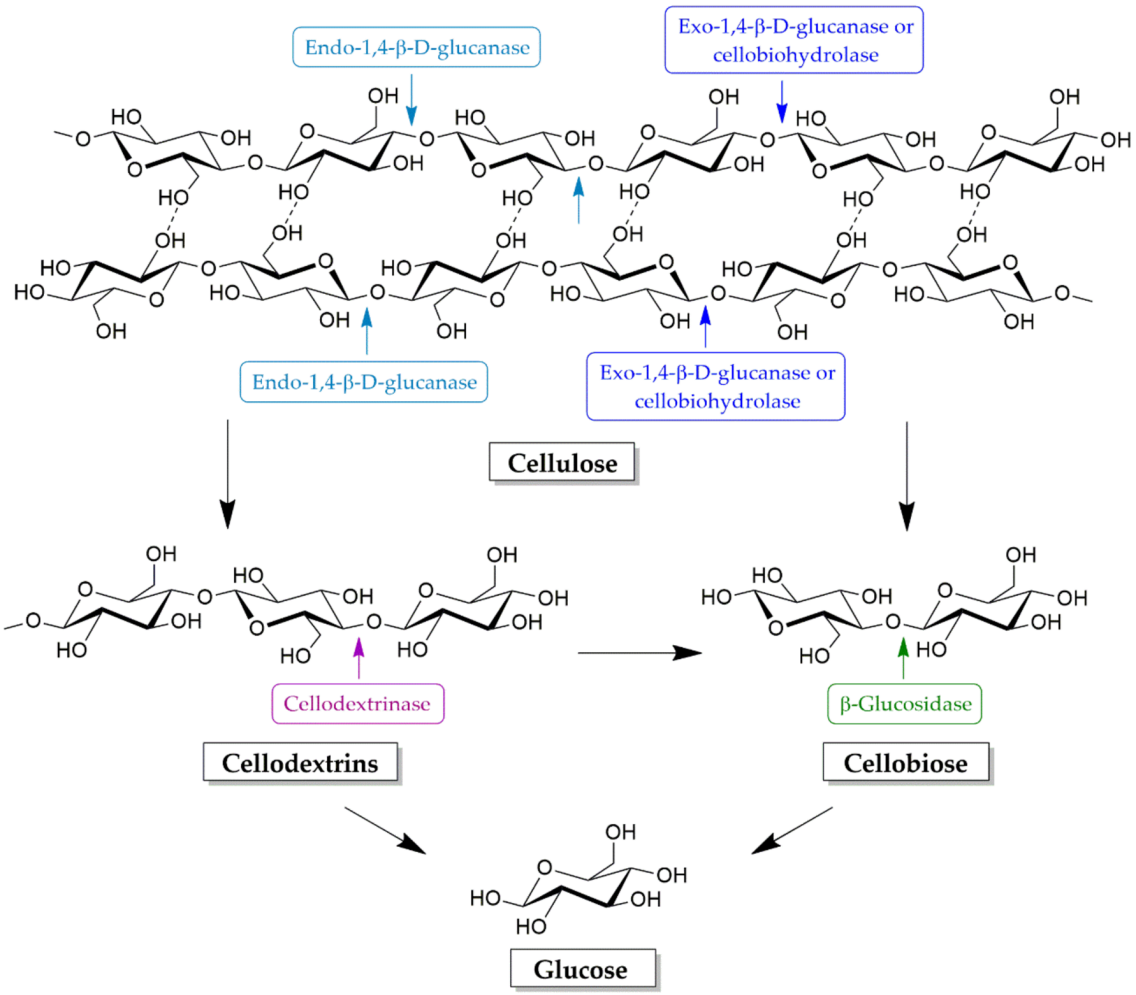

Figure 1.5. Enzymes involved in cellulose degradation. From Kumla et al. (2020).

1.5. Vibrational spectroscopic techniques for studying lignocellulose degradation and mushrooms

Spectroscopy is a branch of the natural sciences that studies the absorption and emission of light and other electromagnetic radiation by matter, and the interactions between particles (*e.g.*, electrons, protons, and ions) as a function of their collision energy (Bunaciu et al., 2020).

In particular, vibrational spectroscopy includes several techniques among which infrared (IR) spectroscopy (absorption) and Raman (emission). These techniques measure the vibrational energy levels associated with the vibration

of the chemical bonds of a studied molecule. The vibrational spectrum of each molecule corresponds to a fingerprint (Campanella et al., 2021) and its molecular and structural information is obtained through the examination of the spectra obtained, considering the position of the band and its intensity. While IR bands result from an electric dipole-mediated transition between vibrational energy levels due to absorption of mid-IR radiation, Raman bands result from a change in the polarizability of the molecule (Gierlinger, 2018). These two techniques provide complementary information on the molecular structure of the analyzed molecules (Gierlinger, 2018) and in particularly, Raman spectroscopy is commonly used to study symmetric vibrations of non-polar groups while mid-IR spectroscopy for study asymmetric vibrations of polar groups (Campanella et al., 2021) (Table 1.3).

Table 1.3. IR and Raman frequencies of common functional groups. From Bunaciu et al. (2020).

			Intensity	
Functional group	**Position**	**Assignment**	**IR**	**Raman**
OH for water	3700–3300		s	w
H bonded OH	3550–3230	str	br	
OH group	3670–3680	str	ms	
R-CH_3	2975–2950	asym str	vs	vs
R-CH_3	2885–2860	sym str	vs	vs
R-CH_3	1470–1440	asym bend	ms	ms
R-CH_3	1380–1370	sym bend	m	vw
R-$CH(CH_3)_2$	1385–1380	Bend-bend	m	vw
R-$CH(CH_3)_2$	1373–1365	Bend-open	m	vw
Aryl-CH_3	2935–2915	Sym str+bendovertone	ms	ms
Aryl-CH_3	2875–2855	Sym str+bendovertone	m	m
$R(CH_3)_3$	1395–1385	Bend-bend	m	vw
$R(CH_3)_3$	1373–1365	Bend-open	ms	ms
Aliphatic CH_2	2936–2915	asym str	vs	vs
Aliphatic CH_2	2895–2833	sym str	vs	vs

Aliphatic CH_2	2920–2890	Fermi resonance	w	m
Aliphatic CH_2	1475–1445	Bend	ms	ms
$(CH_2)_{>3}$	1305–1295	In-phase twist	—	m
$(CH_2)_{>3}$	736–720	In-phase rock	m	—
R_3CH	1360–1320	CH bend	m	m
C-C≡C-H	3340–3267	CH str	s	w
C-C≡C-H	2140–2100	C≡C str	w	vs
C-C≡C-H	710–578	CH wag	sbr	w
>C=C< trans, tri, tetra	1600–1665	C=C str	w-0	s
>C=CH-R mono, cis, trans	3020–2995	CH str	m	m
C=C mono, cis 1,1	1660–1630	C=C str	m	s
$>C=CH_2$ mono 1,1	3090–3075	CH_2 asym str	m	m
$>C=CH_2$ mono 1,1	3000–2980	CH_2 sym str	m	s
$>C=CH_2$ mono 1,1	1420–1400	CH_2 bend	w	m
$R-CH=CH_2$	995–985	trans CH_2 in-phase wag	s	w
$R-CH=CH_2$	910–905	$>CH_2$ wag	s	w
Aryl CH	3100–3000	CH str	mw	s
Aromatic ring	1620–1585	Quadrant str	var	m
Aromatic ring	1590–1565	Quadrant str	var	m
Aromatic ring	1525–1470	Semicircle str	var	vw
Aromatic ring	1465–1400	Semicircle str	m	vw
Mono, meta, (1,3,5), (2,4,6)	1010–990	In-phase str	vw	vs
Meta, (1,2,4), (1,3,5)	9365–810	Lone H wag	m	—
Para, (1,2,4)	880–795	2 adj. H wag	s	—
Meta, (1,2,3)	825–750	3 adj. H wag	s	—
Ortho, meta	800–725	4 and 5 adj. H wag	s	—
Mono, meta, (1,3,5)	710–665	Ring out-of-planebend	s	—
Para	650–630	Ring in-plane bend	—	m
Mono	630–605	Ring in-plane bend	w	m
R-CO-H	1740–1720	C=O str	s	m
Conj -CO-H	1710–1685	C=O str	s	w
R-CO-R	1725–1705	C=O str	s	m
Conj -CO-R	1700–1670	C=O str	s	m
H-CO-O-R	1725–1720	C=O str	s	m
R-CO-O-R	1750–1735	C=O str	s	m
R-CO-OH dimer	1720–1680	C=O out-of-phase str	s	—

R-CO-OH dimer	1670–1630	C=O in-phase str	—	m
R-COO^-	1650–1540	C=O out-of-phase str	s	w
R-COO^-	1450–1360	C=O in-phase str	ms	s
R-CO-O-CO-R	1755–1745	C=O out-of-phase str	mw	m
R-CO-O-CO-R	1825–1815	C=O in-phase str	s	m
R_2CH-OH	1150–1075	C-O str	m	mw
R_2CH-OH	900–800	C-O str	mw	s
R_3C-OH	1210–1180	C-O str	s	mw
R_3C-OH	800–750	C-O str	mw	s
Ar-OH	1260–1180	C-O str	s	w
O=C-O-C	1300–1140	C-O str	s	w
O=C-OH	1300–1200	C-O str	s	w
CH_2-NH_2	3500–3300	NH_2 out-of-phase str	m	vw
CH_2-NH_2	3400–3200	NH_2 in-phase str	m	m
CH_2-NH_2	1630–1590	NH_2 bend	m	vw
CH_2-NH_2	900–600	NH_2 wag	sbr	w
-CH_2-NH-CH_2-	3450–3250	NH str	vw	w
-CH_2-NH-CH_2-	1150–1125	C]N]C out-of-phasestr	m	mw
O=C-NH-	About 3300	NH str	s	w
O=C-NH-	Near 3100 (overtone of1550)	NH str	w	w
C-C≡C-C	2245–2100	C≡C str	—	s
CH_2-C≡N	2260–2240	C≡N str	m	vs
CH_2-C≡N	1440–1405	CH_2 bend	m	m
Conj -C≡N	2235–2185	C≡N str	var	s
Ar-NH_2	1380–1260	C-N str	sbr	m
C-NH_3^+…X^-	3200–2700	NH_3 str	s	vw
C-NH_3^+… X^-	1625–1560	NH_3 out-of-phase str	mw	vw
C-NH_3^+… X^-	1550–1505	NH_3 in-phase str	w	vw
$C_2NH_2^+$… X^-	1620–1560	NH_2 bend	mw	w
$C_2NH_2^+$… X^-	3000–2700	NH_2 str	sbr	w
C_3NH^+…X^-	2700–2300	NH_2 str	s	w
CH_2-NO_2	1600–1530	NO_2 out-of-phase str	s	mw
CH_2-NO_2	1380–1310	NO_2 in-phase str	s	vs
Ar-NO_2	1555–1485	NO_2 out-of-phase str	s	—
Ar-NO_2	1357–1318	NO_2 in-phase str	s	vs
-CH_2-Cl	830–560	C-Cl str	s	s

-CH_2-Br	700–515	C-Br str	s	vs
-CH_2-F	1100–1000	C-F str	s	w
Pyridine	3100–3300	Aryl CH str	m	m
Pyridine	1615–1570	Quadrant str	s	m
Pyridine	1400–1440	Semicircle str	s	mw
Pyridine	1035–1025	2,4,6 carbon radial str	m	vs
Pyridine	995–985	Ring breath/str	m	s
Pyridine	660–600	Quadrant in-plane bend	—	m
Pyrrole	3500–3000	NH str	s	m-w
Pyrrole	3135–3103	=CH str	m	s
Pyrrole	1530	Quadrant str + CHrock	s	—
Pyrrole	1468	Quadrant str + CHrock	m	s
Pyrrole	1418	Semicircle str+CHrock	m	—
Pyrrole	1380	Semicircle str+CHrock	s	m
Pyrrole	1143	Ring in-phase str	m	vs
Furan	3156, 3121, 3092	=CH str	m	s-m
Furan	1590	Quadrant str + CHrk	s	w
Furan	1483	Quadrant str + CHrk	s	vs
Furan	1378	Semicircle str+CHrock	s	s
Furan	1140	Ring in-phase str	—	vs
η-Lactones	1795–1760	C=O str	s	m
Cyclic anhydride	1870–1845	C=O sym str	m	s
Cyclic anhydride	1755–1745	C=O asym str	s	mw
Epoxy	1270–1245	Ring sym str	m	s
Epoxy	935–880	Ring asym str	s	m
Epoxy	880–830	Ring asym str	s	m

s, strong; m, medium; w, weak; v, very; br, broad; var, variable; –, zero.

Among the different accessories of IR, Attenuated Total Reflectance – Fourier Transform Infrared (ATR-FTIR) as well as Raman techniques, are commonly used in chemistry, pharmacy, physics, biology, medicine, and environmental research as well as in industry, biotechnological, art, forensic, and archaeology areas. They are non–destructive and non–invasive tools with high sensitivity

and specificity capable to provide detailed information about the molecular composition, structure and interactions within a sample.

ATR-FTIR spectroscopy exploits a crystal with a high refractive index such as Ge, ZnSe, thallium halides, and diamond through which the IR beam emitted by the source passes before reaching the analyte. The sample is placed directly in contact with the crystal, and thanks to the principle of the evanescent wave, the IR beam penetrates for a few μm (0.5 μm-2μm) in the sample (Bunaciu et al., 2020).

In Raman spectroscopy, the radiation scattered from a molecule irradiated with a monochromatic light, usually a laser in the visible, near IR, or near UV regions, is detected. The scattered radiation is originated when the incident photon excites the molecule into a virtual state. The Raman effect know as Stokes scattering, occur when a molecule, which undergo in a change in polarizability, is excited from a ground vibrational state to a virtual energy state, and relax into a higher energy vibrational excited state. However, even an anti-Stokes scattering can occur when some molecules present in a vibrational excited state, scattering from these states to the ground state through a transfer of energy to the scattered photon (Smith and Dent, 2019).

Raman scattering is very weak and for some samples (*e. g.*, biological samples) a large background fluorescence emission can overlap the Raman signal (Stöckel et al., 2016). To overcome these problems, Surface-enhanced Raman Scattering (SERS) represents a great advance in the field of Raman spectroscopy. This technique, thanks to the use of noble metal (*e. g.*, copper, silver or gold) nanoparticles (NPs) allow to overcome the weakness of the normal Raman signal (Aroca, 2006, 2013). The NPs interacting with the incident light of the laser beam generate a Localized Surface Plasmonic Resonance (LSPR) that allow an enhancement of the Raman scattering of the molecules adsorbed or located

near of the metal NPs, up to 10^{14} orders of magnitude (Butler et al., 2016; Le Ru and Etchegoin, 2009; Lee et al., 2019; Zhang et al., 2017).

ATR-FTIR and Raman SERS spectroscopy have been successfully applied to the study of complex matrices such as biological ones. In particular, several studies have applied ATR-FTIR spectroscopy to study the composition and structural changes that occur during the degradation of the lignocellulosic component of wood (Báder et al., 2020; Bock et al., 2020; Gao et al., 2022; Javier-Astete et al., 2021; Lupoi et al., 2015). Moreover, ATR-FTIR and SERS spectroscopy have been successfully used to study the chemical composition of different foods, including mushrooms (Jiang et al., 2021; Meenu and Xu, 2019; Neng et al., 2020; Zaukuu et al., 2022).

CHAPTER 2

THE MAIN OBJECTIVES OF THE THESIS

The current grow rate of the world population is progressively increasing anthropogenic pressure on natural resources.

To meet the relative demand for food it is essential to satisfy in a more equitable and sustainable way a growing need for energy, water, and soil. In this context, the recovery and enhancement of waste and by-products from the agri-food chain play a key role.

The main objective of this dissertation thesis was to study the role of fungi in the recovery or degradation of agro-industrial wastes and to evaluate their production and/or degradation capacity through the application of vibrational spectroscopy.

Emphasis is given to the study of 3 types of agro-industrial waste:

- The solid fraction of CD resulting from the anaerobic digestion (AD) of agricultural biomass for biogas production, characterized by having high amounts of nitrogen, in particular ammonia, and high amounts of lignin, cellulose and hemicellulose.
- Hazelnut shells (HS), produced as a result of the cracking process and generally used for domestic heating, causing air pollution.

- PE films, widely used in agriculture whose disposal at the end of the crop cycle, is difficult and in some cases can not be completely removed from the ground.

CHAPTER 3

DEGRADATIVE ABILITY OF MUSHROOMS CULTIVATED ON CORN SILAGE DIGESTATE

From Fornito et al., 2020

The current management practice of digestate from biogas plants involves its use for land application as a fertilizer. Nevertheless, the inadequate handling of digestate may cause environmental risks due to losses of ammonia, methane and nitrous oxide. Therefore, the key goals of digestate management are to maximize its value by developing new digestate products, reducing its dependency on soil application and the consequent air pollution. The high nitrogen and lignin content in solid digestate make it a suitable substrate for edible and medicinal mushroom cultivation. To this aim, the mycelial growth rate and degradation capacity of the lignocellulosic component from corn silage digestate, undigested wheat straw and their mixture were investigated on *Cyclocybe aegerita*, *Coprinus comatus*, *Morchella importuna*, *Pleurotus cornucopiae* and *Pleurotus ostreatus*. The structural modification of the substrates was performed by using ATR-FTIR spectroscopy. Preliminary *in vitro* results demonstrated the ability of *P. ostreatus*, *P. cornucopiae* and *M. importuna* to grow and decay hemicellulose and lignin of digestate. Cultivation trials were carried out on *C. aegerita*, *P. cornucopiae* and *P. ostreatus*.

Pleurotus ostreatus showed the highest BE and fruiting body production (FBP) in the presence of digestate; moreover, *P. ostreatus* and *P. cornucopiae* were able to degrade the lignin. These results provide attractive perspectives both for more sustainable digestate management and for the improvement of mushroom cultivation efficiency.

3.1. Introduction

Managing organic waste streams is a major challenge for the agricultural industry. Anaerobic digestion treatment process is considered the most suitable bio-energy technology to treat wastes for biogas production from agriculture, industry and household food wastes (Appels et al., 2011). Public policies of several EU Member States have promoted the use of AD to treat organic wastes and to generate renewable energy. According to the estimates, about one-third of the EU's 2020 target for renewable energy in transport could be met by using biogas produced from bio-waste, while around 2% of the EU's overall renewable energy target could be met if all bio-waste was turned into energy (European Commission, 2010).

Digestate is a heterogeneous material produced in large amounts during the AD process (Dahlin et al., 2017). The physico-chemical characteristics of digestate depend on the nature and composition of feedstocks, as well as on the operational parameters of the process. Agricultural wastes typically have a high content of lignocellulose. In this rigid structure, lignin coats cellulose and hemicellulose while blocking their degradation by anaerobic bacteria (Ahmed et al., 2019; Dashtban et al., 2009). Pretreatment methodologies utilizing energy-intensive processes (high pressures and temperatures) and harsh chemical compounds (NaOH, H_2SO_4) are currently used, in order to better perform their utilization in the AD process (Grigatti et al., 2015; Plácido and Capareda, 2015).

One of the main questions about the reuse of digestate is how to prevent nutrient imbalances in the receiving environment. In agriculture, digestate is considered a useful nutrient source, but its use is influenced by the disposal limits for N and P (Mucha et al., 2019). Moreover, the digestate used as a fertilizer is still a source of greenhouse gases (GHGs). These gases can be produced and emitted during digestate storage and during its spreading upon

the field although their impact is relatively lower than untreated biomass (Czubaszek and Wysocka-Czubaszek, 2018). However, the ammonia release and nitrate leaching are still a critical point with respect to N_2O and CH_4 emissions from digestate (Paolini et al., 2018).

Therefore, new strategies and alternative uses of digestate are necessary in view of the growth of biogas plants (Hidalgo et al., 2019).

Lignocellulolytic mushrooms are an attractive resource that allows the biotransformation of lignocellulosic wastes into a value-added bioproduct (Peng et al., 2020). White-rot mushrooms such as *Cyclocybe aegerita* (V. Brig.) Vizzini, *Ganoderma lucidum* (Curtis) P. Karst., *Ganoderma resinaceum* Boud., *Lentinula edodes* (Berk.) Pegler, *Pleurotus cornucopiae* (Paulet) Rolland, *Pleurotus ostreatus* (Jacq.) P. Kumm. and *Schizophyllum commune* Fr. are the most effective mushrooms for delignification due to the production of a large variety of ligninolytic extracellular enzymes such as laccase, lignin manganese and versatile peroxidases, galactose oxidase, glyoxal and alcohol oxidase, benzoquinone reductases and lytic polysaccharide monooxygenases (Gupta et al., 2018; Janusz et al., 2017; Sista Kameshwar and Qin, 2018). On the other hand, brown root mushrooms such as *Laetiporus sulphureus* (Bull.) Murrill, some coprophilous mushrooms like *Coprinus comatus* (O.F. Müll.) Pers. and the post-fire mushroom *Morchella importuna* M. Kuo, O'Donnell & T.J. Volk, have been shown to also be able, although to a lesser extent, to produce oxidative enzymes for lignin degradation (Janusz et al., 2017; Lu and Ding, 2010; Sista Kameshwar and Qin, 2018; Tan et al., 2019). Most of these mushrooms are edible and/or have medicinal proprieties and have been successfully cultivated (Dasanayaka and Wijeyaratne, 2017; Oei, 2003; Pleszczyńska et al., 2013). *Coprinus comatus* is also cultivated on a biogas residue mixture and is patent-protected (Debin et al.,

2008). Only *M. importuna* has begun to be cultivated recently predominately in open fields in China (Q. Liu et al., 2018).

In the past, several analytical approaches were carried out to study the ability of fungal species to decompose lignin. Since lignin is closely associated to cellulose and hemicellulose, its separation is considered problematic because the extraction procedures take time and lead to chemical and structural changes caused by condensation and oxidation reactions (Lu et al., 2017). There are two main conventional techniques to separate lignin from hemicellulose and cellulose: the first is to remove cellulose and hemicellulose leaving most of the lignin as a solid residue, and the second is to extract lignin using fractionation procedures leaving the other components (Tribot et al., 2019). As a result, the original structural characteristics of lignin may be missing.

ATR-FTIR spectroscopy is a non-destructive technique that has been successfully used for detecting chemical compounds present in complex mixtures because each molecule is characterized by a specific spectrum. Pandey and Pitman (2003); Gupta et al. (2015) have widely used this technique to monitor the chemical variations that occur during wood degradation by chemical and biological treatments. However, some spectra may appear poorly resolved, due to the existence of highly overlapping and hidden peaks. Consequently, it is not possible to assign specific peaks to the vibrations of specific functional groups. In such cases, the application of a curve-fitting analysis has become an important tool for qualitative and quantitative analyses of IR spectra (Griffiths and De Haseth, 2007).

In this context, the main goal of the project was to use mushroom cultivation for degrading the ligninolytic fraction of digestate. Several edible and medicinal mushroom species were tested and their ability to degrade the lignin fraction was assessed by using ATR-FTIR spectroscopy.

3.2. Materials and Methods

3.2.1. Substrates

The CD was obtained from a biogas plant that is located in Malalbergo (Bologna, Italy). The biogas plant can be classified as "single-phase, two-stage", is designed to work in semi-dry conditions (Total Solid 13%) and is fed exclusively with energy crops (maize, sorghum, triticale silage). This plant can be considered to be of compact dimension, compared to other technical solutions with the same productive capacity (4100 m^3 of volume for 1 MW of installed electrical power), due to the ability to develop the process with high concentrations of substrate. The average biomass consumption is approximately 18,500 tons/year for a biogas production of 4,050,000 m^3 (8,500,000 kWh/year of gross renewable electric energy production). The mean hydraulic retention time (HRT) of the biomass is 70 days, after which the digestate is separated into solid and liquid fractions through a mechanical screw separator. The solid digestate (SD) production is 2500 tons/year and after separation is stored in trench silos, similar to those commonly used for silomais. The liquid digestate (10,000 tons/year) is stocked in a specifically covered tank. The SD used in this work was produced in February and collected as soon as it fell out of the mechanical separator.

Durum wheat straw and *Populus* spp. chips (PC) were kindly provided by the Cadriano farm of the University of Bologna. In particular durum wheat straw was used in the farm to produce compost and it was stored under aerobic conditions in the field. All raw materials were dehydrated at room temperature and kept in the stove at 60°C for 24 hours. They were subsequently crushed with scissors and a manual grinder into fragments smaller than 0.5 cm and autoclaved at 121 ± 1°C for 60 minutes to prevent any contamination during their storage. The dried raw materials were stored in a desiccator at 22°C.

Organic soft wheat bran and Alabastrine gypsum ($CaSO_4 \cdot 2\ H_2O$, Lab grade) were used for the mushroom cultivation trials.

3.2.2. Mushrooms cultures and mycelial growth rate evaluation

Experimental trials were carried out by using 9 strains of basidiomycetes (*C. aegerita*, *C. comatus*, *G. lucidum*, *G. resinaceum*, *L. sulphureus*, *P. cornucopiae*, *P. ostreatus*, *S. commune*) and ascomycetes (*M. importuna*) isolated from fruiting bodies collected in the wild; *L. edodes* (belonging to Basidiomycota division) strain was brought by the Fungal Institute of Jinxiang (Shan-dong province, China) (Table 3.1).

Table 3.1. Strain numbers and species used in this work.

Strain n.*	Species
CAe4	*Cyclocybe aegerita*
CCo10	*Coprinus comatus*
GLu16	*Ganoderma lucidum*
GRe5	*Ganoderma resinaceum*
LSu10	*Laetiporus sulphureus*
LEd5	*Lentinula edodes*
MIm6	*Morchella importuna*
PCo3	*Pleurotus cornucopiae*
POs15	*Pleurotus ostreatus*
SCo3	*Schizophyllum commune*

The mycelial pure cultures were stored in the Mycological and Applied Botany Laboratory (CMI-UNIBO strain collection) of the Department of Agricultural and Food Sciences (DISTAL), University of Bologna (Italy).

All the isolates were kept on Potato Dextrose Agar (PDA, Difco) half strength, at 22 ± 1°C in darkness, and subcultured every two months.

For mycelial growth rate evaluation, plugs of 10 mm diameter were taken by 15-day-old colonies of each species and inoculated in the center of 9 cm sterilized Petri dish previously filled with 15 g of three different substrates at 80% humidity: CD, Corn Digestate-Wheat Straw (CD-WS) (1:1, w/w) and Wheat Straw (WS) as control. Five replicates were made for each combination of species and substrate. All plates were incubated at 22 ± 1°C in darkness. The mushroom growth was assessed by measuring the diameter of the colony along two preset diametrical lines every day. Radial daily growth rate (rGR) was calculated during the first 3 days of the exponential phase as:

$$rGR = \frac{(D_1 - D_0) / 2}{(T_1 - T_0)} \times 24$$

where D_0 and D_1 are the colony diameter during the exponential growth phase at time T_0 and T_1, respectively (Trinci, 1971) (modified).

3.2.3. Inoculum preparation and cultivation trials

Cultivation tests were carried out for *C. aegerita*, *P. cornucopiae* and *P. ostreatus*. The grain spawn was prepared by inoculating 15-day-old mycelial plugs in glass tubes containing sorghum kernels and distilled water in a 1:2 (v/v) ratio previously sterilized at 121 ± 1°C for 20 minutes. For each species-substrate combination 5 replicates were prepared. The tubes were incubated in the dark at 22 ± 1°C for 30 days. The spawn was ready when the mycelium had colonized all the kernels.

Three different solid substrates were tested: a digestate based substrate (97% corn digestate), a substrate with 48% of digestate and as control, a substrate based on PC or WS according to the mushroom substrates preferences (Oei, 2003; Stamets, 2000) (Table 3.2). Homogeneous substrate mixtures were prepared by mixing component materials based on their dry weight (w/w).

The substrates were inserted into autoclavable polypropylene (PP) transparent bags (20 × 30 cm). Dried mixed substrates (1.5 L per bag: 120 g for CD, 110 g for CD-WS-WB, 100 g for WS-WB; 160 for CD-PC-WS and 200 g for PC-WS) were moistened with 500 mL (per bag) of distilled water for 24 hours and the excess of water was removed by squeezing the bags.

Table 3.2. Composition of the substrates used for cultivation trials.

Species	Substrates and mixing ratio[1]	Code
P. cornucopiae *P. ostreatus*	97% CD:3% gypsum	CD
	48% CD:46% WS:3% WB:3% gypsum	CD-WS-WB
	92% WS:5% WB:3% gypsum (control)	WS-WB
C. aegerita	97% CD:3% gypsum	CD
	48% CD:44% PC:5% WS:3% gypsum	CD-PC-WS
	88% PC:9% WS:3% gypsum (control)	PC-WS

[1] dry weight (w/w). Abbreviations: CD (Corn Digestate); WS (Wheat Straw); WB (Wheat Bran) and PC (Poplar wood Chips).

Bags were closed with a hydrophobic cotton cap, autoclaved at 121 ± 1°C for 60 minutes; inoculated with grain spawn by opening the bag, inserting the inoculum inside of it (45 g per bag), mixing the inoculum with the substrate and incubated it in the darkness at 22 ± 1°C until complete colonization of the substrate. For each species-substrate combination, five bags were prepared. Mycelial bag colonization was evaluated.

After 20 or 35 days of mycelial growth of the two *Pleurotus* species and *C. aegerita* respectively, the bags were moved to a climatic chamber with a temperature of 19 ± 1°C during the day and 14 ± 1 °C during the night, relative humidity between 80% and 85%, and 12 hours light/dark photoperiod with a light intensity of 700 ± 100 lux. The mature fruiting bodies were collected for 3 months; the fresh weight was recorded for the evaluation of the BE (Chang et

al., 1981), then they were dried in a stove at 65°C for 24 hours and weighed. The BE was calculated as:

$$\text{BE}\ (\%) = \frac{\text{fresh weight of mushrooms}}{\text{dry weight of substrate}} \times 100$$

3.2.4. Chemical analyses

In order to evaluate changes in the chemical composition of the different substrates before and after the 12 days of mycelial growth, the elemental analysis of C and N was carried out. Five replicates of each substrate before and after inoculation were collected from the Petri dishes. All samples were mixed, washed five times with distilled water, dried in a stove at 35°C for 48 hours and crushed in a ball mill (RETSCH MM 400, Germany) to produce a homogeneous mixture of each material. The elemental analysis was carried out using Flash EA 2000 Elemental Analyzer (Thermo Scientific, Germany) on 2 mg and performed on triplicate samples.

3.2.5. ATR-FTIR spectroscopy analysis

The FTIR spectra were recorded by using an ALPHA FTIR spectrometer (Bruker Optics, Ettlingen, Germany) equipped with a diamond crystal ATR device. The substrates were analyzed after 12 days of in vitro mycelial growth and after the FBP (4 months after inoculation) were analyzed. Each sample was deposited on the surface of the crystal and the spectra were acquired against a pre-established background by averaging 64 scans from 4000 to 400 cm^{-1} at 4 cm^{-1} resolution. Spectra were collected in triplicate for each sample and then averaged.

In order to determine the main structural changes in the spectra that had undergone different treatments, a curve fitting using the Grams/386 spectroscopic software (version 6.00, Galactic Industries Corporation, Salem,

NH) was performed. The second derivative of the IR spectra in the 1800–1200 cm^{-1} region was smoothed using the Savitzky–Golay function. The IR spectra were fitted with Gaussian bands, the best fitting parameters were determined by minimization of the reduced Chi-square (χ^2). Agreement between experimental and calculated profiles was obtained, with coefficients of determination, R^2, ranging from 0.990 to 0.980 and the standard error (SE) from 0.001 to 0.005.

3.2.6. Statistical analyses

Statistical analyses were assessed by using the XLSTAT software version 7.5.2 (Addinsoft). Student t-test was performed to compare the C and N content of the substrates after mushrooms mycelial growth with the initial substrates. The analysis of variance (ANOVA) was used to determinate a significant difference in mycelial growth rate, FBP and BE among different substrates. Tukey post hoc test ($p \leq 0.05$) was used to compare the means.

3.3. Results

3.3.1. In vitro mycelial growth and elemental analysis of C and N of substrates

Ganoderma lucidum, G. resinaceum, L. sulphureus, and *L. edodes* did not grow or grow very slowly on digestate whereas *C. aegerita*, *M. importuna*, *P. cornucopiae* and *P. ostreatus* grew similarly or significantly more (*P. ostreatus*) on the corn digestate (CD) compared to the straw (Table 3.3). For this reason, the C and N content and ATR-FTIR spectra were carried out only on the latter four species. *Coprinus comatus* was also included because recently a substrate containing biogas residues has been patented for its cultivation (Debin et al., 2008).

Table 3.3. Radial growth rate (mm/day) of the tested mushroom species on different substrates.

Strain n.	Species	CD	CD-WS	WS
CAe4	*Cyclocybe aegerita*	5.34 ± 1.22 A	4.77 ± 1.04 A	5.33 ± 0.31 A
CCo10	*Coprinus comatus*	2.46 ± 0.64 B	9.26 ± 0.76 A	8.24 ± 1.15 A
GLu16	*Ganoderma lucidum*	0.32 ± 0.10 B	0.38 ± 0.21 B	4.08 ± 0.09 A
GRe5	*Ganoderma resinaceum*	1.37 ± 0.45 C	5.4 ± 0.55 B	8.18 ± 0.92 A
LSu10	*Laetiporus sulphureus*	0.00 B	0.11 ± 0.16 B	6.74 ± 1.24 A
LEd5	*Lentinula edodes*	0.00 B	0.59 ± 0.57 B	2.82 ± 0.41 A
MIm6	*Morchella importuna*	21.50 ± 1.00 AB	23.50 ± 3.09 A	20.20 ± 1.01 B
PCo3	*Pleurotus cornucopiae*	8.18 ± 0.68 A	8.37 ± 0.71 A	7.88 ± 0.86 A
POs15	*Pleurotus ostreatus*	4.83 ± 0.75 A	4.10 ± 1.60 A	2.25 ± 0.33 B
SCo3	*Schizophyllum commune*	6.59 ± 1.72 C	8.52 ± 0.33 B	10.60 ± 0.20 A

The data are the mean of 10 measurements ± standard deviation. Different letters on the same row indicate significant difference for $p \leq 0.05$ by post-hoc Tukey test.

Table 3.4 shows the C and N values determined in CD, CD-WS and WS before inoculation (control) and after 12 days of mycelial growth. The C percentage of CD-WS, showed no intermediate value, due to the high chemical complexity of CD. The C content of substrates inoculated with several mushrooms showed no considerable variation (Table 3.4). C content was significantly lower in *C. aegerita* on CD, and significantly higher in *C. comatus, M. importuna, P. cornucopiae* and *P. ostreatus* on WS than in the untreated substrates (control).

The nitrogen content on WS inoculated with the different mushrooms was generally significantly lower than the control (Table 3.4). These changes led to a significant increase in the C/N ratio on WS which was 31 in the control and ranged from 59 to 69 after the fungal growth (Table 3.5). On the CD substrate, there were no significant differences between treatments although a slight decrease of N was apparent in the presence of *C. comatus* and *P. cornucopiae* (Table 3.4). In the CD-WS substrate, only *C. aegerita, P. ostreatus* and *M. importuna* significantly decreased the N content. No variation was observed for the other species. Considering the C/N ratio, no variation was observed on CD,

while, on CD-WS, the C/N ratio was 34 in the control and 49 after the growth of *P. ostreatus* (Table 3.5).

Table 3.4. Total content of C and N on different substrates before inoculation with the fungi studied (control) and after a 12 days period of mycelium growth following inoculation.

Species	**Substrates**					
	CD		**CD-WS**		**WS**	
	C (%)	**N (%)**	**C (%)**	**N (%)**	**C (%)**	**N (%)**
Control	39.07±0.07	1.59±0.01	39.57±1.04	1.18±0.005	36.26±0.005	1.16 ±0.04
C. aegerita	38.67±0.02**	1.54±0.04	39.18±0.004	1.13±0.01*	37.93±0.99	0.62±0.008**
C. comatus	39.60±0.47	1.51±0.07	39.43±0.18	1.15±0.01	39.55 ±0.27**	0.67±0.01**
M. importuna	38.94±0.04	1.55±0.04	39.81±0.29	1.08±0.02**	39.86±0.79*	0.68±0.02**
P. cornucopiae	39.07±0.05	1.37±0.10	38.80±0.32	1.20±0.04	38.52±0.05**	0.61±0.01**
P. ostreatus	39.86±0.59	1.59±0.05	39.39±0.96	0.81±0.007**	39.61±0.68**	0.57±0.009**

The data are the mean of 3 replicates ± standard error. Asterisks indicate significant differences from the control (* $p \leq 0.05$; ** $p \leq 0.01$) using Student's t-test.

Table 3.5. C/N ratio on different substrates before and after inoculation with mushrooms.

Species	**Substrates**		
	CD	**CD-WS**	**WS**
	C/N	**C/N**	**C/N**
Control	24.57	33.53	31.26
C. aegerita	25.11	34.54	61.16
C. comatus	26.20	34.29	59.03
M. importuna	25.12	37.21	58.62
P. cornucopiae	28.51	33.16	63.15
P. ostreatus	25.23	48.63	69.49

3.3.2. ATR-FTIR of substrates after in vitro mycelial growth

Figure 3.1 shows the ATR-FTIR spectra of the substrates (CD, CD-WS and WS) after 12 days of mycelial growth with different mushrooms species. The ATR-FTIR spectra clearly showed a significant structural variation of the main functional groups in the region between 1800-1200 cm^{-1} in which many clearly defined peaks provided information on their modification during degradation. The major peaks can be listed as follows: 1740 cm^{-1} is ascribed to unconjugated C=O in xylans (hemicellulose) or in the heterocyclic cellulosic rings (Rahman et al., 2017); 1727 cm^{-1} is due to H-bonded acid/ketone carbonyl groups; ~1645 cm^{-1} is assigned to C=O stretching in conjugated ketones, water and amide I (proteins); ~ 1590 and 1510 cm^{-1} are attributed to aromatic skeletal vibrations (C═C) and aromatic breathing in lignin, respectively (Mohebby, 2005; Popescu et al., 2010; Singh et al., 2014); ~ 1547 cm^{-1} is related to amide II (proteins); 1457 cm^{-1} is due to C–H bending in lignin and hemicelluloses; 1423 and 1370 cm^{-1} are assigned to CH_2 and CH_3 bending vibrations, respectively. These bands are typical of the mixture of both crystalline and amorphous cellulose (Huang et al., 2012); 1318 cm^{-1} is attributed to C-H bending in crystallized cellulose I (Colom et al., 2003); ~1240 cm^{-1} is assigned to the syringyl ring in lignin and C–O stretching in xylan of hemicellulose (Pandey and Pitman, 2003; Yilgor et al., 2013).

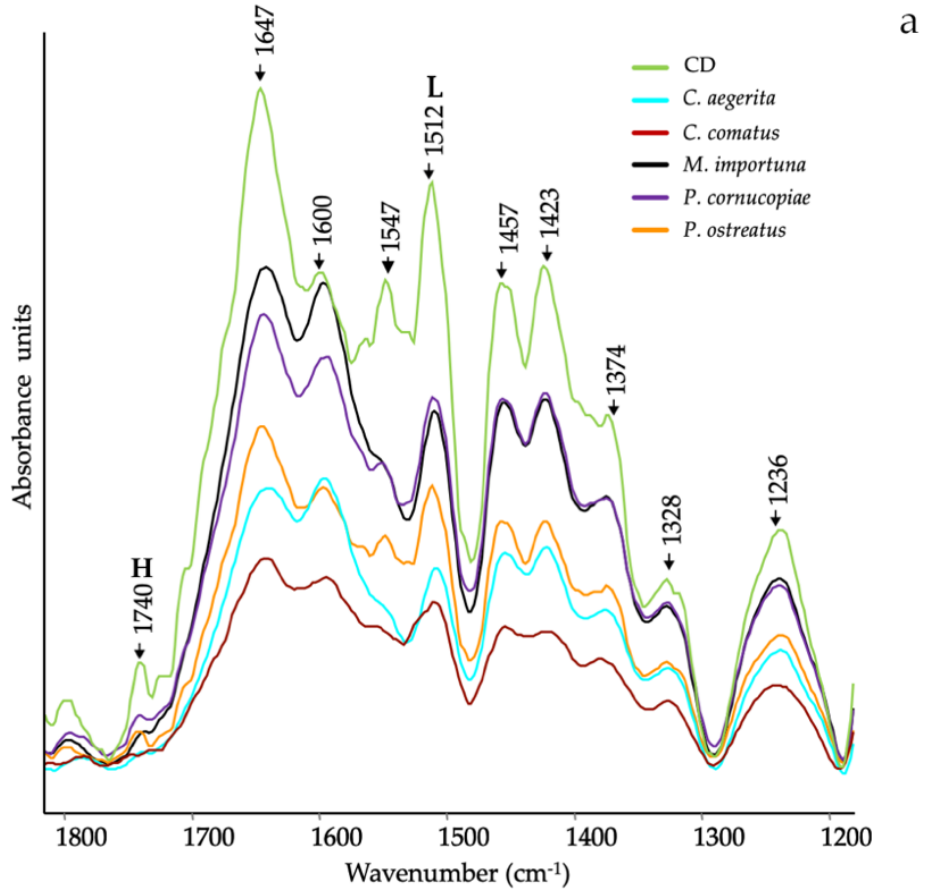
a
Absorbance units
1647
1600
1547
1512
L
1457
1423
1374
1328
1236
H
1740
CD
C. aegerita
C. comatus
M. importuna
P. cornucopiae
P. ostreatus
1800
1700
1600
1500
1400
1300
1200
Wavenumber (cm-1)

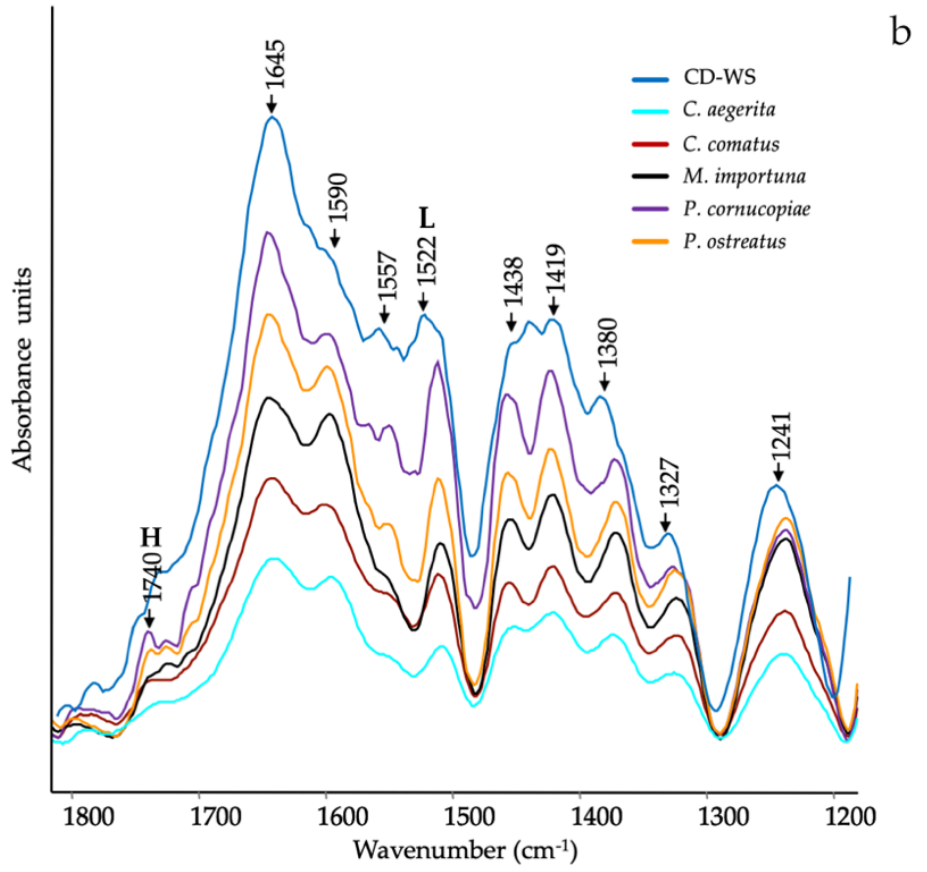
b
Absorbance units
1645
1590
1557
1522
L
1438
1419
1380
1327
1241
H
1740
CD-WS
C. aegerita
C. comatus
M. importuna
P. cornucopiae
P. ostreatus
1800
1700
1600
1500
1400
1300
1200
Wavenumber (cm-1)

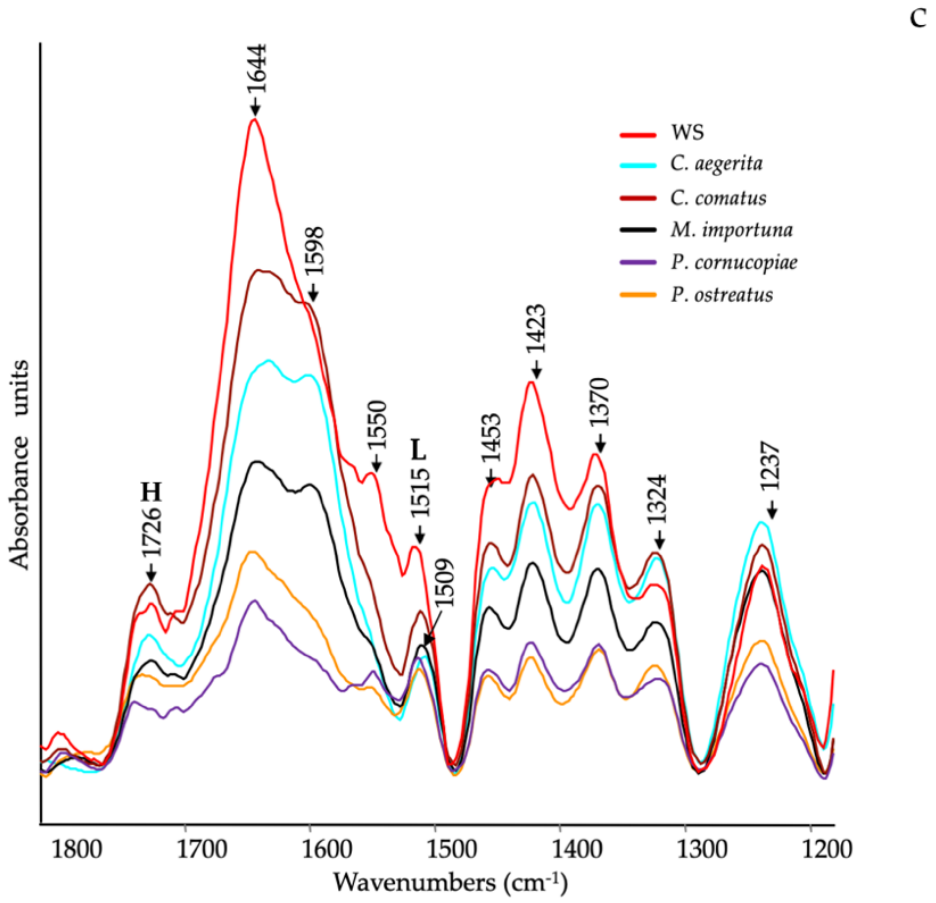

Figure 3.1. ATR-FTIR spectra of (a) Corn Digestate (CD, green line), (b) Corn Digestate 50% - Wheat Straw 50% (CD-WS, blue line) and (c) Wheat Straw (WS, red line) after 12 days of mycelial growth of *C. aegerita* (cyan line), *C. comatus* (dark red line), *M. importuna* (black line), *P. cornucopiae* (purple line) and *P. ostreatus* (orange line). H= hemicellulose; L= lignin [as references for lignin: (Mohebby, 2005; Popescu et al., 2010; Singh et al., 2014)].

In more detail, the ATR-FTIR spectra of the CD substrate after mycelium growth, as compared to untreated CD (Figure 3.1a), showed a significant decrease in the relative intensity of the bands assigned to hemicellulose (1740 cm^{-1} and 1236 cm^{-1}), proteins (1647 cm^{-1} and 1547 cm^{-1}), and lignin (1600 cm^{-1} and 1512 cm^{-1}). All these compounds changed in relation to the inoculated mushroom species.

In some instances, ester bands in hemicellulose have disappeared in CD treated with *C. aegerita* and *C. comatus*, as well as amide (II) in proteins, as supported by

the slight reduction in total nitrogen (Table 3.4). Concerning the lignin bands (1600 cm^{-1} and 1512 cm^{-1}), they progressively decreased in the series: *C. comatus* < *C. aegerita* < *P. ostreatus* < *P. cornucopiae* < *M. importuna*.

In the case of the ATR-FTIR spectra of CD-WS substrate after mycelium growth, a slight difference compared to the untreated substrate was observed (Figure 3.1b). The relative intensities of hemicellulose bands considerably decreased in substrate treated with *C. aegerita* and *C. comatus* as well as in the protein bands (1645 cm^{-1} and 1557 cm^{-1}), although no correspondence with total N was found. Regarding the peaks taken as a reference of lignin (1590 cm^{-1} and 1522 cm^{-1}) they progressively decreased in the series: *C. aegerita* < *C. comatus* < *M. importuna* < *P. ostreatus* <*P. cornucopiae*.

Figure 3.1c showed the ATR-FTIR spectra of WS substrate. As already observed on CD and CD-WS, the intensity of the hemicellulose bands (1726 cm^{-1} and 1237 cm^{-1}) decreased in treatments with *P. cornucopiae* and *P. ostreatus*. As regards to the amide bands, a considerable reduction appeared in all treatments, as also supported by the variation of total N (Table 3.4). The intensity of the band at 1509 cm^{-1} (lignin) was significantly reduced in all spectra, although it was more consistent in *P. ostreatus* and *P. cornucopiae*.

3.3.3. Fruiting body production

For the cultivation test, *C. aegerita*, *P. cornucopiae* and *P. ostreatus* were used. The choice was made based on the results obtained from the measurements of the mycelial growth rate on CD (Table 3.3) and the commercial potential of the species. The species *M. importuna*, even though it has rapid development in in vitro tests, was not selected for cultivation trials as its production of fruiting body is still difficult in controlled conditions (Masaphy, 2010).

The different species used during the cultivation tests showed a FBP (Figure 3.2a) and a BE similar in the different substrates used. Although there were no

statistically significant differences between substrates, *P. ostreatus* grown on CD exhibited a FBP and a BE apparently higher than PC-WS or WS-WB. On the other hand, *P. cornucopiae* showed not significantly higher production and BE compared to WS (Figure 3.2a, b).

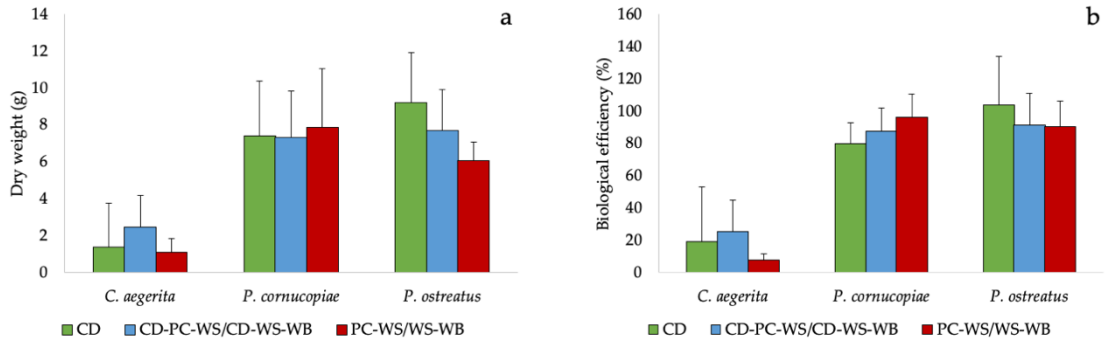

Figure 3.2. (a) Fruiting body production and (b) biological efficiency of the tested mushrooms species on CD and on Corn Digestate-Poplar Chips-Wheat Straw (CD-PC-WS) or Corn Digestate-Wheat Straw-Wheat Bran (CD-WS-WB) and on PC-WS/WS-WB.

3.3.4. Structural evaluation of substrates after FBP

Gaussian curve fitting procedure applied to the substrates ATR-FTIR spectra (CD, CD-WS-WB and WS-WB) after production of the fruiting body provided additional quantitative results. The area under the entire band was considered as 100%, and each component after fitting was expressed as a percent area. *Cyclocybe aegerita* was not included in the spectroscopic analyses because its mycelium did not completely colonize the substrate and the FBP was low.

The percentage area of each functional group can be considered representative of structural modification as a consequence of the FBP.

Histograms of the percentage area of each considered band of CD, CD-WS-WB, and WS-WB substrate spectra of untreated and after the FBP of *P. ostreatus* and *P. cornucopiae* are shown in Figure 3.3. The ester in hemicellulose (1740 cm^{-1}) in the untreated CD accounts for 1.4%; while it completely disappeared in the

substrates with *P. cornucopiae,* and at the same time represented 7.1% with *P. ostreatus.*

The band at 1680 cm^{-1} (C=O conjugated ketone stretch) accounted for 7.3% and was only present on untreated CD (Figure 3.4a). The protein content in CD was evaluated by amide I (1648 cm^{-1}) and amide II (1546 cm^{-1}) that accounted for 11.3% and 6.5%, respectively. In the composition of anaerobic digestate, the presence of bioactive substances such as proteins or amino acids was clearly identified (Möller and Müller, 2012). Besides, the variation of the band at 1648 cm^{-1} may be also due to the deformation vibration of adsorbed water (Pandey and Pitman, 2003).

On the contrary, both amide groups increased considerably by 49.8% and 7.5% in the substrate with *P. ostreatus* and 37.4% and 11.3% with *P. cornucopiae*, respectively. In CD substrate, lignin bands (~1580 cm^{-1} and 1508 cm^{-1}) contributed to 20% and 11.5%, respectively. After the FBP of *P. ostreatus* and *P. cornucopiae,* the band at 1508 cm^{-1} disappeared completely, while the band at ~1580 cm^{-1} accounted for 13.5% with *P. ostreatus* and 21.8% with *P. cornucopiae* (Figure 3.3b, c). Variations in lignin peaks would indicate the opening of the lignin reticles through the removal of lignin subunits.

In untreated CD-WS-WB substrate (Figure 3.3d), the CD presence could be recognized from the C=O conjugated ketone (1690 cm^{-1}), amide I (1645 cm^{-1}) and amide II (1550 cm^{1}) bands. All these functional groups were respectively 2.2%, 26.2% and 16.7%. As previously mentioned in the CD substrates, the band at 1690 cm^{-1} disappeared with *P. ostreatus* and *P. cornucopiae* (Figure 3.3e, f). In the substrate with *P. cornucopiae,* the contents of amide I and amide II were respectively 40.8% and 17.9%. The high value of amide I may also be due to the influence of the absorbed water (Pandey and Pitman, 2003). On the other hand, in *P. ostreatus,* amide I decreased by 23%, while amide II was missing. The ester

in hemicellulose (~1730 cm^{-1}) in untreated CD-WS-WB accounted for 4.5%, on the contrary in *P. ostreatus* it increased by 11.4% and it was missing in *P. cornucopiae*. Regarding the lignin in the untreated substrate (~1596 cm^{-1} and 1509 cm^{-1}), it accounted for 4.8 % and 6.0%, respectively.

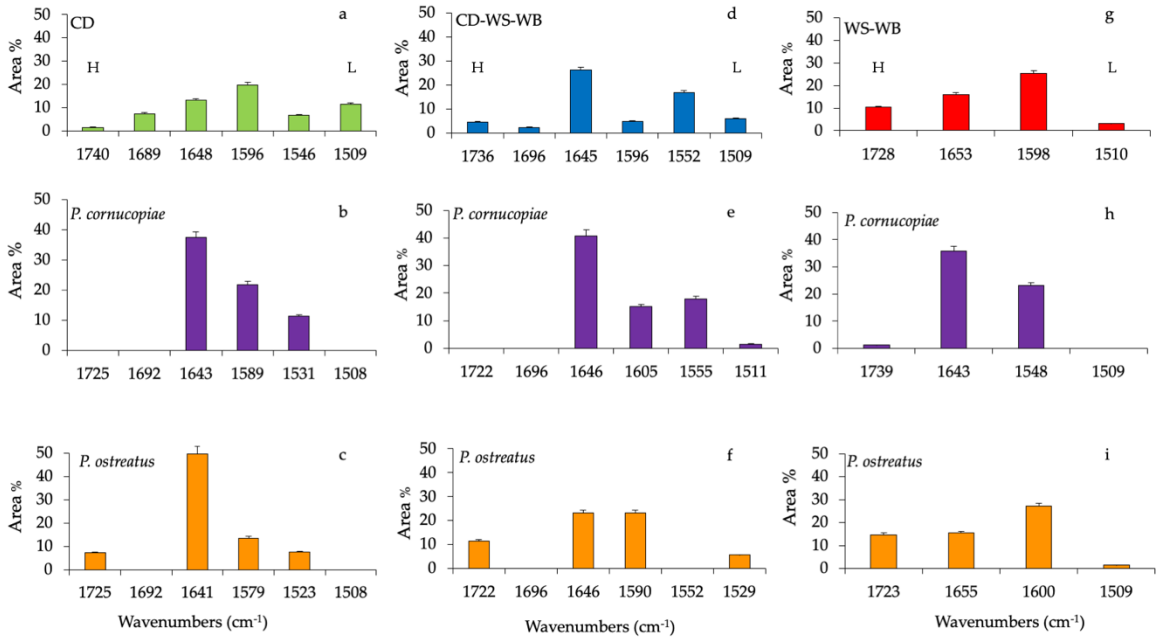

Figure 3.3. Histograms of peak areas (%) processed by using a curve fitting in the region from 1800 to 1200 cm^{-1}. The best-fitting parameters were determined by the minimization of the reduced Chi-square (χ^2) and R^2 that ranging from 0.990 to 0.980. The bar corresponds to the standard error. CD (green), CD-WS-WB (blue) and WS-WB (red) correspond to untreated substrates (top), while in the middle and bottom part there were the substrates after the fruiting body production of *P. cornucopiae* (purple) and *P. ostreatus* (orange). H= hemicellulose; L= lignin [as references for lignin: (Mohebby, 2005; Popescu et al., 2010; Singh et al., 2014)].

As a result of the production of fruiting bodies, lignin components with *P. ostreatus* changed only for the band at 1590 cm^{-1} by 23%, but no variation of the band at 1529 cm^{-1} (5.6%) was observed. In the substrates with *P. cornucopiae*, the band at 1605 cm^{-1} was around 15% and the band at 1511 cm^{-1} was 1.5%. The delignification process in the substrate with *P. ostreatus*, led to an increase in aromatic rings (1590 cm^{-1}) and to the formation of new carbonyl groups in hemicellulose esters (Mohebby, 2005). In the substrates with *P. cornucopiae*,

lignin degradation was associated with the disappearance of the bands at 1509 cm^{-1} arising from the aromatic skeletal vibration of the benzene ring and also that of hemicellulose.

In untreated WS-WB substrate (Figure 3.3g), the ester in hemicellulose was 10.3% and the lignin accounted for 25% and 3%, respectively. After the fruiting body production of *P. cornucopiae* (Figure 3.3h) and *P. ostreatus* (Figure 3.3i), the hemicellulose accounted for 1.3%, and 14.7% respectively. The lignin was 27% (1600 cm^{-1}) and 1.6% (1508 cm^{-1}) with *P. ostreatus* and 23% (1548 cm^{-1}) with *P. cornucopiae.* As already observed in CD-WS-WB substrate, the delignification and degradation process involved the same compounds.

3.4. Discussion

The anaerobic digestate from biogas plants has considerable operational and environmental drawbacks caused by the releasing of GHG (NH_3, CO_2, N_2O) and by the presence of non-digested organic compounds (Gioelli et al., 2011; Menardo et al., 2011; Monlau et al., 2015). The management of digestate with mushrooms that can decay the lignocellulosic component is creating a new scenario in biomass recycling in agriculture (Peng et al., 2020).

In this work, the mycelial growth *in vitro* and the BE of different mushroom species cultivated on CD-based substrates were explored. The structural modifications, as a result of the growth of different mushroom species, were monitored by using ATR-FTIR spectroscopy.

The results of the tests in the Petri dishes (Table 3.3) showed that *P. ostreatus* and *M. importuna* exhibited a higher growth rate on CD than on WS used as a control. Although these species are characterized by varying nutritional needs, the alkaline pH of the digestate has encouraged the growth of *M. importuna* (Q. Li et al., 2017). Furthermore, for *P. ostreatus* the higher nitrogen content in CD

than in WS has contributed to a faster development, as already demonstrated in other studies (Fanadzo et al., 2010; Royse et al., 2004) where a higher yield was obtained with straw that was enriched with nitrogen-rich plant supplements. As already shown by Santi et al. (Santi et al., 2015a), the CD substrate would be suitable for the growth of lignivorous species such as *Pleurotus* spp. compared to digestates obtained from other biomasses.

The changes in substrate compositions in terms of elemental C and N (Table 3.4) after the mycelial growth in Petri dishes have shown an overall increase in the C/N ratio in CD-WS and especially in WS. Similar results were previously obtained in other works after 12 days of mycelial growth (Rajarathnam et al., 1979).

The variations observed in WS may be due to the low C/N ratio of the durum wheat straw used in this trial. However, the biomasses from agro-wastes are characterized by a great variation of N amount and thus of carbon-to-nitrogen (C/N) ratios. A considerable variation in the C/N ratio may also be assumed when the biomass is stored under aerobic conditions, as in our experiment and consequently an undesirable decomposition is expected. It was also reported that residues from crops with a C/N ratio below 30 should lead to a net N mineralization, while residues with a C/N ratio above 30 should promote immobilization (Alexander, 1977).

In most cases, fungi are stimulated to incorporate N into proteins when the C source is lower than the N source. This could explain the significant reduction of N and the variation of amide bands in the FTIR spectra of WS after mycelial growth.

The increase in total C may be explained as a combination of depolymerization of the lignocellulosic component and conversion of the labile C into mycelial biomass. Generally, mushrooms in the early stages of lignin decomposition

degrade it in more labile component and consequently an apparent increase in recalcitrant fraction may be observed (Guo et al., 2018). All these variations are associated to structural alterations as it was observed in our 12 days-study (Guo et al., 2018). The structural variations of the substrates were dependent on the biomass type and mushroom species. After 12 days of mycelial growth, all tested species showed to be able to initiate depolymerization and subsequently decay the lignocellulosic component of CD. For example, in this early stage, *C. aegerita* and *C. comatus* degraded hemicellulose (1740 cm^{-1}) and proteins (1647 cm^{-1} and 1547 cm^{-1}), as demonstrated by the significant decrease in the relative intensity of the bands. Concerning lignin decay (1600 cm^{-1} and 1512 cm^{-1}), *M. importuna* and both *Pleurotus* spp. were more active compared to *C. comatus* and *C. aegerita*. Recent studies carried out on *M. importuna* genome have shown that the laccase-like multicopper oxidase (LMCO) gene was present in the genome and may therefore support the observed effects (Tan et al., 2019).

In the case of the CD-WS, the substrate modifications were very similar to those observed for the CD with the involvement of *C. aegerita* and *C. comatus* for hemicellulose and protein degradation and both *Pleurotus* and *M. importuna* for lignin. As for the WS substrate, all species were able to modify it, in particular, *P. cornucopiae* and *P. ostreatus* which attacked lignin more readily than hemicellulose.

Cultivation trials conducted on *C. aegerita*, *P. cornucopiae* and *P. ostreatus* highlighted the suitability of CD for the cultivation of edible mushrooms. Their BE on CD (19%, 80% and 103.3% respectively) was in line with those previously obtained on other substrates (Isikhuemhen et al., 2009; Royse et al., 2004). *Pleurotus ostreatus* and *P. cornucopiae* showed good BE, proving capable of exploiting digestate based substrates, as shown in previous studies conducted on *Pleurotus* spp. (Brezáni et al., 2019; Isikhuemhen and Mikiashvilli, 2009;

Kataki et al., 2019; Udayasimha and Vijayalakshmi, 2012; Zhou et al., 2019). In particular, *P. ostreatus* grown on CD exhibited a higher FBP (34% more) and BE (9% more) than WS, the most used substrate for its cultivation (Islam and Riaz, 2017; Oei, 2003; Vieira and de Andrade, 2016). The CD allowed to obtain a good FBP of *Pleurotus* without the addition of WB for its high N content (Table 3.4). In fact, WB is commonly added to WS as nitrogen supplement for increasing the production (Stamets, 2000).

Results on spent substrates after the production of the fruiting bodies showed a different decay of lignocellulosic constituents depending on the mushroom species. The most important change was observed for hemicellulose and lignin which were completely decayed in the spent substrate of *P. cornucopiae*. Results showed that *P. cornucopiae* performed an efficient degradation of the lignocellulose component, particularly with only the digestate. Nevertheless, the constant presence of hemicellulose residues in all spent substrates of *P. ostreatus* was unexpected, although an increase in cellulose content after mushroom growth on WS was also reported (Dias et al., 2010; Santi et al., 2015a). Moreover, lignin decomposed in CD and WS-WB spent substrates. That is coherent with the activity of white-rot mushrooms. These mushrooms generate a mixture of ligninolytic enzymes that catalyze the oxidation of aromatic substrates, by producing aromatic radicals and modifying the structure of biomasses that contain lignocellulose and lignin (Udayasimha and Vijayalakshmi, 2012). White-rot mushrooms, carry out delignification through 2 main patterns: non-selective delignification or selective delignification (Martínez et al., 2005). In non-selective delignification, the degradation of lignin, cellulose and hemicellulose occurs simultaneously. Selective delignification, typical of different species of fungi including *Pleurotus* spp., involves the degradation of lignin and hemicellulose before the attack of

cellulose (Boddy et al., 2008; Kubicek, 2012; Martínez et al., 2005). However, the chemical analyses in this study revealed a non-selective delignification for our strain of *P. cornucopiae*.

After lignin removal, spent substrates may be suitable for biogas production as the materials are biologically predigested and are more available for bacterial degradation through anaerobic digestion (Chiu et al., 2000; Mohd Hanafi et al., 2018; Rinker, 2002). Several works have underlined that pre-treating different lignocellulosic biomasses with *Pleurotus* spp. before feeding them into the biogas plant leads to higher biogas production compared to the untreated biomasses with mushrooms (Amirta et al., 2016; Mehta et al., 1990; Mustafa et al., 2016; Tuyen et al., 2013). Additionally, soil fertilization with spent digestate obtained after mushroom growth, produces benefits to the soil microbial communities for the availability of the released nutrients (Brabcová et al., 2016). Consequently, the effect of fungi can be a powerful protective tool against soil fungal diseases (Yusidah and Istifadah, 2018).

The results obtained confirm the possibility to economically utilize the digestate for mushroom cultivation. Moreover, lignin removal by mushroom mycelium improves the degradation of hemicellulose and cellulose, and this is one of the strategies needed to improve its further utilization as fertilizer and opens up the possibility to obtain new bio-based products.

CHAPTER 4

VALORIZATION OF HAZELNUT SHELLS AS GROWING SUBSTRATE FOR EDIBLE AND MEDICINAL MUSHROOMS

From Puliga et al., 2022a

Recently, the cultivation of hazel is undergoing a large expansion. Italy is the world's second largest producer of hazelnuts, with a production of around 98,530 tons in 2019. The processing of hazelnuts produces large amounts of waste, especially woody pericarps, due to the cracking process, generally used for domestic heating, causing air pollution. The high lignin content present in the pericarps makes them a suitable substrate for the cultivation of edible and medicinal mushrooms. To this aim, *G. lucidum*, *L. edodes,* and *P. cornucopiae* were grown and cultivated on different hazelnut-shell-based substrates: HS, HS-WS, and WS mixed with Beech Chips (BC) as control. In vitro mycelial grow rate, the degradation capacity of the lignocellulosic fraction, the BE, and the qualitative differences between mushrooms growing on different substrates by using ATR-FTIR spectroscopy were investigated. Our results suggested the ability of *G. lucidum*, *L. edodes,* and *P. cornucopiae* to grow and decay the lignocellulosic fraction of HS. Cultivation trials showed a similar BE but a different FBP in the presence of HS with respect

to the control. ATR-FTIR analysis provided a chemical insight for the examined fruiting bodies, and differences were found among the substrates studied. These results provide attractive perspectives both for more sustainable management and for the improvement of mushroom cultivation efficiency.

4.1. Introduction

The hazel, *Corylus avellana* L., is the world's leading nut crop with a production of 1,125,178 tons in 2019 (FAOSTAT, 2019). Turkey, Italy, and Azerbaijan are the three lay producers with a production of 776,046; 98,530 and 53,793 tons, respectively (FAOSTAT, 2019). Ninety percent of the hazelnuts produced are intended for processing (Król and Gantner, 2020), deprived of the woody pericarp, and used in chocolate, pastry, confectionery, as well as in the preparation of numerous foods and liqueurs (Król et al., 2021; Silvestri et al., 2021).

One of the main concerns associated with hazelnut production is due the large amount of by-products. Hazelnuts are mechanically collected by compact harvesters in-shell covered by husks that are mechanically separated during harvesting. In-shell nuts need to be opened in order to be introduced into the industrial food chain. The woody biomass produced as a result of the cracking process accounts for more than 50% of the total nut weight (Rivas et al., 2020). Lignin, present in a percentage between 40% and 50%, is the main constituent of the HS, followed by hemicellulose and cellulose present in percentages between 13–32 and 16–27 percent, respectively (Hoşgün and Bozan, 2020; Pérez-Armada et al., 2019; Rivas et al., 2020).

In recent years, there has been marked attention to climate change, the preservation of species biodiversity, environmental sustainability by sustainable and environmentally friendly use, and the recycling of waste in line with the circular economy approach. Consequently, the scientific community is encouraged to seek new methods and strategies for exploiting the by-products of agricultural activities.

Traditionally, HS are mainly used as a boiler fuel for domestic heating causing air pollution (Arslan et al., 2012; Guney, 2013; Özçelik and Pekşen, 2007) and for

landscaping (Uzuner et al., 2017). Several studies have been conducted in order to enhance and valorize this waste by-product with the aim to obtain new materials, chemical compounds, and bioactive ingredients. In particular, HS were found to be suitable for the production of particleboard and Medium Density Fiberboard (MDF) (Barbu et al., 2020; Çöpür et al., 2008), activated carbons capable of adsorbing and removing different heavy metals and CO_2 (Cimino et al., 2000; Demirbaş, 2003; Demirbas et al., 2009; Kazemipour et al., 2008; Kobya et al., 2002; Lewicka, 2017; Pehlivan et al., 2009; Şencan et al., 2015; Sert et al., 2017), antioxidant phenolics (Contini et al., 2008; Esposito et al., 2017; Pérez-Armada et al., 2019; Yuan et al., 2018b, 2018a), fermentable sugars and xylooligosaccharides (Surek and Buyukkileci, 2017; Uzuner et al., 2017), hydrogen production (Midilli et al., 2001, 2000), ethanol (Hoşgün et al., 2017) and some prebiotic compounds (Fuso et al., 2021).

Mushrooms are considered an important source of food and biologically active compounds with several medicinal proprieties (Badalyan and Zambonelli, 2022). Various lignocellulolytic mushrooms such as oyster mushrooms, shiitake, and *Ganoderma* sp. are cultivated on different pasteurized or sterilized lignocellulosic substrates. While oyster mushroom (*Pleurotus* spp.) and shiitake (*Lentinula edodes* (Berk.) Pegler) are cultivated worldwide for their culinary qualities (Royse et al., 2017; Vedder and Van den Munckhof-Vedder, 2020), *G. lucidum* sensu latu is the most important medicinal mushroom, and it is specifically cultivated for its pharmacological activities (L. Wang et al., 2020). Moreover, mushrooms can be cultivated on several agricultural wastes, which can be sustainably recycled in the principles of circular economy (Di Piazza et al., 2021).

Some previous works report the possibility of using the hazelnut husk and hazelnut leaves as basal ingredients for substrate preparation in *L. edodes* and

Pleurotus cultivation (Özçelik and Pekşen, 2007; Pekşen and Küçükomuzlu, 2004; Yildiz et al., 2002), but no reference was found by the authors regarding the use of HS as substrate for mushroom cultivation. Due to the high lignin content, this by-product can be used as a substrate for the cultivation of lignocellulolytic mushrooms.

FTIR is widely used for the rapid and non-destructive characterization of the macromolecule structures (lipids, proteins, nucleic acids, and polysaccharides) (Coates, 2006). More specifically, amongst the various techniques used, ATR is viewed as very advantageous as it does not require any sample preparation prior to spectral analysis. In ATR measurements, the depth of penetration of the IR radiation into the sample is independent of the sample thickness. Consequently, by layering the solid sample directly on the micro diamond crystal, structural information at different parts of the sample may be gained. Specifically, it was used to identify species and geographic origin of *Boletus* sp. mushrooms (Y. Li et al., 2017) or quantify the total polysaccharide content in *Ganoderma* mycelia (Li et al., 2020), as well as glucans and ergosterol content in *Pleurotus* (Bekiaris et al., 2020b). In an earlier study, it was also used to show how physical harm had an effect on tissue structure and the aging process (O'Gorman et al., 2010). The most intriguing application of this technique is currently the degradation processes of various agricultural waste for mushroom cultivation (Bekiaris et al., 2020a; Fornito et al., 2020).

To this aim, *G. lucidum*, *L. edodes*, and *P. cornucopiae* were grown on HS substrates in order to evaluate their potential as alternative growth substrates. In order to accomplish this objective, mycelia growth rate and BE were studied. Additionally, micro-ATR-FTIR was applied to explore the substrate breakdown and the composition of the fruiting bodies.

4.2. Materials and Methods

4.2.1. Substrates

The HS were provided by an organic farm located in Carrù (Cuneo, Piedmont, Italy). WS and *Fagus* sp. L. chips (BC) were kindly provided by the Cadriano farm of the University of Bologna. WS and BC were crushed into fragments smaller than 0.5 cm; HS was crushed with a cutting mill (Retsch, SM 100) and autoclaved at 121 ± 1°C for 60 minutes to prevent any contamination during storage. The dried raw materials were stored at 22 ± 1°C.

4.2.2. Mushrooms Cultures and Mycelial Growth Rate Evaluation

Experimental trials were carried out by using three species of basidiomycetes (belonging to Basidiomycota division) mushrooms: *G. lucidum*, *L. edodes*, and *P. cornucopiae*.

Ganoderma lucidum (strain Glu16) and *P. cornucopiae* (strain Pco3) were isolated from fruiting bodies collected in the wild; *L. edodes* strain (LEd5) was brought by the Fungal Institute of Jinxiang (Shandong province, China).

The mycelial pure cultures were stored in the Mycological and Applied Botany Laboratory of the DISTAL at the University of Bologna (Bologna, Italy). The isolates were kept at 22 ± 1°C in darkness on PDA (Difco) half strength and subcultured every two months.

For mycelial growth area evaluation, plugs of 10 mm diameter were taken by 15-days-old colonies of each species and inoculated in the center of 9 cm sterilized Petri dish filled with 30 g of three different substrates previously soaked for 24 hours with distilled water and brought to 70% humidity: HS; WS 50%-HS 50% and WS as control. Five replicates were made for each combination of species and substrate. All plates were incubated at 22 ± 1°C in

darkness. The fungal growth was assessed by measuring the diameter of the colony along two preset diametrical lines every day.

The area (cm^2) covered daily by the mycelium was calculated assuming an elliptical shape as reported by Tryfinopoulou et al. (2020) using the following formula:

$$A = \pi \times R_1 \times R_2$$

where A is the fungal colony area (cm^2) and R_1 and R_2 are the two perpendicular radii, respectively.

The area growth rate of the mycelium (AGR) was calculated with the formula of Sinclair and Cantero (1989) modified as follows:

$$AGR = \frac{A_f - A_i}{T_f - T_i}$$

where AGR is the growth rate ($cm^2\ day^{-1}$); A_f is the final growth area (cm^2); A_i is the initial growth area (cm^2) and T_f is the final growth time (days); T_i is the initial growth time (days).

4.2.3. Mushrooms Cultivation Trials

Spawn production occurs in inoculated glass tubes containing 30 g of sorghum kernels and distilled water in a 1:2 (*v*/*v*) ratio, previously sterilized at 121 ± 1°C for 20 minutes, with two 15-days-old mycelial plugs of 1 cm diameter. Five replicates were prepared for each species-substrate combination. The tubes were incubated in the dark at 22 ± 1°C for 30 days with the aim to obtain the complete colonization of the kernels.

Two different HS-based substrates were used as reported in Table 4.1; a substrate composed of WS 50% and BC 50% was used as a control. Homogeneous substrate mixtures were prepared by mixing component materials based on their dry weight (*w*/*w*).

Table 4.1. Composition and ratios of the substrates used in cultivation trials.

Substrates and Mixing Ratio	Code	Average Dry Weight (g)
Wheat Straw 50%-Beech Chips 50% (control)	WS-BC	400
Wheat Straw 50%-Hazelnut Shells 50%	WS-HS	900
Hazelnut Shells 100%	HS	1500

The substrates were inserted into autoclavable PP transparent bags (20 × 30 cm). Dried mixed substrates were moistened with 1 L (per bag) of distilled water for 24 hours and the excess of water was removed by squeezing the bags.

Bags were closed with a PP plastic cap with a filter, autoclaved at 121 ± 1°C for 60 minutes; inoculated with grain spawn by opening the bag, inserting the inoculum inside it (1 tube per bag), mixing the inoculum with the substrate, and incubated in the darkness at 22 ± 1°C until the complete colonization of the substrate. For each species-substrate combination, five bags were prepared.

After 1 or 2 months of mycelial growth, depending on the substrate (one month on WS and WS-BC and around 2 months on HS), bags were moved to a climatic chamber with different climatic conditions (Table 4.2) according to their biological needs (Oei, 2016).

Table 4.2. Cultivation parameters used in the trials.

	Species		
	Ganoderma lucidum	***Lentinula edodes***	***Pleurotus cornucopiae***
Temperature (°C)	22–30	10–20	18–25
Light intensity (lux)	500–1000	500–1000	500–1000
Relative Humidity (%)	85–95	60–95	80–95

Lentinula edodes fruiting body were collected only when the cap radius reached 5 cm in diameter (Zhang et al., 2020). *Ganoderma lucidum* and *P. cornucopiae* were collected when the cap was completely developed. The duration of the harvest periods, starting from the appearance of the first primordia, was two months

for *L. edodes* and *P. cornucopiae* and 3 months for *G. lucidum*. All fruiting bodies were freshly weighted, dried in a stove at 40°C for 24 hours, and their dried weight was recorded. BE was calculated according to Chang et al. (1981).

4.2.4. Micro ATR-FTIR Spectroscopy Analysis

A Bruker Tensor FTIR instrument (Bruker Optics, Ettlingen, Germany) equipped with an accessory for analysis in ATR was used. The sampling device contained a micro- diamond crystal, single reflection with an angle of incidence of 45° (Specac Quest ATR, Specac Ltd., Orpington, Kent, UK). Spectra were recorded from 4000 to 400 cm^{-1}, with a spectral resolution of 4 cm^{-1} and 64 scans. Background spectra were also taken against air under the same conditions before each sample.

The substrates from in vitro test were analyzed after 30 days of mycelial growth, as previously described by Fornito et al. (2020). Parts of dried fruiting bodies (cap, hymenophore, and stipe) grown on the HS and WS-BC of each species were placed on the diamond crystal, and pressure was applied with a compression clamp. The resulting spectra of each type of sample were averaged. Isopropyl alcohol was used to clean the diamond crystal before each recording.

4.2.5. Statistical Analyses

Statistical analyses were performed using the RStudio graphical interface for the R software environment v.4.0.2 (R Foundation, Vienna, Austria) with the packages agricolae, ggplot2, Hmisc, and mice. The analysis of variance (ANOVA) and Kruskal-Wallis test were used to determine the significant difference of AGR, FBP (expressed as dry weight of mushrooms collected during the harvesting period), and BE among different substrates. Tukey post hoc test ($p \leq 0.05$) was used to compare the means.

4.3. Results

4.3.1. In Vitro Mycelial Growth and ATR-FTIR of Substrates

Figure 4.1 shows the in vitro mycelial growth of the tested fungi in the three different substrates. Only *P. cornucopiae* showed a significantly higher mycelial growth rate on WS (Figure 4.1e, f). The growth of *G. lucidum*, *L. edodes*, and *P. cornucopiae* was significantly lower on HS with respect to the other substrates (Figure 4.1a, c, e). Statistical differences were found between the area growth rate of *G. lucidum* and *L. edodes* grown on HS respect to WS and WS-HS (Figure 4.1b, d).

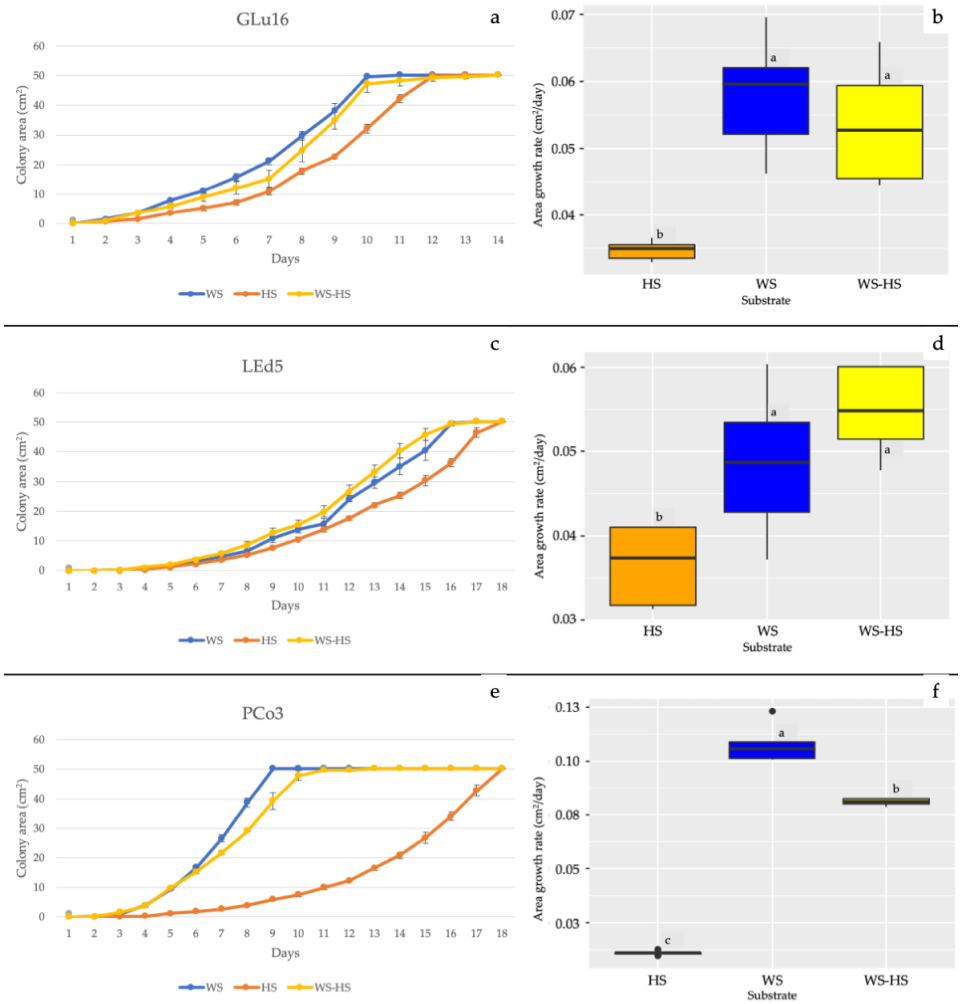

Figure 4.1. Growth and AGR of (a,b) *G. lucidum*, (c,d) *L. edodes*, and (e,f) *P. cornucopiae* in Petri dishes on WS (blue), HS (orange), and WS-HS (yellow). Different letters indicate significant differences at $p \leq 0.05$.

In the fingerprint region (1800–600 cm^{-1}) of the substrate spectra, WS and HS, and after 30 days of mycelial growth, consistent structural variation for both substrates were found for *G. lucidum*, *L. edodes,* and *P. cornucopiae* (Figure 4.2a, b). In the WS spectrum (blue line) (Figure 4.2a), the bands at 1735 cm^{-1}, due to unconjugated C=O, and at 1460 cm^{-1} (C–H deformation), correspond to those of xylan (hemicellulose) or the heterocyclic cellulosic rings (Rahman et al., 2017). The peak at 1623 cm^{-1} may be assigned to carboxylates in aromatic rings. The shoulder at 1517 cm^{-1} was attributed to the aromatic skeletal vibrations (C=C) and aromatic breathing in lignin, respectively (Mohebby, 2005; Popescu et al., 2010; Singh et al., 2014). The bands at 1423 cm^{-1} and 1322 cm^{-1} were assigned to C–H_2 bending at C-6 of the crystalline cellulose (Huang et al., 2012), and that at 1370 cm^{-1} was due to CH_2 bending vibrations in cellulose and hemicellulose. The region between 1100 and 950 cm^{-1} corresponded to that of cellulose and hemicelluloses. The most intense bands centered at 1031 cm^{-1} were assigned to the C–O–C stretching of primary alcohol in cellulose and hemicellulose (Bekiaris et al., 2015). The weak shoulder at 898 cm^{-1} was associated with C1–O–C β-(1–4)-glycosidic linkage in cellulose. The other bands at approximately 700 cm^{-1} and 600 cm^{-1} were assigned to the C–OH bending (De Rosa et al., 2010; Pandey and Pitman, 2003).

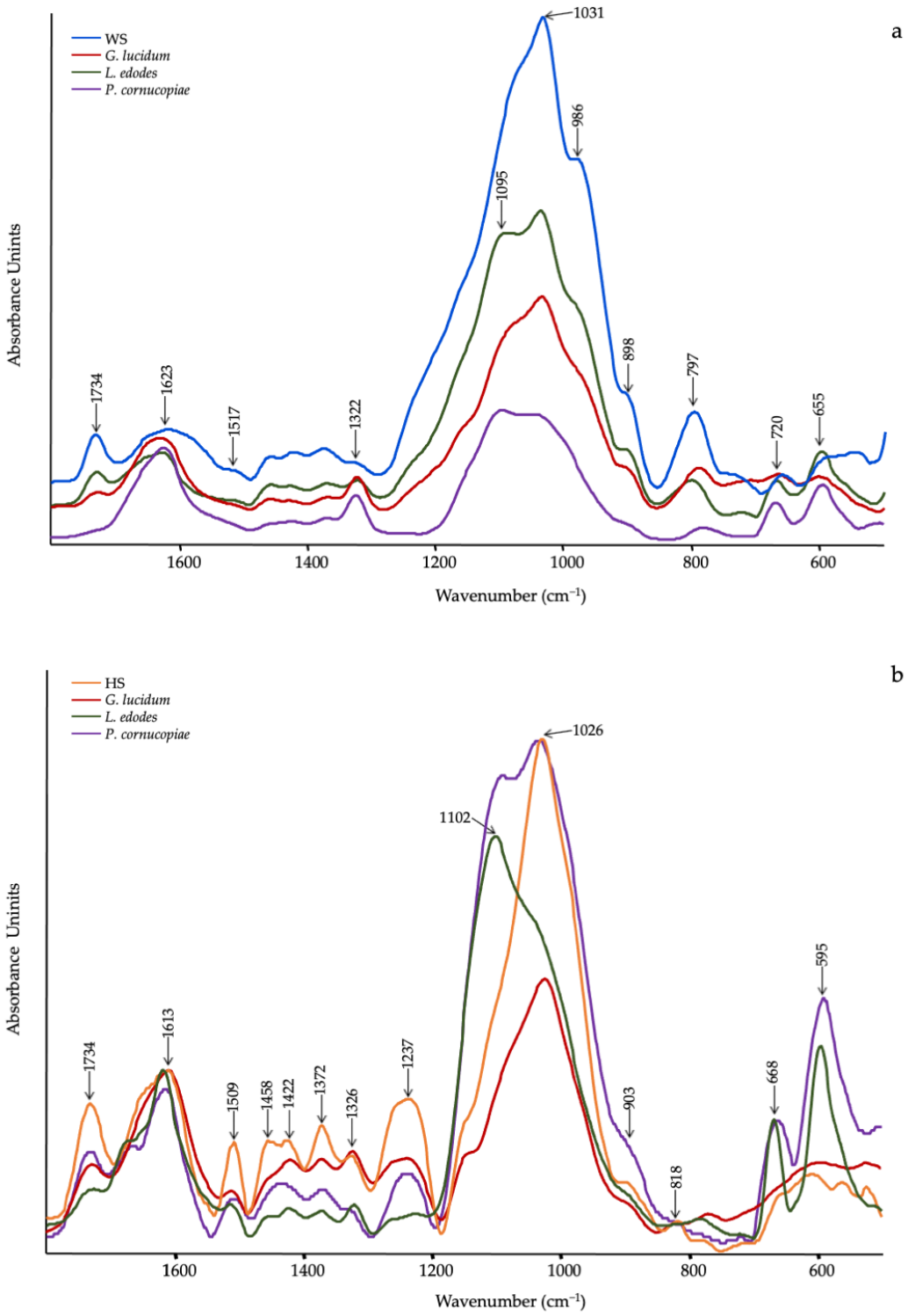

Figure 4.2. ATR-FTIR spectra of (a) WS (blue line) and (b) HS (orange line) after 30 days of mycelial growth of *G. lucidum* (red line), *L. edodes* (green line) and *Pleurotus cornucopiae* (purple line).

After 30 days of mycelial growth, a considerable structural modification was observed. In particular, the progressive decrease of xylan in hemicellulose (1735 cm^{-1} and 1460 cm^{-1}) in *L. edodes* and *G. lucidum* and the total disappearing in *P. cornucopiae* was observed in the spectra (Figure 4.2a).

Lignin decay may be ascertained in the decreased intensity of absorption bands at around 1623 cm^{-1}, appearing more significant in *P. cornucopiae*. Conversely, the band at 1322 cm^{-1} (Figure 4.2a) increased in *G. lucidum* and *P. cornucopiae*. More significant variations were also observed in the glycosidic C–O–C band (1100–950 cm^{-1}), showing an alteration of the linkage C1–O–C β-(1–4)-sugar of the polymeric cellulose in the following order: *P. cornucopiae* > *G. lucidum* > *L. edodes*, probably as a result of cellulose degradation processes. As shown in Figure 4.2b, the HS spectrum (orange line) displayed a number of adsorption peaks, indicating the complex nature of the material examined (Pandey and Pitman, 2003). More precisely, the peak centered at 1734 cm^{-1} could be ascribed to acetyl and uronic ester groups in hemicellulose and ρ-coumaric acids in lignin (Li et al., 2020). The bands at 1613 cm^{-1} and 1509 cm^{-1} corresponded to the aromatic skeletal vibration in lignin (Rahman et al., 2017) as well as the bands at 1458 cm^{-1}. In addition, the bands at 1422 cm^{-1} were derived from C–H bending in lignin. The cellulose and hemicellulose bands appeared at 1372 cm^{-1} and 1326 cm^{-1} (C–H bending). Nevertheless, the last band also may be assigned to C–O vibration in syringyl derivatives as well as the band at approximately 1237 cm^{-1}, due to syringyl ring and C–O stretching in lignin and xylan (Pandey and Pitman, 2003). The most intense region from 1100 to 900 cm^{-1} was attributed to C–O and C–O–C stretching in cellulose and hemicellulose. Spectra after mycelia growth showed a progressive reduction in the relative intensity of the aromatic rings (1509 cm^{-1}, 1326 cm^{-1}, and 1237 cm^{-1}) in this order: *L. edodes* > *G. lucidum* > *P. cornucopiae*. Likewise, the gradual decrease in the peak at 1734 cm^{-1} might be

related to the presence of ϱ-coumaric acids from the lignin rather than the hemicellulose. In the region corresponding to cellulose and hemicelluloses (1100 to 900 cm^{-1}), a significant increase in C–O (1102 cm^{-1}) group in *P. cornucopiae* and *L. edodes* was detected. On the contrary, the C–O–C group decreased in *G. lucidum* and *L. edodes* (Figure 4.2b).

4.3.2. Fruiting Body Production

In Figure 4.3, the FBP and the BE of all the tested fungi in different substrates are reported. The FBP of *L. edodes* was significantly higher on HS than on the other tested substrates (Figure 4.3c). The *P. cornucopiae* FBP on HS was significantly higher than on WS-BC but had similar production as on WS-HS (Figure 4.3e). In contrast, the FBP of *G. lucidum* was significantly lower in HS than WS-BC but similar to FBP on WS- HS (Figure 4.3a). Regarding the biological efficiency, all the tested fungi showed a higher BE on WS-BC with respect to the other substrates (Figure 4.3b, d, f).

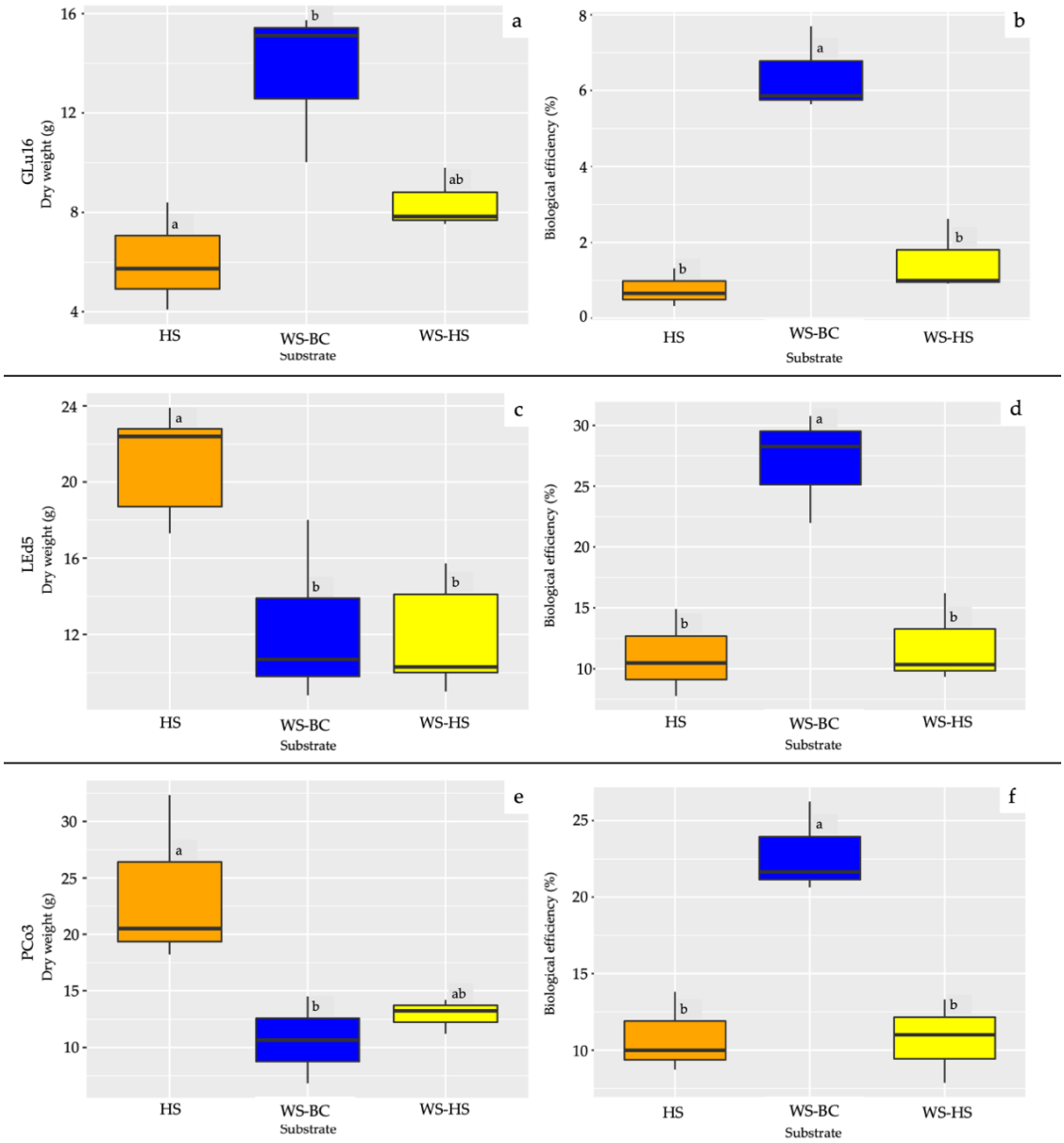

Figure 4.3. FBP and BE of (**a**,**b**) *Ganoderma lucidum*; (**c**,**d**) *Lentinula edodes*, and (**e**,**f**) *Pleurotus cornucopiae* grown on HS (orange), WS-BC (blue), and WS-HS (yellow). Different letters indicate significant differences at $p \leq 0.05$.

4.3.3. Qualitative Evaluation of Mushrooms by ATR-FTIR

The spectra of the fruiting bodies of *G. lucidum*, *L. edodes*, and *P. cornucopiae* produced on different growing media (HS and WS-BC) are shown in Figure 4.4.

As no spectral difference from 1800 cm^{-1} to 800 cm^{-1} was detected between the cap, the gills, and the stipe in either *L. edodes* or *P. cornucopiae*, the spectra were averaged (Figure 4.4a, b). Conversely, in the *G. lucidum* spectra, a significant spectral variation was observed between the cap and the hymenophore (Figure 4.4c, d). The characteristic bands of the main functional groups are listed in Table 4.3.

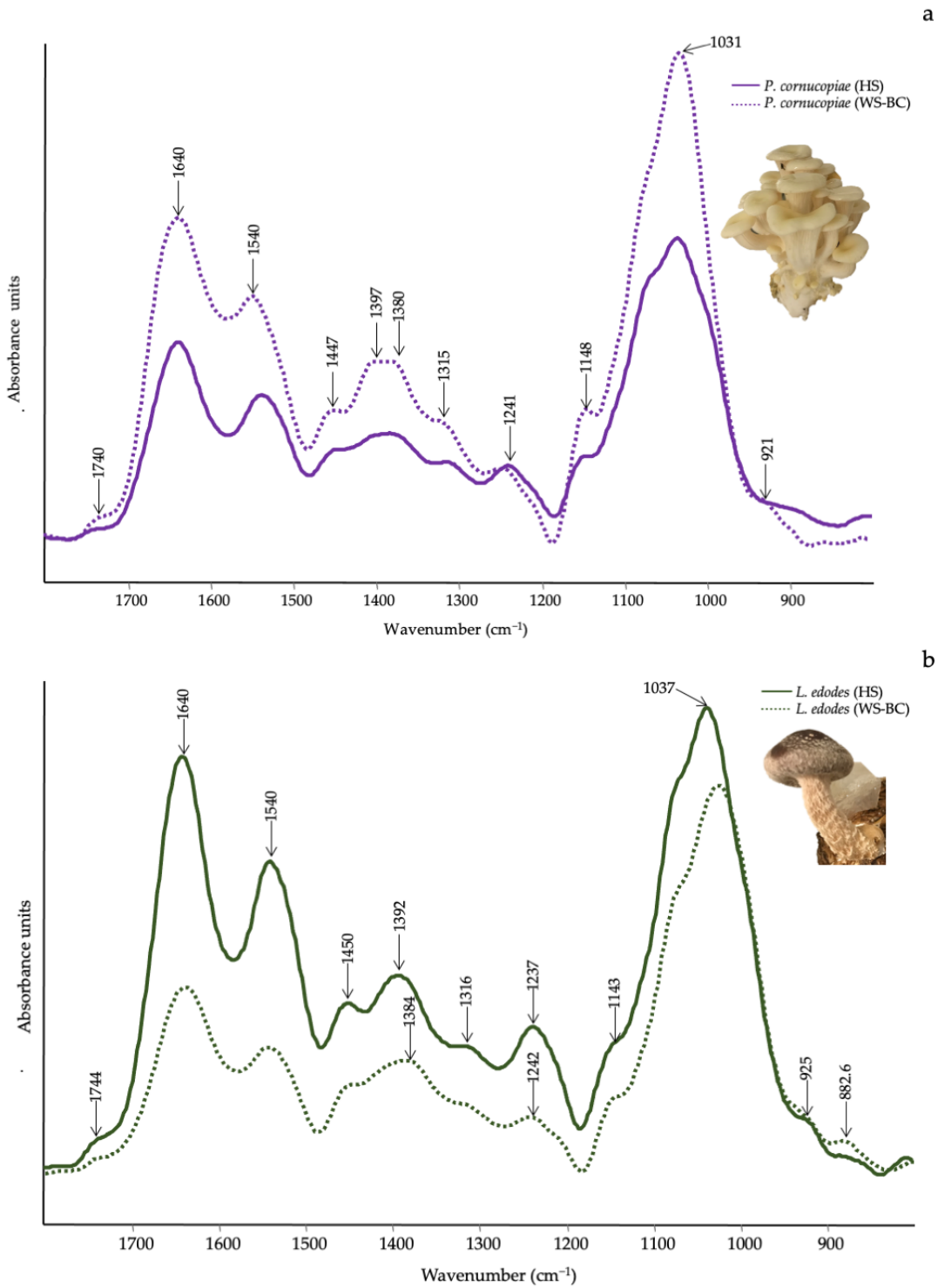
a
1031
P. cornucopiae (HS)
P. cornucopiae (WS-BC)
1640
1540
1447
1397
1380
1315
1241
1148
1740
921
Absorbance units
1700
1600
1500
1400
1300
1200
1100
1000
900
Wavenumber (cm⁻¹)
b
1037
L. edodes (HS)
L. edodes (WS-BC)
1640
1540
1450
1392
1316
1237
1143
1744
1384
1242
925
882.6
Absorbance units
1700
1600
1500
1400
1300
1200
1100
1000
900
Wavenumber (cm⁻¹)

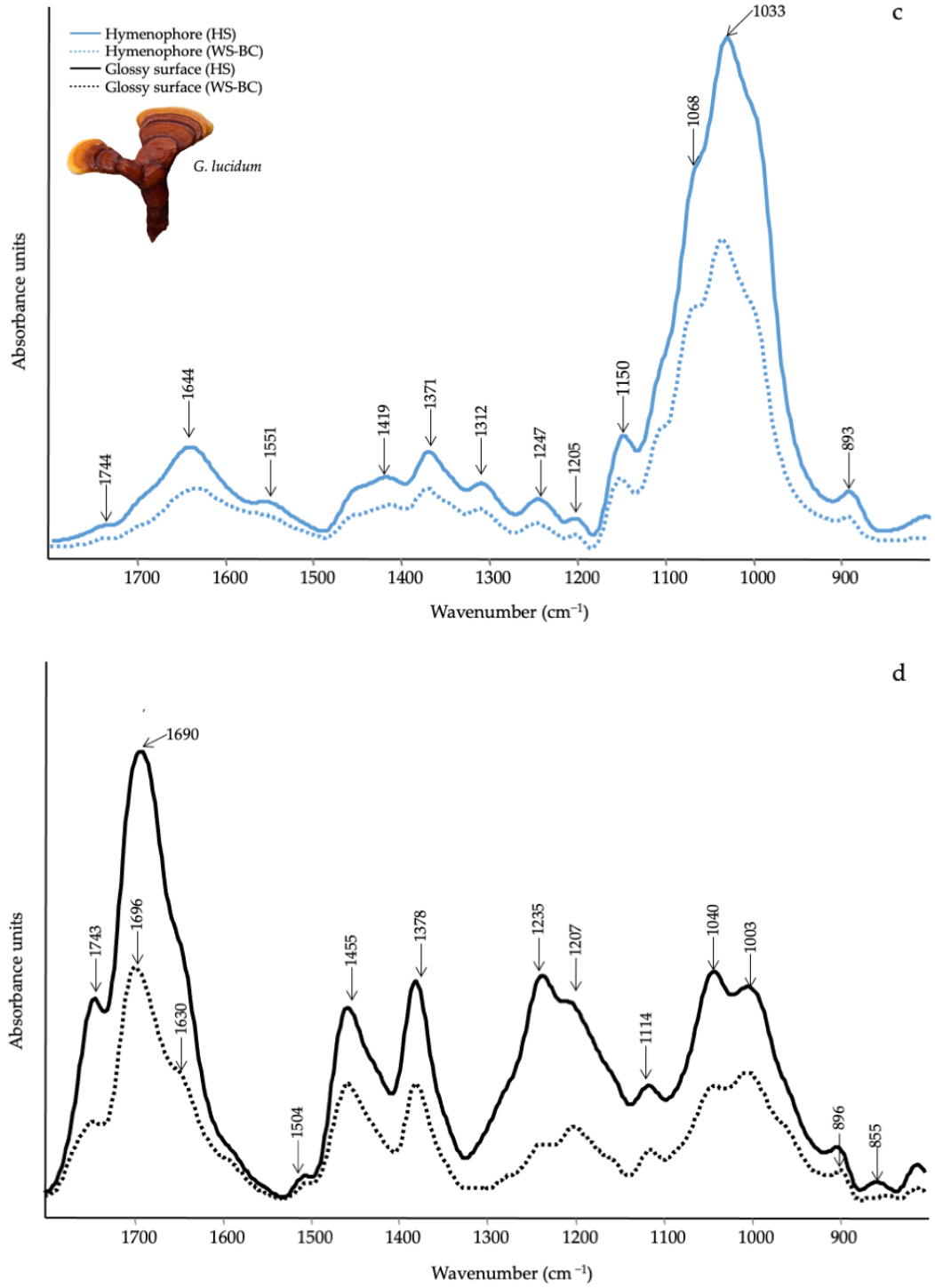

Figure 4.4. ATR-FTIR spectra of the fruiting bodies of (**a**) *P. cornucopiae* cultivated on WS-BC (dotted purple line) and HS (solid purple line); (**b**) *L. edodes* cultivated on WS-BC (dotted green line) and HS (solid green line); (**c**) *G. lucidum* hymenophore on WS-BC (dotted cyan line) and HS (solid cyan line); (**d**) *G. lucidum* glossy surface on WS-BC (dotted black line) and HS (solid black line).

Table 4.3. Attributions of the main characteristic FT-IR bands in the spectra of *G. lucidum*, *L. edodes* and *P. cornucopiae* fruiting bodies according to the literature.

Wavenumber (cm^{-1})	Functional Groups Attributions	Reference
1745–1738	C=O stretching of lipids	(Zervakis et al., 2012)
1696–1690	CHO stretching in aromatic	(Choong et al., 2011)
1640–1638	Amide I, water	(Zervakis et al., 2012)
1540–1548	Amide II	(Zervakis et al., 2012)
1507	Aromatic ring	(Choong et al., 2011)
1455	CH_2 bending in polysaccharides	(Coates, 2006)
1400–1378	C–H in-plane bending vibration	(Mohaček-Grošev et al., 2001)
1245–1235	Amide III and C–O stretching	(Li et al., 2020)
1150–1157	C–O–C asymmetric stretching of glycosidic linkage	(O'Gorman et al., 2010)
1040–1025	stretching vibration of C–O–C group	(O'Gorman et al., 2010)
930–882	Glucan band β anomer; C–H deformation	(Das et al., 2020)
807–796	α (1–6) linked backbone with α (1–3); CH out-of plane bending	(Das et al., 2020)

In the spectra of *P. cornucopiae* and *L. edodes* (Figure 4.4a,b) are well identifiable the Amide I (~1640 cm^{-1}), Amide II (~1540 cm^{-1}) and Amide III (~1240 cm^{-1}) bands of proteins (Zervakis et al., 2012). Another characteristic is valuable in the region of polysaccharides vibrations between 1150–796 cm^{-1} (Table 4.3). More specifically, the bands at about 807 cm^{-1} and 930 cm^{-1} are corroborating for mannan [α (1-6) linked backbone with α (1-3) and α (1-2) linked branches] a type of glucan that is one component of fungal cell walls and chitin (N-acetylglucosamine based polymer), respectively (Das et al., 2020). A weak shoulder at around 1740 cm^{-1} indicated the presence of cell membrane phospholipids (Zervakis et al., 2012). *Pleurotus cornucopiae* grown on WS-BC and HS (Figure 4.4a) showed a similar spectral profile, although an increase in the relative intensity of the bands was seen in presence of WS-BC and more specifically, in the polysaccharide region. At the opposite, the spectra of *L.*

edodes grown on HS consistently showed an increase in the relative intensity of all bands as compared to the WS-BC substrate (Figure 4.4b). However, no relevant structural variation was observed.

Referring to the spectra of *G. lucidum* grown on HS and WS-BC, a different spectral profile was detected both in the external and inner parts of the fruiting body and in the different substrate (Figure 4.4c, d). The glossy surface part of both cap and stipe were characterized by esterified carboxyl groups in lipids at 1745 cm^{-1} and 1235 cm^{-1}, respectively. These bands may also be coupled to vibrations at 1455 cm^{-1} and 1378 cm−1 in C–H bending of aliphatic compounds. The band at 1690 cm^{-1}, 1630 cm^{-1}, and 1504 cm^{-1} were due to aromatic rings vibrations (Choong et al., 2011). The region from 1100 to 896 cm^{-1} belonged to the vibration of C–C–O or C–C–OH in polysaccharides (Table 4.3). In the inner part of the fruiting body and hymenophore, the lipid functional groups (1744 cm^{-1}, 1450 cm^{-1}, 1371 cm^{-1} and 1247 cm^{-1}) become weaker (Figure 4.4c) than those observed in the surface. Instead, the bands of amide I, (1644 cm^{-1}) and amide II (1551 cm^{-1}) were visible. The spectra were also dominated by the intense bands assigned to polysaccharides from 1150 to 893 cm^{-1}. By comparing the spectra of *G. lucidum* grown on HS and WS-BC, the main variations occurred in the polysaccharide region, which appeared more intense in HS than in WS-BC.

4.4. Discussion

The circular economy in the agro-wastes management sector requires reusing these materials as a feedstock in a variety of production cycles. In this context, the high production of hazelnuts has led to a significant accumulation of wood residues frequently involved in manufacturing processes, potentially impacting the environment.

In this work, we explored the potential of HS as a growing substrate for the cultivation of edible and medicinal mushrooms.

Preliminary results in Petri dishes indicated that all the three tested species were able to grow on HS (Figure 4.1), which was never used for mushroom cultivation.

It is well known that the C/N ratio is one of the most important parameters for mushroom growth and cultivation (Melanouri et al., 2022). The C/N ratio of HS ranged from 43.4 to 58 (Kaya et al., 2018; Kumla et al., 2020b; Şenol, 2019); this C/N ratio is optimal for *L. edodes* and *P. cornucopiae* and sub-optimal for *G. lucidum.* In fact, the optimal C/N ratio for *L. edodes* and *P. cornucopiae* ranges from 30–35 and 45–55, respectively, whereas *G. lucidum* development is favored by C/N ratios between 70 and 80 (Kumla et al., 2020; Oei, 2016).

All the tested species are considered white-rot fungi naturally found on hardwood (Stamets, 2000). However, *G. lucidum*, *L. edodes,* and *P. cornucopiae* showed a different behavior on the tested substrates. *Pleurotus cornucopiae* grow better on WS and WS-HS with respect to HS (Figure 4.1e,f), this different behavior could be due to the different lignin percentage in HS (ranging from 40 to 50%) (Hoşgün and Bozan, 2020; Pérez-Armada et al., 2019; Rivas et al., 2020) with respect to WS (15%) (Del Río et al., 2013; Tamaki and Mazza, 2011) and the greater presence of soluble sugars and nutrients present in WS. In fact, *P. cornucopiae* on WS and WS-HS rapidly covered the surface of the plate and then degraded its cellulose and available hemicellulose. In contrast, in HS substrate, lesser soluble nutrients were released, and lesser cellulose and hemicellulose were available without previous degradation of lignin. Moreover, *P. cornucopiae* is typically found on poplar wood which contains a percentage of lignin ranging from 16 to 21% (Pettersen, 1984). On the other hand, *G. lucidum* and *L. edodes* are commonly found on oaks and on chestnut trees, whose lignin content

ranging from 18–30% in oak wood to 26% in chestnut wood (Le Floch et al., 2015; Vinciguerra et al., 2011).

The efficiency of mycelial growth on different substrates may be related to the structural modification detected in the spectra (Figure 4.2a, b). Since the lignocellulose is the major component of any substrate, the changes observed in the spectra presumed a synergistic action of several enzymes (Kumla et al., 2020; Madeira et al., 2017). As expected, the mycelial growth of *P. cornucopiae* in WS-BC resulted in a change in the acetyl and uronic ester groups of hemicellulose (1734 cm^{-1}) and in those bound to the C1–O–C β-(1-4)-sugar bond of cellulose. Based on these structural changes, we can surmise that enzymatic hydrolysis led to a total degradation of β-(1,4) glycosidic bonds with the missing band at 898 cm^{-1} and the production of new simple molecules, most likely as sugar acids (Figure 4.2a). Substrate degradation activity by *G. lucidum* and *L. edodes* did not lead to significant structural changes in WS-BC, even though in *G. lucidum* is visible light degradative activity of acetyl and uronic ester groups of hemicellulose (1734 cm^{-1}).

As previously reported, the higher mycelia growth capacity of *G. lucidum* and *L. edodes* on HS could be related with the high lignin, cellulose, and hemicellulose contents. Specifically, *G. lucidum* caused a modification of the HS substrate with reduction of the acetyl and uronic ester groups of hemicellulose (1734 cm^{-1}) and of those linked to the C1–O–C β-(1-4)-sugar bond of cellulose. In addition, the typical lignin aromatic ring (1509 cm^{-1}) showed consistent degradation that, coupled with the gradual decrease of the peak at 1734 cm^{-1} related to ϱ-coumaric acids rather than to hemicellulose, suggests that lignin degradation is the first level of lignocellulose degradation in order that cellulose and hemicellulose accessibility is more feasible (Jurak et al., 2015). With *L. edodes* and *P. cornucopiae,* the alterations were mainly related to the region of cellulose

and hemicelluloses (1100 to 900 cm^{-1}). The increase in these bands may indicate that a variety of hydrolytic enzymes could be released during fungal attacks specifically to modify and break the bonds of the lignin and hemicellulose; the chemical changes in these compounds signal that the fungus could take them as carbon sources.

After in vitro preliminary tests, cultivation trials conducted on *G. lucidum*, *L. edodes,* and *P. cornucopiae* showed a BE on HS (0.8, 11.0, and 10.8%, respectively) lower than those obtained on WS-BC (6.4, 21.9, and 22.9%, respectively), but the biological efficiency on WS-BC are in line with those previously obtained by other authors (Ćilerdžić et al., 2018; Kalmiş and Sargin, 2004; Nandni and Mishra, 2018). The lower BE on HS could be attributed to the higher dry weight of the substrate used to fill each bag. *Lentinula edodes* and *P. cornucopiae* showed a good FBP, proving capable of exploiting HS-based substrates, although the growth of *P. cornucopiae* in vitro was slower than WS and WS-HS. In contrast, *G. lucidum* had a lower FBP on HS despite rapid development in vitro. The mycelial colonization and the FBP could not be strictly correlated as in not ideal substrates; several fungi show a faster colony expansion for a foraging strategy (Ritz and Crawford, 1999).

A spectroscopic comparison of *P. cornucopiae* fruiting bodies grown on WS-BC displayed a higher content in polysaccharide than those on HS (Figure 4.4a). The higher biosynthesis of polysaccharides in *P. cornucopiae* is strongly influenced by the chemical composition of the substrates, and in particular, by cellulose and hemicellulose availability as also claimed by Bekiaris, (2020b). Conversely, in *L. edodes* grown on HS, polysaccharides increased, chitin in particular, confirming the role of the substrate composition. It is known that *L. edodes* grown on a wood log have a greater economic value than those grown on WS for their better quality (Bruhn and Hall, 2008). Our preliminary sensory

data showed that the fruiting bodies of *L. edodes* grown on HS have a better texture, probably due to the higher chitin content (Zivanovic et al., 2000), aroma, and color than those grown on WS-BC (data not shown). These differences could be due to the high lignin content present in HS, which could provide a fruiting body qualitatively similar to those obtained on wood logs. This result also suggests that a high chitin and polysaccharide content in the *L. edodes* fruiting bodies could be an indicator of the quality of its fruiting bodies. On the other hand, differences in the chemical composition of the medicinal mushroom *G. lucidum* were found both on the glossy surface and in the inner part of the fruiting bodies grown on WS-BC and HS. It is confirmed that the HS substrate led to the enhancement of polysaccharides with respect to those grown on WS-BC. Polysaccharides are the most biologically active substances in *G. lucidum* endowed with antitumor, antiviral, antioxidant, and immunomodulatory activities and for medicinal uses of *Ganoderma* spp. the Chinese Pharmacopoeia has established a minimum content of polysaccharides in the dry fruiting body (L. Wang et al., 2020).

CHAPTER 5

APPLICATION OF SURFACE-ENHANCED RAMAN SCATTERING (SERS) FOR MUSHROOM CHARACTERIZATION

From Puliga et al., 2022b

Mushrooms have always been considered an important source of food and biologically active compounds with several medicinal properties. In recent years, different methods were used to study the quality and chemical composition of mushrooms. Among these, FTIR and FT-Raman spectroscopy techniques have been successfully applied to identify different mushroom species. However, the structural biomolecule components existing in the mycelium or in the fruiting bodies may produce strong fluorescence emission that overlaps the Raman radiation, thus avoiding their analyses by Raman. SERS spectroscopy is a powerful technique which uses metal NPs to enhance the Raman signal of molecules adsorbed on the NPs surface. In addition, SERS is able to quench the macromolecule florescence. In this work we have employed silver NPs in order to get mushroom fingerprints based on SERS as quick procedure to analyze and identify different chemical compounds from the fruiting bodies of six edible and/or medicinal mushrooms:

Lentinula edodes, *Ganoderma lucidum*, *Pleurotus cornucopiae*, *Pleurotus ostreatus*, *Tuber aestivum* and *Tuber magnatum*.

SERS analyses performed directly on fruiting body fragments produced characteristic spectra for each species. One group of mushrooms (*L. edodes*, *G. lucidum*, *T. aestivum* and *T. magnatum*) was dominated by the bands of nucleic acids; and the other one (*P. cornucopiae* and *P. ostreatus*), by the bands of pigments such as melanins; carotenoids; azafilones; polyketides; and flavonoids located in the cell wall. Additionally, bands corresponding to cell wall polysaccharides, particularly chitosan and 1,3-β D-glucan, were identified in the extracts of *P. cornucopiae*, *P. ostreatus* and *L. edodes*. No signal of cell wall polysaccharides was found in *G. lucidum* extract. Raman mapping of the analyzed samples was useful in tracking the spatial distribution of the marker bands. Moreover, the Principal Component Analysis (PCA) carried out on the acquired SERS spectra, allows to discriminate the analyzed mushroom species.

The SERS technique has the ability to generate a strong Raman signal from mushroom fruiting bodies using Ag-NPs deposited directly on intact, untreated mushroom tissues. Using this methodology, commonly applied laboratory time-consuming methods can be avoided or bypassed as well as analysis time can be reduced.

5.1. Introduction

Fungi are a kingdom of unicellular or multicellular eukaryotic organisms which it has recently been estimated to include up 12 millions of species (Wu et al., 2019). Most of them are free-living in soil or water as saprotroph; others establish parasitic or symbiotic relationships with plants or animals. Depending on their aspects, they can be empirically divided in yeasts, filamentous molds, and mushrooms. In particular, mushrooms are defined as the fungi that form a distinctive fruiting body which can be either hypogeous or epigeous, large enough to be seen with the naked eye and to be picked by hand (Chang and Miles, 1992; Wasser, 2002). Mushrooms have always been considered an important source of food and biologically active compounds with several medicinal properties (Badalyan and Zambonelli, 2019). Traditionally, characterization of fungi has been based on phenotypic characteristics or molecular analysis. However, most of the described fungal species (about 70%) have not yet been sequenced (Raja et al., 2017). All these issues reduce the authenticity of the data and the reliability of the analysis. In addition, another concern relates to the time required for analysis, which is both time consuming and often very expensive.

In recent years, vibrational spectroscopy techniques allow a range of qualitative or quantitative information to be obtained, representing a new frontier for fungal identification (Motteu et al., 2022), as well as FTIR and FT-Raman techniques have been successfully applied to identify different fungal species (*Boletus* spp., *Ganoderma* spp., *Agaricus bisporus* (J.E. Lange) Imbach, *Mucor rouxii* (Calmette) Wehmer and *Mortierella* sp.) (Edwards et al., 1995; Li et al., 2020; Y. Li et al., 2017). However, FT-Raman analysis of biological materials can produce a weak signal, which is often covered by the large fluorescence emitted by the sample after excitation (Stöckel et al., 2016). Likewise, FTIR analysis of

biological materials can produce low-quality spectra due to different tissue hydration. As a result, this may lead to an information loss in the amide region caused by the broad adsorption of water molecules at around 1640 cm^{-1} (Faghihzadeh et al., 2016)

SERS, thanks to the use of nanostructured metals (Au and Ag), allows to overcome the intrinsic weakness of Raman spectroscopy combining high molecular specificity with a high sensitivity (Aroca, 2006, 2013). The signal enhancement strongly depends on the NPs optical properties (*i.e.*, composition, size, and shape), the laser excitation characteristics, the nature of the molecule and its Raman cross-sections (Moskovits, 1985; Moskovits and Suh, 1984). When incident light interacts with the NPs, a localized electric field is generated producing a LSPR that allows a strong increase in the Raman scattering up to 10^{14} orders of magnitude compared to the normal Raman technique (Butler et al., 2016; Le Ru and Etchegoin, 2009). Thus, only molecules adsorbed or located near the plasmonic substrate produce noticeable amplification of the Raman signal (Lee et al., 2019; Zhang et al., 2017). Moreover, the maximum intensification of the signal occurs at the tips of protruding elements and, even more, in the interparticle nanoscale spaces called "hot spots" (Giannini et al., 2004). These “hot spots” result from plasmonic coupling between NPs and increase rapidly as the interparticle distance becomes shorter (Guerrini et al., 2010). As a result of their efficacy the SERS-based metallic NPs have been used to characterize complex biological samples such as nucleic acids (Barhoumi and Halas, 2010; Calderon et al., 2021; Kneipp and Flemming, 1986) and proteins (Almehmadi et al., 2019; Fazio et al., 2016; Han et al., 2009) as well as for the study of different microorganisms, including fungi (Dina et al., 2018; Petersen et al., 2021; Prusinkiewicz et al., 2012; Wang et al., 2018; Witkowska et al., 2016), yeasts (Lemma et al., 2019), and plant pathogens (Ramirez-Perez et al., 2022;

Yüksel et al., 2015). Moreover, SERS spectroscopy coupled with the PCA has been employed by several authors to discriminate different fungal species on the basis of their spectra (Dina et al., 2018; Ramirez-Perez et al., 2022; Witkowska et al., 2016).

In the present work we have analyzed six different mushrooms species having a high economical interest: *Lentinula edodes* (Berk.) Pegler, *Ganoderma lucidum* (Curtis) P. Karst., *Pleurotus cornucopiae* (Paulet) Rolland, *Pleurotus ostreatus* (Jacq.) P. Kumm, *Tuber magnatum* Picco and *Tuber aestivum* Vittad. The basidiomycetes *L. edodes*, *G. lucidum, P. cornucopiae* and *P. ostreatus* are between the most popular and cultivated mushrooms in the world (Bijalwan et al., 2021; Royse et al., 2017). On the other hand, *T. magnatum* and *T. aestivum* are two truffles (hypogeous ascomycetes into the genus *Tuber*) which are ones of the most highly prized food (Zambonelli et al., 2021). Accordingly, the main objective of this work was to develop a fast and simple method for identifying mushrooms with no chemical processing. In addition, in situ analysis of tiny mushroom parts is likely to be a low-cost winning procedure for the characterization of different edible and medicinal mushrooms by SERS spectroscopy combined with chemometric analysis.

5.2. Materials and Methods

5.2.1. Mushroom samples and conservation

The fruiting bodies of *G. lucidum* (Glu), *L. edodes* (Led), *P. cornucopiae* (Pco), *P. ostreatus* (Pos), *T. aestivum* (Tae) and *T. magnatum* (Tmg) were analyzed. The fruiting bodies of *G. lucidum*, *L. edodes*, *P. cornucopiae* and *P. ostreatus* were obtained through cultivation on sterilized substrates as described in previous works (Fornito et al., 2020; Puliga et al., 2022a). Samples of *T. aestivum* (herbarium No. 5259) and *T. magnatum* (herbarium No. 3956) were collected in

the wild in the provinces of Bologna and Ferrara, Italy, respectively, and stored in the CMI-Unibo Herbarium at the University of Bologna. All samples were dried at 40°C for 24 hours and stored in a desiccator until used.

5.2.2. Raw polysaccharide extraction

Polysaccharide extraction was carried out on 1 g of dried and powdered Glu, Led, Pco and Pos fruiting bodies, following the protocols described by Ma et al. (2014). The powder was initially treated overnight by immersing it in an 85% ethanol solution. Samples were then centrifuged at 4500 × *g* for 15 minutes and the precipitate was extracted in distilled water (25 mL for each g of precipitate) at 70°C for 140 minutes. The solution obtained was filtered and centrifuged for 10 min at 4500 × *g*. The supernatant was deproteinized with Sevag reagent (Butanol: Chloroform, 1:4 v/v) and centrifuged at 4500 × *g* for 10 minutes. The upper layer was removed and mixed with 4-fold volume of absolute ethanol in order to precipitate the crude polysaccharides for 12 hours at 4°C. Crude polysaccharides were centrifuged at 4500 × *g* for 15 minutes and the precipitate was washed with ethanol and acetone and lyophilized.

5.2.3. Chemical reagents

Silver nitrate, trisodium citrate dihydrate, hydroxylamine hydrochloride and other reagents were of analytical grade and purchased from Sigma-Aldrich. All solutions were freshly prepared with Milli-Q® ultrapure distilled water before experiments and used immediately.

5.2.4. Silver NPs preparation

Before Silver NPs preparation all glassware was cleaned with aqua regia and rinsed with Milli-Q® ultrapure distilled water to remove any impurities present on glass surface. Solutions of silver nitrate, hydroxylamine hydrochloride, and

sodium hydroxide were used for silver colloid preparation as described by Leopold and Lendl (2003). Briefly, 10 mL of silver nitrate solution (10^{-2} M) was droply added while stirring to 90 mL of a hydroxylamine hydrochloride solution (1.67×10^{-3} M) containing 3.33×10^{-3} M sodium hydroxide. After preparation the colloidal solution was stored at 4°C in darkness.

5.2.5. Sampling for SERS spectroscopy and mapping

For SERS analyses, small fragments (3×3 mm) from the cap and pileus of dry fruiting bodies of Led, Glu, Pco and Pos and fragments from the sterile tissue of the gleba of the two *Tuber* species, were placed for 24 hours into a 1.5 mL microcentrifuge tube containing 1 mL of Milli-Q® ultrapure distilled water. After 24 hours the tubes were centrifuged at 11,000 × *g* for 10 minutes and all the water was removed. The small wet fragments of each mushroom species were placed on a microscope slide glass and covered with 5 μL of a concentrated Ag-NPs suspension obtained by centrifugation of 500 μL and successive redispersion to 10% of the original volume. Samples were dried at room temperature before SERS analyses. For each mushroom species three biological replicates were made.

5.2.6. Instrumentation

The silver NPs ware characterized by using an UV-VIS spectrophotometer (UV-3600, Shimadzu, Japan). Raman, SERS, and mapping were performed by using the portable spectrometer Renishaw Raman Virsa™ with a 785 and 532 nm lasers. Before measurements a calibration was performed by using a Si reference sample. Mushroom fragments were analyzed under a 50× objective long focal lens and the laser power was set at 2 mW with an integration time of 1 second. Samples were mapped by recording the spectra of an area of around 40×40 μm for a total of 800 spectra for each sample. The spectra were acquired

using the Renishaw WiRE 5.5 program and processed by the OriginPro 2019 software (OriginLabs). The Scanning Electron Microscope (SEM) picture was obtained in an environmental scanning electron microscope, Philips XL30 (Philips, the Netherlands), with a tungsten filament operating in high vacuum mode. The acceleration voltage was 25 kV.

5.2.7. Statistical analysis

The PCA was applied to evaluate variations in the data matrix between the analyzed mushrooms in order to identify the single species. Spectra were previously normalized as reported by Dina et al. (2018) on the basis of the νAgX band which represents the most intense peak. Processed spectral data were used because of providing much more accurate information on the sample by solving the bands that were previously overlapped in the raw spectra. The PCA was performed by using the OriginPro software with a matrix having a dimension of 18 samples × 2303 variables (wavenumbers units, covering the range 100–1800 cm–1). PCA was performed on the variance-covariance matrix band.

5.3. Results and discussion

5.3.1. Ag-NPs characterization

The successful Ag-NPs formation strictly depends on the preparation parameters that can be easily handled to produce Ag-NPs of well-defined shape, structure, and size distribution. Based on previous studies (Lemma et al., 2019; Prusinkiewicz et al., 2012; Zanasi et al., 2021) the Ag-NPs formation was confirmed by the presence of a narrow band with an absorption maximum at 400 nm in UV-Vis spectroscopy (Figure 1a). The higher absorption intensity indicates that the number of Ag-NPs formed in the solution rise with increasing

reaction time (Figure 5.1a). The nanoparticles produced had an average radius of 40 nm. SEM imaging (Figure 5.1b) of Ag-NPs confirmed the particles' diameter and spherical shape.

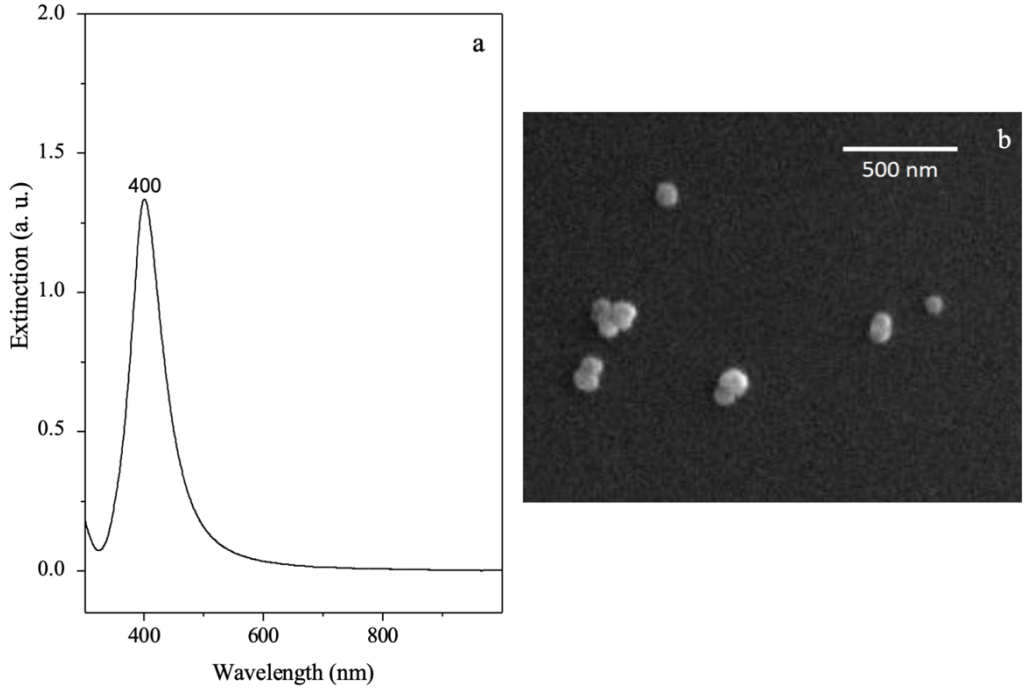

Figure 5.1. (a) UV-Vis extinction spectrum of the Ag-NPs and (b) SEM image showing Ag-NPs.

5.3.2. Normal Raman and SERS spectroscopy

One of the main objectives of the present work was to characterize the different molecular species present in mushrooms by using the Raman spectroscopy under the specific excitation at 785 nm. The latter excitation wavelength is usually employed in the analysis of biological materials because it leads to a reduced fluorescence. However, the Raman spectra registered at 785 nm produced no vibrational signals (Figure 5.2b). Likewise, a broad background fluorescence at 532 nm was detected as a result of pigment molecules excitation within the mushroom cell wall (data not shown). Therefore, normal Raman

spectra collected with two different excitation wavelengths were unable to generate spectra from the mushroom samples. By contrast, the direct deposition of a concentrated drop of Ag-NPs on the mushroom surface was sufficient to generate an enhancement of the SERS signal with 785 nm radiation. (Figure 5.2a). The spectra registered on different points of the analyzed surface revealed few spectral changes between spectra, thus indicating the reproducibility of the analysis (data not shown).

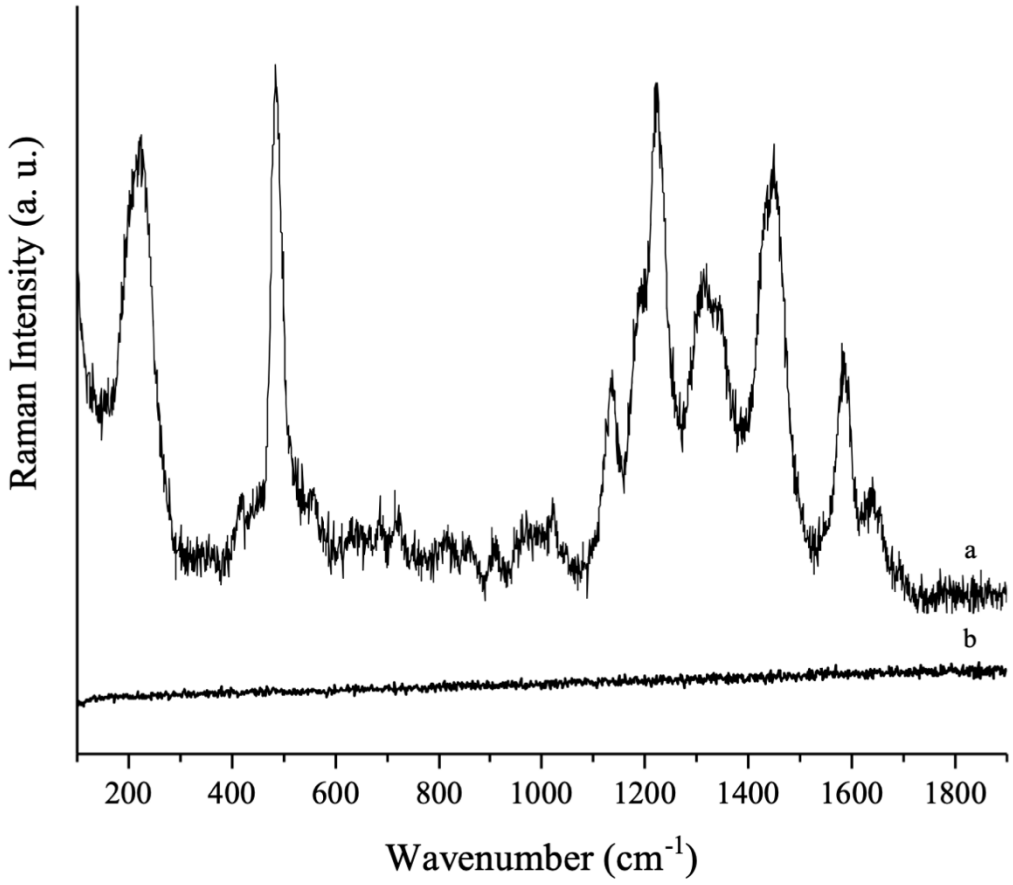

Figure 5.2. (a) SERS and (b) Normal Raman spectra of small fragments of Pco fruiting body.

The SERS analyses performed on the six different fungal species (Figure 5.3) rendered different spectral responses that can be roughly classified into two main groups. The first one is dominated by nucleic acid signals (Adenine (A),

Guanine (G), Thymine (T) and Phosphate groups (P)). The second one is characterized by other set of bands that we have assigned to fungal pigments localized in the mushroom cell wall: melanins (M); carotenoids; azaphilones; polyketides, flavonoids, etc (Lin and Xu, 2020). However, we can not exclude that these bands are related to the polysaccharides existing in the fungal cell wall as reported by Gieroba et al. (2022). These two different groups will henceforth be referred to as A-group and B-group, respectively.

In particular, in A-group, the bands of adenine at 735 and 1335 cm^{-1}, and guanine at 660 and 1568 cm^{-1} were clearly visible (Otto et al., 1986). The band at 796 cm^{-1} can be assigned to the ring breathing band of cytosine and thymine coupled with phosphate vibrations (Otto et al., 1986). Other less intense bands in the 960-1100 cm^{-1} region corresponded to the A-group DNA phosphate and to some ring bands of the purine and pyrimidine bases (Kneipp and Flemming, 1986; Otto et al., 1986).

The presence of nucleic acid bands in the SERS spectra of fungi was detected in the extracted DNA of *Phytophthora ramorum* Werres, De Cock & Man in 't Veld , and in the analysis of micro-fungi cells (Prusinkiewicz et al., 2012; Yüksel et al., 2015). The detection of nucleic material by SERS in the intact non-treated mushroom fragments is an interesting result, because we expected to detect biomolecules localized in the outer part of fungal cell walls. The fact that the fungal genetic material can be put in evidence under the presence of the Ag-NPs implies two possible effects: a) diffusion of the nanoparticles inside the fungal cells through the wall, and b) the disruption of the fungal cell wall and the direct interaction of silver with the intracellular material. Both effects are possible and also they were previously described in the literature (Kim et al., 2012; Panáček et al., 2009; Xia et al., 2016).

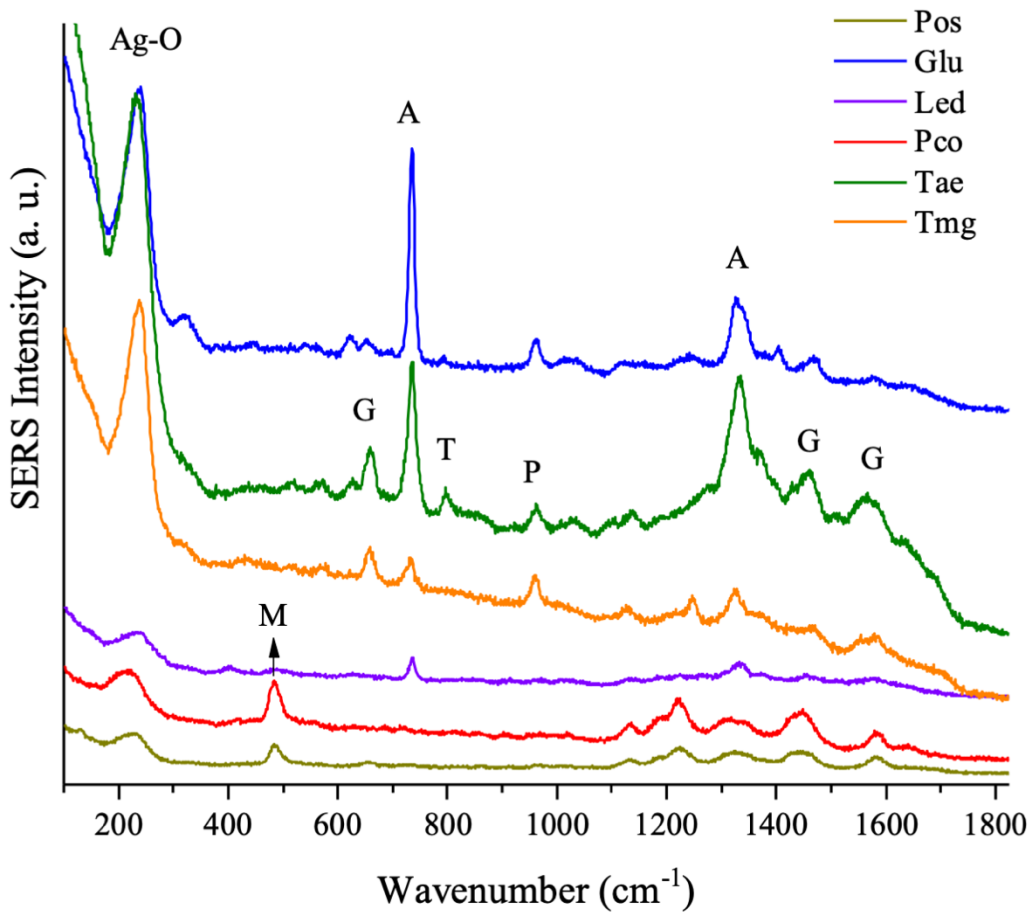

Figure 5.3. SERS spectra of Glu (blue line), Tae (green line), Tmg (orange line), Led (purple line), Pco (red line) and Pos (yellow line). A: Adenine, G: Guanine, M: Melanins, P: Phosphate groups and T: Thymine.

On the other hand, Ag-NPs have been reported to interact with the fungal membranes through electrostatic interactions (Kim et al., 2007) or through specific covalent interactions with SH-containing groups leading to the protein denaturation (Dibrov et al., 2002). The latter effect could increase the permeability of the fungal membrane resulting in disruption of the cell membrane (Kim et al., 2009). Based on previous studies (Kim et al., 2009, 2007), the appearance of intense bands of nucleic acids (DNA and RNA) in SERS spectra might be due to the disruption of the fungal membrane through the formation of holes in the fungal cell wall and the formation of pores in the plasma membrane through which the cell material can flow outward.

The strong effect of Ag-NPs on DNA and RNA was likely induced by the high affinity of silver for purine and pyrimidine bases. In particular, the interaction of Ag with adenine and guanine has been widely demonstrated in previous SERS analyses of nucleic acids (Otto et al., 1986; Rivas et al., 2000). Our outcomes exhibited changes that may be related to different interaction of DNA and/or possibly RNA with Ag-NPs, as shown in Figure 5.3 (Glu, Led, Tae and Tmg species). Specifically, the ratio between the ring breathing bands corresponding to adenine (735 cm^{-1}) and guanine (656 cm^{-1}) changed from Glu, where it was maximum and it was dominated by the adenine bands, to Tmg, where the guanine bands were more enhanced in the SERS spectrum. On the other hand, the A/G ratio can be related in SERS with the different hybridization degree of the double stranded DNA chain (Barhoumi and Halas, 2010). Therefore, in terms of the SERS spectra of mushrooms, this ratio could be related to an effect of silver on the DNA structure.

In the case of B-group (Pos and Pco, Figure 5.3), no band corresponding to nucleic acids were observed. Conversely, broad and weak bands were observed at 483, 1223, 1312, 1445 and 1585 cm^{-1}. Similar bands were observed in the case of some pathogenic fungi (*Scopulariopsis Brumptii* Salv.-Duval, *Candida krusei* (Castell.) Berkhout, *Trichophyton rubrum* (Castell.) Sabour., *Alternaria alternata* (Fr.) Keissl., *Aspergillus flavus* Link, *Fusarium verticillioides* (Sacc.) Nirenberg, *Aspergillus parasiticus* Speare) previously analyzed by SERS (Ramirez-Perez et al., 2022; Witkowska et al., 2016). In addition, these Raman spectra showed a high similarity with the SERS of some of the pigments existing in the fungal cell wall, such as flavonoid pigments (Jurasekova et al., 2006). More specifically, bands at 1223, 1312 or 1445 cm^{-1} are visible in fungal melanins that were identified in the fungus *Ochroconis* sp. by SERS (De La Rosa et al., 2017; Martin-Sanchez et al., 2012). The prevalence of bands corresponding to pigments

presumably embedded in the fungal wall indicated that the cell wall of Pos and Pco remained intact in the presence of Ag-NPs. Therefore, the absence of cell wall rupture resulting in the opening of the plasma membrane could be related to its organization. In fact, it is structured in several layers, with the innermost layer consisting of a covalently bound β-(1,3) glucan core and branched chitin (Chen et al., 2014; Mirończuk-Chodakowska and Witkowska, 2020). The outer layers, in contrast, are more heterogeneous and adapted to the physiology of particular fungi and generally composed of polysaccharides such as β-(1,6) glucan, mannan, galactomannan, and also highly mannosylated glycoproteins (Gow et al., 2017). In addition, pigments such as melanin are found in this outer layer, as was detected in the SERS of Pco. This peculiar organization of the cell wall provides greater resistance to Ag-NPs.

In addition, another important difference between the mushrooms of the A and B-group is the position of the stretching Ag-X band (νAgX), where X can designate the atom (normally O, S or N) of the fungal biomolecule directly interacting with the metal. This band appeared at 237 cm^{-1} in the case of the A-group mushrooms, while it is shifted to 220 cm^{-1} in the mushrooms of the B-group.

For assessing the origin of the SERS Pco and Pos spectra shown in Figure 5.3, polysaccharides from fungi of A-group (Glu and Led) and B-group (Pco and Pos) were investigated.

The SERS spectra of polysaccharides are displayed in Figure 5.4. The bands corresponding to the cell wall from 1100 to 1600 cm^{-1} were evident in the Glu, Pos and Pco. However, in the case of Glu (A-group), these bands were not detected in the SERS of intact fruiting body fragments demonstrating the disruption of the cell wall of this mushroom at the presence of Ag-NPs. In the specific case of Led, the adenine bands are still strong in the SERS spectrum of

the extracted polysaccharides. This is likely due to the adsorption of Led A-rich DNA sequences to the wall fragments.

Polysaccharides, mainly β-glucans, are particularly important as they are linked to the medicinal properties of mushrooms (*e.g.*, immunomodulatory, anticancer, and antioxidant). In particular, Glu and Led mushrooms are among of the most important medicinal mushrooms cultivated in the world (Venturella et al., 2021).

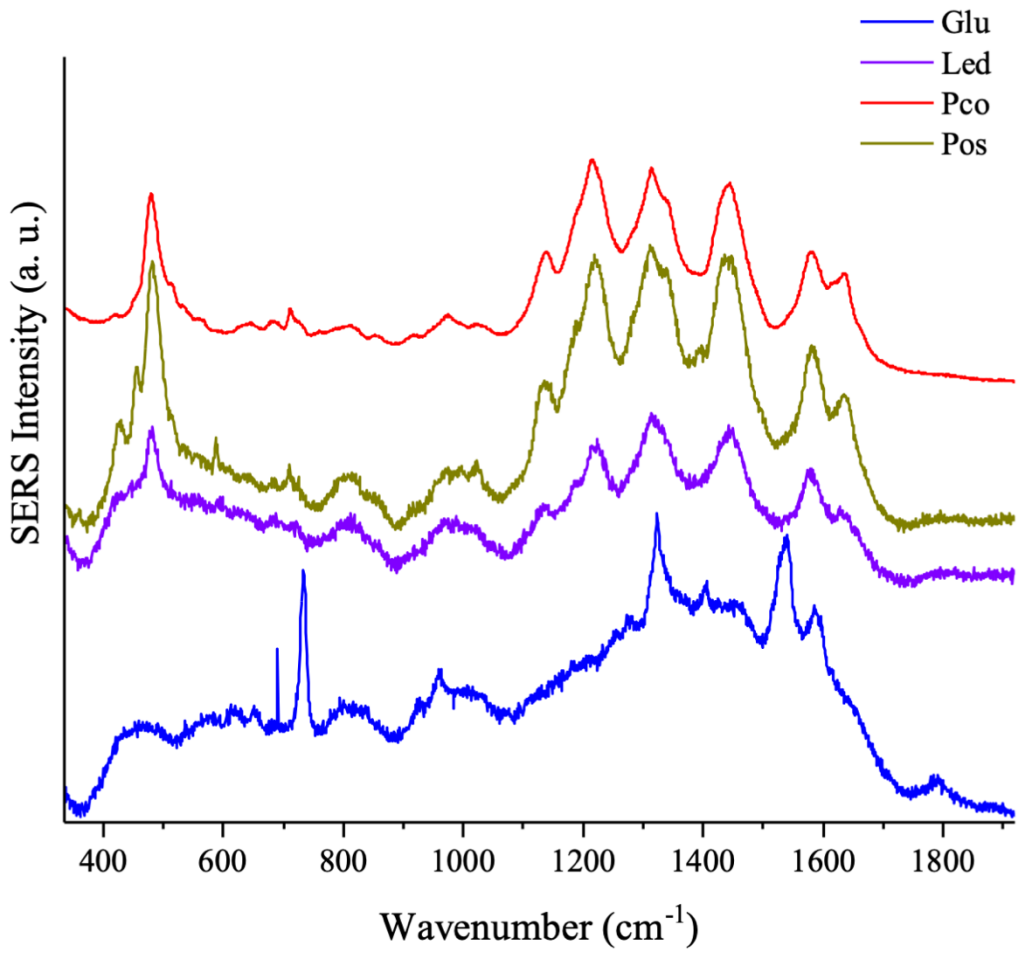

Figure 5.4. SERS spectra of the crude o raw polysaccharides from Pco (red line), Pos (yellow line), Led (purple line) and Glu (blue line).

5.3.3. Raman mapping and PCA analysis

SERS mapping of Glu and Pco (Figure 5.5) were carried out in order to investigate the spatial distribution of bands corresponding to nucleic acids and the fungal cell wall pigments. Figure 5.5b shows the optical direct image of Glu where the hyphae of the fungus are clearly observed. Figure 5.5c displays the intensity (purple) of the adenine marker band (735 cm^{-1}). An individual spectrum of a certain point is shown for comparison in Figure 5.5a. From this mapping it is possible to corroborate that the signal is located in the hyphae. In the case of Pco, the spectrum corresponds to the fungal cell wall (Figure 5.5d), as well as the direct image (Figure 5.5e) and the mapping of the marker band distribution at 1218 cm^{-1} (Figure 5.5f). The distribution maps were also recorded to demonstrate the method's reproducibility, since the areas with the most intense spectra exhibited no significant variation in the SERS spectral pattern.

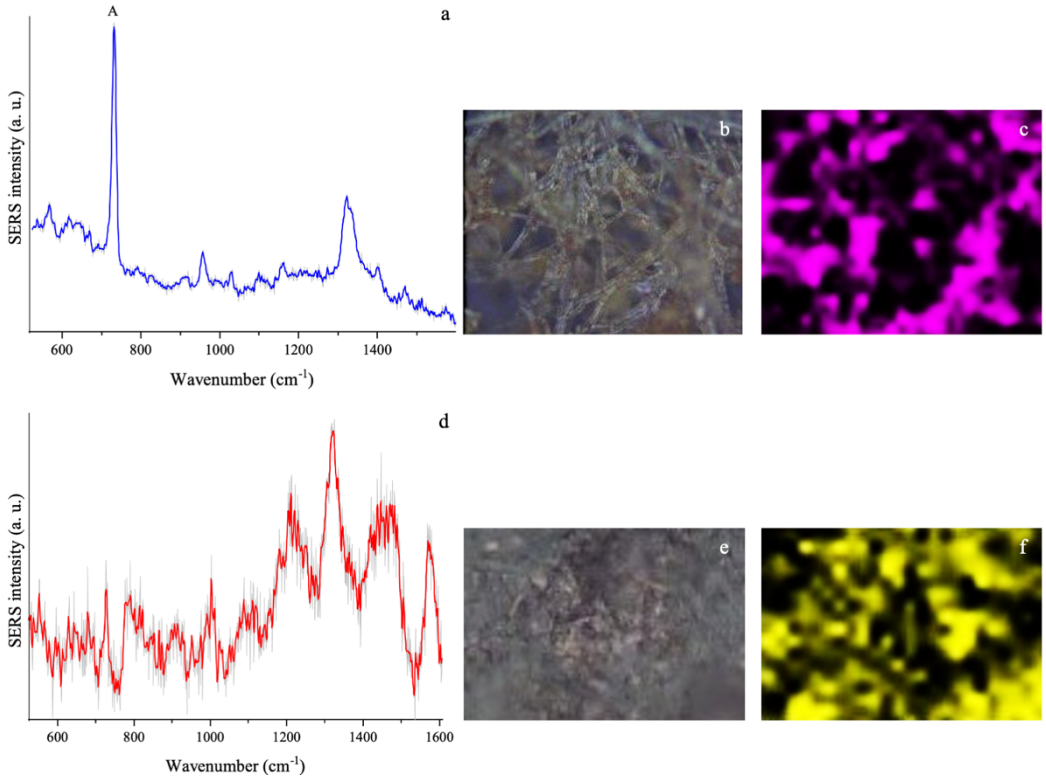

Figure 5.5. SERS mapping of Glu and Pco mushrooms: a) Glu spectrum; b) direct image of Glu hyphae; c) adenine mapping intensity (purple); d) Pco cell wall spectrum; e) direct image of Pco; f) mapping of the marker band distribution at 1218 cm-1 (yellow).

The PCA analysis of the Raman-SERS spectra (100–1800 cm–1) allows to discriminate different mushroom species. PC-1 scores accounted for 71% of the total variance of the analyzed dataset. Thereby demonstrating separation of the studied mushrooms into three separate clusters (Figure 5.6). The first one cluster comprises Led, Pco and Pos which belongs to Agaricales order; the second one is represented by Glu species which belong to the Polyporales order. The latter group include Tae and Tmg belonging to Tuberales order.

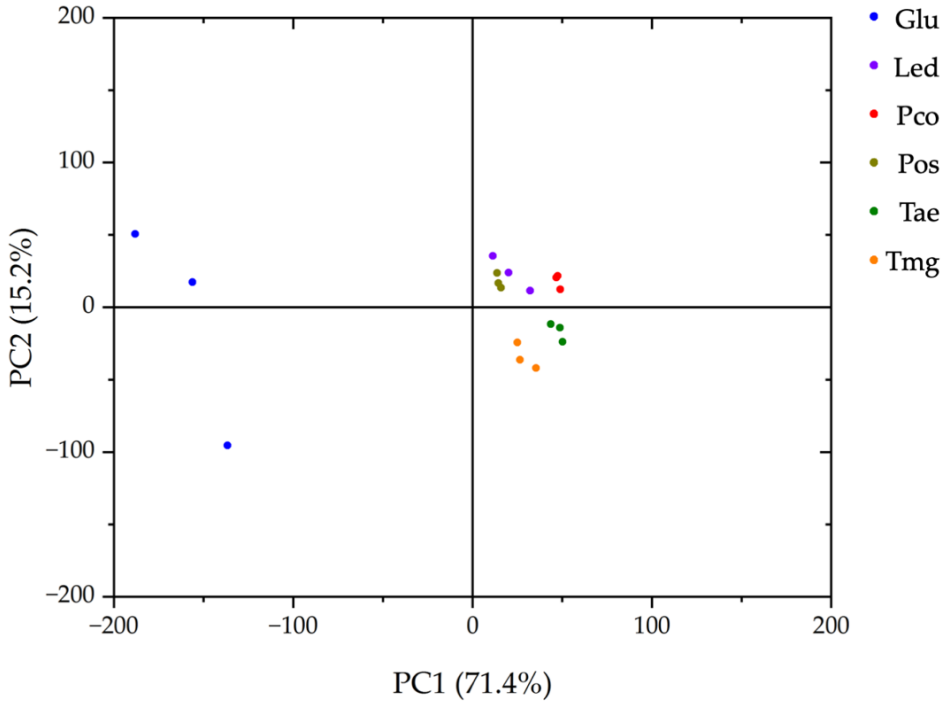

Figure 5.6. PCA analysis of the Raman-SERS spectra of the six mushroom species used in this work. The PCA scores of the first two principal components PC-1 (71.40% of total variance) and PC-2 (15.20% of total variance) indicate the formation of three distinct clusters.

5.4. Conclusions

In conclusion, only the SERS technique can afford significant Raman signals from the analyzed mushrooms by the use of Ag-NPs directly dropped onto the intact non-treated biological tissue of the fruiting bodies. The normal Raman spectroscopy is not able to provide vibrational signals due to the high fluorescence emission. SERS provides a very simple and rapid protocol to identify marker biomolecules of cell wall or the nucleic acid components, that can serve to univocally identify the species. Accordingly, two main groups of mushrooms can be recognized from the SERS data based on different spectral patterns: a) Those dominated by nucleic acid signals; and b) those dominated to other set of bands that we have assigned to fungal pigments localized in the mushroom cell wall. The pigments identified in the fungal cell wall are of polyphenolic nature and could be related to melanins and flavonoids present in this wall. The polysaccharide bands of the cell walls, particularly chitosan and 1,3-D glucan, were exclusively visible in the Pco and Pos spectra and extremely weak in Led, although these bands are also mixed with those of fungal pigments. Raman mapping of fungi was useful for tracing the spatial distribution of marker bands and getting a large number of spectra from a given area, confirming a high repeatability of the analysis. Additionally, the SERS data were processed with the PCA algorithm, and the outcomes revealed that they explained 94% of the variance among the data. Based on above, the PCA clearly exhibits its applicability with a limited number of fungal species as well. Thus, by using this methodology, more time-consuming methods commonly applied in the laboratory can be avoided or bypassed as well as analysis time can be reduced.

CHAPTER 6

CLADOSPORIUM CLADOSPORIOIDES (STRAIN Clc/1) A POTENTIAL CANDIDATE FOR LOW-DENSITY POLYETHYLENE DEGRADATION.

Plastic is one of the most widely used materials in the world in various fields, including packaging and agriculture. The large quantities of this material require proper disposal and for this reason more and more attention is paid to the issue of degrading plastic materials. Thanks to the production of non-specific enzymes, fungi are able to attack complex and recalcitrant xenobiotics such as plastics. In this work, the isolation of different strains of fungi from plastic residues collected in the fields and the ability of these strains to growth and colonizing the Low-density Polyethylene (LDPE) were explored. The structural modifications of the LDPE, as consequence of their growth were monitored by using SEM and ATR-FTIR spectroscopy. Isolation trials allow to obtain 47 strains belonging to 10 genera among them only 11 were able to grow and colonize the LDPE substrate. However, from SEM observations, only *Cladosporium cladosporioides* Clc/1 strain was able to carry out an initial degradation of the LDPE film after 90 days trial. In particular, small cavities and depressed areas of circular shape are visible in the

sample treated. ATR-FTIR analyses conducted on these treated samples after 90 days of fungal growth supports the SEM observed structural changes. Our results suggests that *Cladosporium cladosporioides* Clc/1 is able to carry out an initial degradation of LDPE but further studies will be necessary in order to investigate the enzymes involved in the degradation.

6.1. Introduction

Plastics are represented by a wide range of synthetic or semi-synthetic materials, obtained from oil and natural gas, which under certain conditions of temperature and pressure, undergo permanent variations in shape (Gourmelon, 2015).

Plastics tend to be exceptionally stable and durable, which is why they have gained popularity and wide application in society. However, these same qualities make them persistent in the environment and resistant to decay when it is desired to dispose of them (Rhodes, 2018).

World plastics production is estimated at around 400 million tons per year and of these, a good 90% is plastic produced from fossil sources (Carus et al., 2020). The trend is not declining especially as the annual growth rate of the plastics market is estimated at 4% at least until 2025 (Carus et al., 2020). Geyer and collaborators (2017) estimated that from 1950 to 2015 the world production of resins and plastic fibers increased from 2 million tons to 380 million tons, respectively. From the first years of use to 2015, 8,300 million tons of virgin plastic were produced. In the same year, about 6,300 million tons of plastic waste were produced, of which about 9% was recycled, 12% incinerated and 79% accumulated in landfills or in the natural environment. These data show the great problem caused by the accumulation of plastics that affects numerous habitats: oceans, seas, rivers, lakes, soil, air, ice (Windsor et al., 2019) and living organisms (F. Wang et al., 2020), even accumulating in the human placenta (Ragusa et al., 2021).

PE is one of the most widespread and used plastics in the world (Yin et al., 2020), it is used to produce plastic films, shopping bags and food packaging, and represents up to 64% of single-use plastics that are discarded within a short

period after use, resulting in massive and rapid accumulation in the environment (Harshvardhan and Jha, 2013; Ragaert et al., 2017).

PE films are widely used in agriculture as they allow to improve the efficiency of water use by the crop (Zhou et al., 2009), reduce weeds growth (Ashworth and Harrison, 1983; Qin et al., 2018) and the use of herbicides (Martín-Closas et al., 2017), increases soil temperature and humidity (Ding et al., 2019), prevent soil erosion, and consequently improve crop yield and quality (Greer and Dole, 2003). On the other hand, mulching films represent a problem: at the end of the crop cycle, their disposal is difficult and in some cases they cannot be completely removed from the soil (Wang et al., 2021). This causes an accumulation of plastic residues which over the years, due to different environmental conditions such as solar radiation, wind and current flushing (Roy et al., 2011; Steinmetz et al., 2016), fragment and decompose to sizes below 5 mm (Law and Thompson, 2014; M. Liu et al., 2018; Thompson et al., 2004; Zhang and Liu, 2018).

To the traditional mechanical and chemical recycling strategies of plastics, in recent decades, modern research has investigated new degradation methods that involve the use of different microorganisms (Lear et al., 2021; Shah et al., 2008). Different fungal species have been recognized to produce enzymes capable of degrading plastic under laboratory conditions (Sumathi et al., 2016). The reason why fungi are widely used in degradability assays of various plastic materials lies in the large number of enzymes and other substances they produce (Rhodes, 2014). Different ascomycetes such as: *Aspergillus* spp. (Ameen et al., 2015; Balasubramanian et al., 2014; Brunner et al., 2018; Das and Kumar, 2014; Deepika and Jaya, 2015; Esmaeili et al., 2013; Khan et al., 2017; Muhonja et al., 2018; Munir et al., 2018; Raaman et al., 2012; Raghavendra et al., 2016; Sakhalkar and Mishra, 2013; Sangale et al., 2019; Sindujaa et al., 2011; Singh and

Gupta, 2014; Zahra et al., 2010), *Cladosporium cladosporioides* G.A. de Vries (Brunner et al., 2018), *Fusarium* spp. (Das and Kumar, 2014; Ronkvist et al., 2009; Sakhalkar and Mishra, 2013; Singh and Gupta, 2014; Tachibana et al., 2010; Zahra et al., 2010) and *Penicillium* spp. (Brunner et al., 2018; Liebminger et al., 2007; Ojha et al., 2017; Raghavendra et al., 2016; Sakhalkar and Mishra, 2013; Sepperumal et al., 2013), basidiomycetes (da Luz et al., 2019; Perera et al., 2020) and zigomycetes (Sakhalkar and Mishra, 2013; Singh and Gupta, 2014) have been found to be capable to degrade different petroleum-based plastics. Although the knowledge regarding the enzymes involved in the fungal degradation of PE are few (Santacruz-Juárez et al., 2021), several studies have reported that peroxidases, oxidase, cutinases and lipases plays a crucial role in the degradation (Sánchez, 2020 and references therein). It is known that both enzymatic and abiotic factors can mediate the initial degradation of PE chains, which once reached a length of between 10 and 50 carbons can be enzymatically degraded taking the metabolic path of hydrocarbons degradation (Restrepo-Flórez et al., 2014). Moreover, fungi can produce small wall proteins, called hydrophobins, responsible for attaching the fungal hypha to the plastic material (Sánchez, 2020).

Most of the studies have investigated the degradation of PE by ascomycete fungi through the use of various techniques such as, for example, the FTIR spectroscopic technique and SEM observations (Sánchez, 2020).

The aim of this work was to test the ability of different fungal species isolated from plastic residues to grow and degrade LDPE by using different analytical approach: ATR-FTIR spectroscopy, and SEM observation.

6.2. Materials and Methods

6.2.1. Sampling, mycelial isolation and molecular analyses

Samplings were carried out during June and August 2020, in agricultural fields located in the province of Rimini and Bologna (Emilia-Romagna, Italy). Fifteen samples for each province, of small plastic fragments were taken from the soil and placed in sterile plastic containers, in the dark at room temperature.

Mycelial isolations were carried out the same day of sampling by placing a small plastic fragment inside Petri dishes containing PDA medium (20 g/L) supplemented with chloramphenicol and streptomycin. For each plastic sample five Petri dishes were made.

After 24 hours, under a stereomicroscope, the single small colonies originated on the surface of the plastic fragment were transplanted into new Petri dishes.

Mycelial pure cultures were morphologically assigned to a fungal genus by using taxonomic keys (von Arx, 1970).

Molecular analyses were carried out only by amplification of the Internal Transcribed Spacer (ITS) region of the rDNA using primer pairs ITS1F/ITS4 (Gardes and Bruns, 1993; White et al., 1990) in a direct approach (Iotti and Zambonelli, 2006). Direct Polymerase Chain Reactions (PCRs) were carried out in 50-µL reaction volumes using 2x BiomixTM (Bioline) and amplifications were run in a SimpliAmp thermal cycler (ThermoFisher) as follows: 95°C for 6 minutes, followed by 30 cycles of 94°C for 30 seconds, 56°C for 30 seconds. PCR products were purified using NucleoSpin® Gel and PCR Clean-up kit (Macherey-Nagel, Düren, Germany) and sequencing was performed with both ITS forward and reverse. Sequences generated in this work were compared with existing sequences in the GenBank using BLASTn considering for species identification an identity greater than or equal to 98% and deposited in GenBank.

6.2.2. Plastic degradation assay

For the 90 days plastic degradation assay, an LDPE film was cut into discs about 5.5 cm in diameter and sterilized at 121°C for 20 minutes. After sterilization, the LDPE discs were inserted inside sterile Petri dishes 6 cm in diameter. Each disc was wetted with 300 µL of a liquid mineral salts media devoid of any carbon source as reported by Das and Kumar (2014). The prepared Petri dishes were than inoculated with a 0.6 cm diameter plug of 15 days old colony and five replicates were made for each isolated species. One week after inoculation, the agar plug from each plate was removed and every 10 days 50 µL of mineral salt medium were administered to the colonies. At the end of the trials, the plates were open, and the LDPE disks were freeze-dried in a Virtis Benchtop 2 K lyophilizer (SP Industries, Warminster, Pennsylvania) for further investigations.

6.2.3. SEM analyses

SEM microscopy was carried out in order to verify the adhesion and growth of the fungal hyphae and the degradation of the plastic substrate. A small piece of LDPE disk of 1 cm^2 of each species was washed and firstly fixed in 5% glutaraldehyde solution for 24 hours at 4°C. Subsequently, 2 washes of 7 minutes each in 0.1 M phosphate buffer and a series of washes in ethanol at different percentage (2 washes of 7 minutes each at 20%, 30%, 50%, 75%, 90% and 100%) were done. All washes were done ad 4°C cold and in agitation. The prepared samples were stored in absolute ethanol (99.9%) and subsequently using liquid CO_2 the supercritical dehydration of the samples was conducted.
For observations, the samples were placed on an aluminum stub (26 mm) and coated with gold in real time for 100 seconds using an ionic sputter (E-1010; Hitachi, Tokyo, Japan). The coated samples were taken for image analysis using

a scanning electron microscope (Philips 515; Philips, Amsterdam, The Netherlands), with an acceleration voltage of 20.0 kV.

6.2.4. ATR-FTIR spectroscopy

The spectra were acquired using a TENSOR 27 FTIR Bruker spectrophotometer (Bruker, Ettlingen, Germany), equipped with an ATR module with a micro-diamond crystal. Each sample was deposited on the crystal surface, and the spectra were acquired an average of 32 scans from 4000 to 400 cm^{-1} with a resolution of 4 cm^{-1}. Background spectra were also taken against air under the same conditions before each sample.

The spectra obtained were processed with the Grams/386 software (Galactic Industries, Salem, NH, USA).

6.3. Results

6.3.1. Fungal identification and plastic degradation assays

From the mycelial isolation carried out in this work, it has been possible isolate from the plastic matrices collected in the field a total of 47 strains divided into 10 genera belonging to Ascomycota and Mucoromycota (Figure 6.1). Of these, only 11 strains were capable to grow on the LDPE substrate and thus selected for further analyses. Molecular analyses showed that these strains belong to 9 species as reported in Table 6.1. These strains were deposited in the CMI-Unibo culture collection at the University of Bologna and their ITS sequences were deposited in GenBank (Table 6.1).

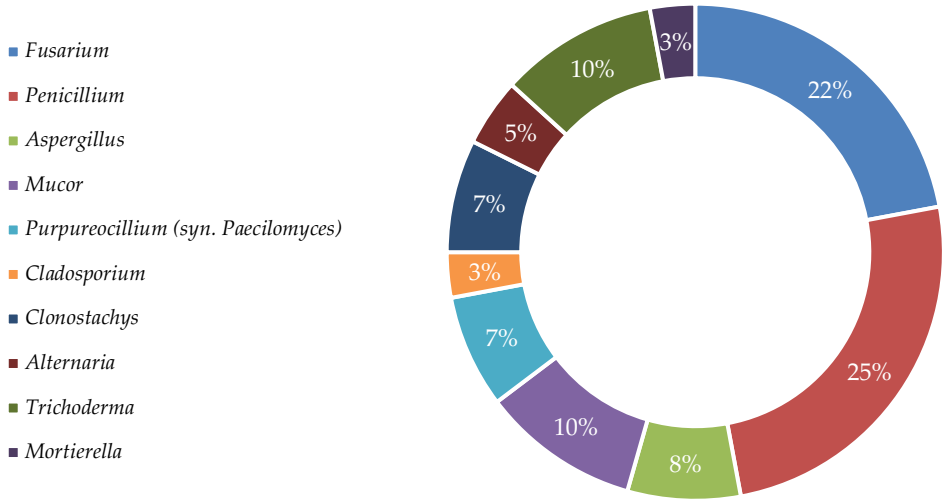

Figure 6.1. Genera identified in this work.

Table 6.1. Species and their accession number molecularly identified.

Species	Strain (CMI-Unibo)	GenBank accession n°
Cladosporium cladosporioides G.A. de Vries	Clc/1	OP729904
Clonostachys rosea (Preuss) Mussat	Clr/1	OP729905
Clonostachys rosea (Preuss) Mussat	Clr/2	OP729906
Fusarium sp.	Fus/1	OP729903
Fusarium equiseti (Corda) Sacc.	Fue/1	OP729900
Fusarium equiseti (Corda) Sacc.	Fue/2	OP729907
Fusarium oxysporum Schltdl.	Fuo/1	OP729901
Fusarium sp.	Fus/2	OP729910
Linnemannia elongata Linnem.	Moe/1	OP729902
Mucor fragilis Bainier	Muf/1	OP729908
Purpureocillium lilacinum (Thom) Luangsa-ard, Houbraken, Hywel-Jones & Samson	Pul/1	OP729909

6.3.2. SEM and ATR-FTIR analyses

SEM observations were carried out on the 11 fungal strains capable to grow on the LDPE substrates. All fungi tested were able to adhere to the LDPE substrate

but only *C. cladosporioides* Clc/1 strain was able to carry out an initial degradation. In particular, small cavities and depressed areas of circular shape are visible in the sample treated with the Clc/1 strain (Figure 6.2b, c) with respect to the untreated LDPE film which is characterized by a smooth surface (Figure 6.2a).

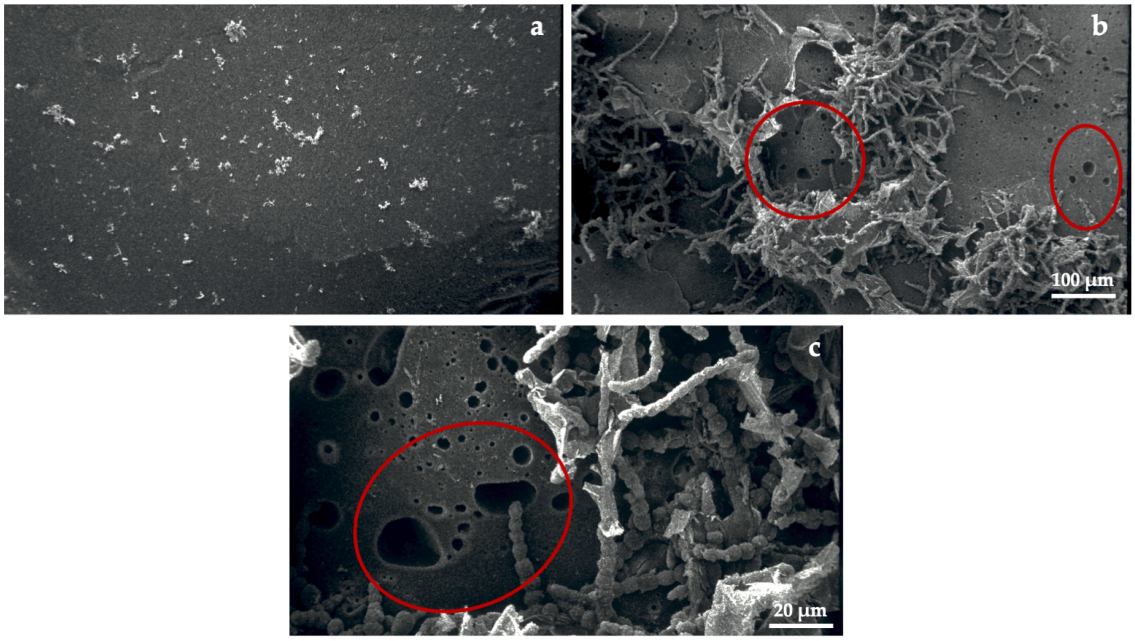

Figure 6.2. SEM images of the LDPE film (a) untreated and (b, c) treated with *C. cladosporioides* Clc/1 strain after 90 days mycelia growth.

ATR-FTIR analyses were conducted on samples treated with *C. cladosporioides* Clc/1 as the only species that following SEM observations clearly showed signs of degradation of the plastic surface. The spectra recorded are presented in Figure 6.3.

The characteristic absorption bands of the main functional groups as reported by Jung et al. (2018); Rajandas et al. (2012) and, Gulmine et al. (2002) are listed in Table 6.2.

Table 6.2. Absorption bands and main functional groups of PE.

Wavenumbers (cm^{-1})	Functional group attribution	Intensity
2914-2915	-CH_2 asymmetric stretching	S
2845-2847	-CH_2 symmetric stretching	S
1467-1470	-CH_2 scissoring	M
1378	CH_3 umbrella mode	Vw
1303	-CH_2 wagging	Vw
720	-CH_2 rocking	M

"S" strong, "M" medium, "Vw" very weak

In the untreated LDPE film spectrum (Figure 6.3, grey dotted line) It is possible to see two very intense bands, at about 2915 cm^{-1} and 2845 cm^{-1} due to the -CH_2 asymmetric and symmetric stretching vibrations, respectively. The bands of medium intensity at 1467 cm^{-1} and 720 cm^{-1} correspond to the -CH_2 scissoring and rocking motions. Finally, the peak at 1378 cm^{-1}, allows the correct discrimination between LDPE and HDPE (Jung et al., 2018).

In the spectrum of the treated LDPE (Figure 6.3, red line), a significant decrease in the relative intensity of the bands at 2915, 2845, 1467, and 720 cm^{-1} can be seen, indicating an initial degradation of the methylene groups. The appearance of other bands in the spectrum, particularly the one at 3251 cm^{-1}, corresponding to the stretching of -OH groups, as well as the one at 1644 cm^{-1} due to amide I and H_2O, and the region between 1100-1030 cm^{-1} assigned to C-O-C, C-C, C-OH stretching groups of the pyranose ring may be associated with the mycelium adhering to the surface of the LDPE film.

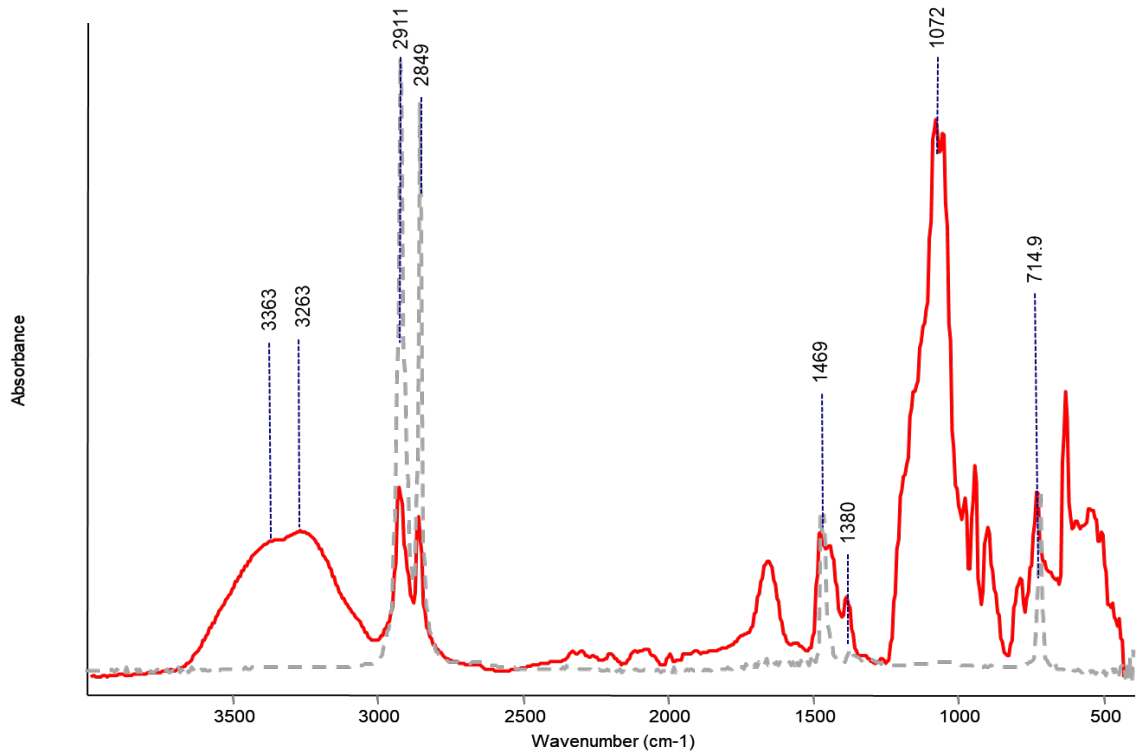

Figure 6.3. ATR-FTIR spectra of the untreated LDPE film (control, gray dotted line) and treated LDPE film with *C. cladosporioides* Clc/1 strain after 90 days of fungal growth (red line).

6.4. Discussion

Plastic, with a production of more than 380 million tons per year (Geyer et al., 2017), is one of the most used materials in the world in various fields, including packaging and agriculture. With a population forecast of 9.2 billion in 2050 (Bongaarts, 2009), the demand for plastic is expected to grow steadily. These large quantities of material require proper disposal, and for this reason more and more attention is paid to the issue of the possibility of degrading plastic materials. Recently, several studies have been carried out in this area, highlighting the ability of different microorganisms to degrade some plastic materials (Lear et al., 2021; Shah et al., 2008). Among these microorganisms, there are also fungi, ubiquitous organisms that, play a fundamental role in the decomposition of organic matter, and are also considered an essential resource

for the development of various biotechnological applications. Thanks to the production of non-specific enzymes, they are able to attack complex and recalcitrant xenobiotics such as plastics (da Luz et al., 2019; Sánchez, 2020).

In this work, the isolation of different strains of fungi from plastic residues collected in the fields and the ability of these strains to growth and colonizing the LDPE were explored. The structural modifications of the LDPE, as consequence of their growth were monitored by using SEM and ATR-FTIR spectroscopy.

Isolation trials allow to obtain 47 strains belonging to 10 genera, among which the most abundant were *Penicillium* (25%) and *Fusarium* (22%) followed by *Mucor* (10%) and *Trichoderma* (10%). These results are in line with those previously obtained by Spina et al. (2021), where a small number of genera were found associated with plastic residues.

As reported by Lear et al. (2021), the presence of PE in the soil lead to a shaping of a peculiar microbiome. Therefore, this can lead to a decrease in the fungal community with a dominance of a small number of species, mainly ascomycetes, in plastic-polluted soils as already observed by Raghavendra et al. (Raghavendra et al., 2016).

Of all the 47 isolated and tested strains, 11 were able to grow and colonize the LDPE substrate, but only *C. cladosporioides* Clc/1 strain was able to carry out an initial degradation of the PE substrate. Brunner et al. (2018) showed that a strain of this species, isolated from plastic debris floating in the shoreline of a lake, was able to degrade polyurethane but not PE. Since our results are in contrast with those reported by Brunner and collaborators (2018), we could hypothesize that the ability of *C. cladosporioides* to degrade LDPE is strain-specific.

ATR-FTIR analysis carried out after 90 days of fungal growth supports the observed structural changes. In fact, similar results were found by other authors

(Das and Kumar, 2014; Muhonja et al., 2018; Spina et al., 2021) and the most significant changes involved the methylene chains. The decrease in the relative amount of these functional groups suggest that *C. cladosporioides* Clc/1 strain may be capable to break the C-H bonds of the PE chains.

The degradative signs observed with the SEM are similar to those reported in the literature by Austin et al. (2018) and are probably due to the action of extracellular enzymes. In fact, these enzymes are involved in the depolymerization of the long carbon chains of plastic polymer into simpler and more degradable oligomers, dimers, and monomers (Amobonye et al., 2021) and in PE degradation, the main fungal enzymes involved seem to be the ligninolytic laccases and peroxidases (Temporiti et al., 2022).

The ability of *C. cladosporioides* to produce laccases and peroxidase was previously reported by Aslam et al. (2012), Bonugli-Santos et al. (2010), Chinaglia et al. (2014) and, Halaburgi et al. (2011).

Further studies will be necessary in order to investigate the enzymes involved in LDPE degradation by the Clc/1 strain.

CHAPTER 7

GENERAL CONCLUSIONS AND FUTURE PROSPECTIVES

The results obtained in chapters 3 and 4 of this dissertation thesis have shown that it is possible to use the solid fraction of the CD and the HS as substrates for the cultivation of different species of edible and medicinal mushrooms.

In particular, the studies conducted on the two types of substrates have allowed to verify through ATR-FTIR spectroscopy, the degradation of the lignocellulosic component present in the cultivation substrate and to evaluate the production of different species of fungi of high economic value on unconventional substrates, considered agro-wastes.

The results obtained open interesting scenarios for the improvement of the efficiency of indoor mushroom cultivation with suitable substrates available locally. For companies with anaerobic digestion plants, the management of CD is a problem due to the high quantities produced daily (about 8 t/day), the highest emissions of greenhouse gases that are released into the environment, and its high concentration of ammonia nitrogen. Although since 2016 it is possible to use CD both as a soil amendment and fertilizer, the high lignin

content present in the solid fraction, make this product difficult to degrade. Moreover, the high amount of nitrogen contained in it, places limits on spreading in the field in nitrate vulnerable zones. On the other hand, the cultivation of the hazel is increasing, this leads to a high production of processing waste represented by the HS produced during the cracking process. This agro-waste, mainly used for domestic heating, also release CO_2 causing air pollution.

As we demonstrated, these agro-wastes can be a valid substrate for the cultivation of edible and medicinal mushrooms allowing their enhancement, reducing management costs, and making them a resource. From the point of view of mushroom producers, the possibility of having an economically and locally available material that offers yields comparable to the conventional substrate, creates indisputable advantages.

These results provide interesting prospects both for more sustainable management of CD and HS and for the improvement of the efficiency of mushroom cultivation. Moreover, in a circular economy perspective, at the end of the production cycle spent mushroom substrate, can be reintroduced into the biogas plant for the production of biogas by activating virtuous circular processes of reuse of materials and elimination of waste. Tests to evaluate the methane power of these spent substrates are currently underway.

ATR-FTIR and SERS analyses conducted to study the chemical composition of fruit bodies in chapters 4 and 5 showed differences between mushrooms grown on the different substrates studied. In particular, the ATR-FTIR analysis provided information on the chemical composition of the fruit bodies highlighting differences in polysaccharides and proteins content between mushrooms grown on the HS-based substrate and the control. Through Raman-SERS spectroscopy and the production of functionalized silver NPs, it was

possible to obtain complementary information to that obtained with ATR-FTIR. Through the application of SERS, it has been possible to develop a rapid, simple, and highly sensitive method for the non-destructive analysis of fruit bodies. The results obtained also made it possible to differentiate the different species analyzed on the basis of their SERS spectrum.

The results obtained in chapter 6 demonstrate the potential for the use of fungal species for bioremediation activities and in particular for plastics degradation.

The strain of *C. cladosporioides* isolated from plastic materials found in the field, has allowed to obtain interesting preliminary results. This species through its enzymatic system has been able to use the PE substrate as the only source of carbon. Since the production of enzymes is also influenced by abiotic factors, and *C. cladosporioides* is widely diffused in the environment, the isolation of fungal strains from different plastic matrices sampled in different environments, would allow the genetic selection of the strains that best adapt to the particular pedo-climatic conditions of the area to be restored. Further investigations will be needed to study and characterize the main enzymes produced by this species. These studies will allow to identify the enzymes responsible for the degradation of the plastic material that can then be synthesized in laboratory and used for different biotechnological applications, including, for example, the bioremediation of agricultural areas polluted by mulch films or other microplastics. In addition, further investigations can be carried out using other types of plastics, in order to verify the degradation capacity of this strain on a wider range of materials.

Bibliography

2030 Water resources group, 2021. From Dialogue to Action: the Road to 2030.

Abe, M., Kobayashi, K., Honma, N., Nakasaki, K., 2010. Microbial degradation of poly(butylene succinate) by *Fusarium solani* in soil environments. Polym. Degrad. Stab. 95, 138–143. https://doi.org/10.1016/j.polymdegradstab.2009.11.042

Ahmed, B., Aboudi, K., Tyagi, V.K., Álvarez-Gallego, C.J., Fernández-Güelfo, L.A., Romero-García, L.I., Kazmi, A.A., 2019. Improvement of anaerobic digestion of lignocellulosic biomass by hydrothermal pretreatment. Appl. Sci. https://doi.org/10.3390/app9183853

Alexander, M., 1977. Mineralization and immobilization of nitrogen., in: Alexander, M. (Ed.), Introduction to Soil Microbiology. Wiley, New York, pp. 225–250.

Almehmadi, L.M., Curley, S.M., Tokranova, N.A., Tenenbaum, S.A., Lednev, I.K., 2019. Surface enhanced Raman spectroscopy for single molecule protein detection. Sci. Rep. 9, 1–9. https://doi.org/10.1038/s41598-019-48650-y

Ameen, F., Moslem, M., Hadi, S., Al-Sabri, A.E., 2015. Biodegradation of low density polyethylene (LDPE) by mangrove fungi from the red sea coast. Prog. Rubber, Plast. Recycl. Technol. 31, 125–144. https://doi.org/10.1177/147776061503100204

Amirta, R., Herawati, E., Suwinarti, W., Watanabe, T., 2016. Two-steps

utilization of Shorea wood waste biomass for the production of oyster mushroom and biogas – A zero waste approach. Agric. Agric. Sci. Procedia 9, 202–208. https://doi.org/10.1016/j.aaspro.2016.02.127

Amobonye, A., Bhagwat, P., Singh, S., Pillai, S., 2021. Plastic biodegradation: Frontline microbes and their enzymes. Sci. Total Environ. 759, 143536. https://doi.org/10.1016/j.scitotenv.2020.143536

Anderson, W.F., Akin, D.E., 2008. Structural and chemical properties of grass lignocelluloses related to conversion for biofuels. J. Ind. Microbiol. Biotechnol. 35, 355–366. https://doi.org/10.1007/s10295-007-0291-8

Andlar, M., Rezić, T., Marđetko, N., Kracher, D., Ludwig, R., Šantek, B., 2018. Lignocellulose degradation: An overview of fungi and fungal enzymes involved in lignocellulose degradation. Eng. Life Sci. 18, 768–778. https://doi.org/10.1002/elsc.201800039

Appels, L., Lauwers, J., Degrve, J., Helsen, L., Lievens, B., Willems, K., Van Impe, J., Dewil, R., 2011. Anaerobic digestion in global bio-energy production: Potential and research challenges. Renew. Sustain. Energy Rev. 15, 4295–4301. https://doi.org/10.1016/j.rser.2011.07.121

Ardon, O., Kerem, Z., Hadar, Y., 1998. Enhancement of lignin degradation and laccase activity in *Pleurotus ostreatus* by cotton stalk extract. Can. J. Microbiol. 44, 676–680. https://doi.org/10.1139/cjm-44-7-676

Aroca, R., 2006. Surface-Enhanced Vibrational Spectroscopy. Wiley.

Aroca, R.F., 2013. Plasmon enhanced spectroscopy. Phys. Chem. Chem. Phys. 15, 5355–5363. https://doi.org/10.1039/c3cp44103b

Arslan, Y., Takaç, S., Eken-Saraçoğlu, N., 2012. Kinetic study of hemicellulosic sugar production from hazelnut shells. Chem. Eng. J. 185–186, 23–28. https://doi.org/10.1016/j.cej.2011.04.052

Ashworth, S., Harrison, H., 1983. Evaluation of mulches for use in the home

garden. HortScience 18, 180–182.

Aslam, M.S., Aishy, A., Samra, Z.Q., Gull, I., Athar, M.A., 2012. Identification, purification and characterization of a novel extracellular laccase from *Cladosporium cladosporioides*. Biotechnol. Biotechnol. Equip. 26, 3345–3350. https://doi.org/10.5504/bbeq.2012.0107

Austin, H.P., Allen, M.D., Donohoe, B.S., Rorrer, N.A., Kearns, F.L., Silveira, R.L., Pollard, B.C., Dominick, G., Duman, R., Omari, K. El, Mykhaylyk, V., Wagner, A., Michener, W.E., Amore, A., Skaf, M.S., Crowley, M.F., Thorne, A.W., Johnson, C.W., Lee Woodcock, H., McGeehan, J.E., Beckham, G.T., 2018. Characterization and engineering of a plastic-degrading aromatic polyesterase. Proc. Natl. Acad. Sci. U. S. A. 115, E4350–E4357. https://doi.org/10.1073/pnas.1718804115

Badalyan, S., Zambonelli, A., 2022. The potential of mushrooms to develop healthy food and biotech products, in: Satyanarayana, T., Deshmukh, S.K. (Eds.), Fungi and Fungal Products in Human Welfare and Biotechnology. Springer nature.

Badalyan, S.M., Zambonelli, A., 2019. Biotechnological exploitation of macrofungi for the production of food, pharmaceuticals and cosmeceuticals, in: Sridhar, K.R., Deshmukh, S.K. (Eds.), Advances in Macrofungi: Diversity, Ecology and Biotechnology. CRC Press, Boca Raton, pp. 199–230.

Báder, M., Németh, R., Sandak, J., Sandak, A., 2020. FTIR analysis of chemical changes in wood induced by steaming and longitudinal compression. Cellulose 27, 6811–6829. https://doi.org/10.1007/s10570-020-03131-8

Balasubramanian, V., Natarajan, K., Rajeshkannan, V., Perumal, P., 2014. Enhancement of in vitro high-density polyethylene (HDPE) degradation by physical, chemical, and biological treatments. Environ. Sci. Pollut. Res. 21,

12549–12562. https://doi.org/10.1007/s11356-014-3191-2

Baldrian, P., 2008. Enzymes of saprotrophic basidiomycetes, in: British Mycological Society Symposia Series. Academic Press, pp. 19–41.

Barbu, M.C., Sepperer, T., Tudor, E.M., Petutschnigg, A., 2020. Walnut and hazelnut shells: Untapped industrial resources and their suitability in lignocellulosic composites. Appl. Sci. 10. https://doi.org/10.3390/APP10186340

Barhoumi, A., Halas, N.J., 2010. Label-free detection of DNA hybridization using surface enhanced Raman spectroscopy. J. Am. Chem. Soc. 132, 12792–12793. https://doi.org/10.1021/ja105678z

Bekiaris, G., Koutrotsios, G., Tarantilis, P.A., Pappas, C.S., Zervakis, G.I., 2020a. FTIR assessment of compositional changes in lignocellulosic wastes during cultivation of *Cyclocybe cylindracea* mushrooms and use of chemometric models to predict production performance. J. Mater. Cycles Waste Manag. 22, 1027–1035. https://doi.org/10.1007/s10163-020-00995-7

Bekiaris, G., Lindedam, J., Peltre, C., Decker, S.R., Turner, G.B., Magid, J., Bruun, S., 2015. Rapid estimation of sugar release from winter wheat straw during bioethanol production using FTIR-photoacoustic spectroscopy. Biotechnol. Biofuels 8, 1–12. https://doi.org/10.1186/s13068-015-0267-2

Bekiaris, G., Tagkouli, D., Koutrotsios, G., Kalogeropoulos, N., Zervakis, G.I., 2020b. *Pleurotus mushrooms* content in glucans and ergosterol assessed by ATR-FTIR spectroscopy and multivariate analysis. Foods 9. https://doi.org/doi:10.3390/foods9040535

Bijalwan, A., Bahuguna, K., Vasishth, A., Singh, A., Chaudhary, S., Dongariyal, A., Kumar Thakur, T., Kaushik, S., Javed Ansari, M., Alfarraj, S., Ali Alharbi, S., Skalicky, M., Brestic, M., 2021. Growth performance of *Ganoderma lucidum* using billet method in Garhwal Himalaya, India. Saudi

J. Biol. Sci. 28, 2709–2717. https://doi.org/10.1016/j.sjbs.2021.03.030

Bock, P., Nousiainen, P., Elder, T., Blaukopf, M., Amer, H., Zirbs, R., Potthast, A., Gierlinger, N., 2020. Infrared and Raman spectra of lignin substructures: Dibenzodioxocin. J. Raman Spectrosc. 51, 422–431. https://doi.org/10.1002/jrs.5808

Boddy, L., Frankland, J., West, P. Van, 2008. Ecology of saprotrophic basidiomycetes. Academic Press, Elsevier, Amsterdam, the Netherlands.

Bongaarts, J., 2009. Human population growth and the demographic transition. Philos. Trans. R. Soc. B Biol. Sci. 364, 2985–2990. https://doi.org/10.1098/rstb.2009.0137

Bonugli-Santos, R.C., Durrant, L.R., da Silva, M., Sette, L.D., 2010. Production of laccase, manganese peroxidase and lignin peroxidase by Brazilian marine-derived fungi. Enzyme Microb. Technol. 46, 32–37. https://doi.org/10.1016/j.enzmictec.2009.07.014

Brezáni, A., Svobodová, K., Jablonský, I., Tlustoš, P., 2019. Cultivation of medicinal mushrooms on spruce sawdust fermented with a liquid digestate from biogas stations. Int. J. Med. Mushrooms 21, 215–223. https://doi.org/10.1615/IntJMedMushrooms.2019030022

Bruhn, J., Hall, M., 2008. Growing shiitake mushrooms in an agroforestry practice. Agrofor. action.

Brunner, I., Fischer, M., Rüthi, J., Stierli, B., Frey, B., 2018. Ability of fungi isolated from plastic debris floating in the shoreline of a lake to degrade plastics. PLoS One 13, 1–14. https://doi.org/10.1371/journal.pone.0202047

Bunaciu, A.A., Aboul-Enein, H.Y., Hoang, V.D., 2020. Vibrational spectroscopy applications in biomedical, pharmaceutical and food sciences. Elsevier, Amsterdam, the Netherlands.

Burlacu, A., Israel-Roming, F., Cornea, C.P., 2018. Depolymerization of kraft

lignin with laccase and peroxidase: A review. Sci. Bull. Ser. F. Biotechnol. XXII, 172–179.

Butler, H.J., Ashton, L., Bird, B., Cinque, G., Curtis, K., Dorney, J., Esmonde-White, K., Fullwood, N.J., Gardner, B., Martin-Hirsch, P.L., Walsh, M.J., McAinsh, M.R., Stone, N., Martin, F.L., 2016. Using Raman spectroscopy to characterize biological materials. Nat. Protoc. 11, 664–687. https://doi.org/10.1038/nprot.2016.036

Calderon, I., Guerrini, L., Alvarez-Puebla, R.A., 2021. Targets and tools: Nucleic acids for surface-enhanced Raman spectroscopy. Biosensors 11. https://doi.org/10.3390/bios11070230

Campanella, B., Palleschi, V., Legnaioli, S., 2021. Introduction to vibrational spectroscopies. ChemTexts 7, 1–21. https://doi.org/10.1007/s40828-020-00129-4

Carus, M., Dammer, L., Raschka, A., Skoczinski, P., 2020. Renewable carbon: Key to a sustainable and future-oriented chemical and plastic industry: Definition, strategy, measures and potential. Greenh. Gases Sci. Technol. 10, 488–505. https://doi.org/10.1002/ghg.1992

Chang, S.T., Lau, O.W., Cho, K.Y., 1981. The cultivation and nutritional value of *Pleurotus sajor-caju*. Eur. J. Appl. Microbiol. Biotechnol. 12, 58–62. https://doi.org/10.1007/BF00508120

Chang, S.T., Miles, P.G., 1992. Mushroom biology—a new discipline. Mycologist 6, 64–65.

Chen, L., Xu, W., Lin, S., Cheung, P.C.K., 2014. Cell wall structure of mushroom sclerotium (Pleurotus tuber regium): Part 1. Fractionation and characterization of soluble cell wall polysaccharides. Food Hydrocoll. 36, 189–195. https://doi.org/10.1016/j.foodhyd.2013.09.023

Chinaglia, S., Chiarelli, L.R., Maggi, M., Rodolfi, M., Valentini, G., Picco, A.M.,

2014. Biochemistry of lipolytic enzymes secreted by *Penicillium solitum* and *Cladosporium cladosporioides*. Biosci. Biotechnol. Biochem. 78, 245–254. https://doi.org/10.1080/09168451.2014.882752

Chiu, S.W., Law, S.C., Ching, M.L., Cheung, K.W., Chen, M.J., 2000. Themes for mushroom exploitation in the 21st century: Sustainability, waste management, and conservation. J. Gen. Appl. Microbiol. 46, 269–282. https://doi.org/10.2323/jgam.46.269

Choong, Y.K., Sun, S.Q., Zhou, Q., Ismail, Z., Rashid, B.A.A., Tao, J.X., 2011. Determination of storage stability of the crude extracts of *Ganoderma lucidum* using FTIR and 2D-IR spectroscopy. Vib. Spectrosc. 57, 87–96. https://doi.org/10.1016/j.vibspec.2011.05.008

Ćilerdžić, J.L., Vukojević, J.B., Klaus, A.S., Ivanović, Ž.S., Blagojević, J.D., Stajić, M.M., 2018. Wheat straw – a promissing substrate for *Ganoderma lucidum* cultivation. Acta Sci. Pol. Hortorum Cultus 17, 13–22. https://doi.org/10.24326/asphc.2018.1.2

Cimino, G., Passerini, A., Toscano, G., 2000. Removal of toxic cations and Cr(VI) from aqueous solution by hazelnut shell. Water Res. 34, 2955–2962. https://doi.org/10.1016/S0043-1354(00)00048-8

Coates, J., 2006. Interpretation of Infrared Spectra, A Practical Approach, in: Meyers, R.A. (Ed.), Encyclopedia of Analytical Chemistry. John Wiley & Sons Ltd., Chichester, UK, pp. 10815–10837.

Coconi-Linares, N., Magaña-Ortíz, D., Guzmán-Ortiz, D.A., Fernández, F., Loske, A.M., Gómez-Lim, M.A., 2014. High-yield production of manganese peroxidase, lignin peroxidase, and versatile peroxidase in *Phanerochaete chrysosporium*. Appl. Microbiol. Biotechnol. 98, 9283–9294. https://doi.org/10.1007/s00253-014-6105-9

Colom, X., Carrillo, F., Nogués, F., Garriga, P., 2003. Structural analysis of

photodegraded wood by means of FTIR spectroscopy. Polym. Degrad. Stab. 80, 543–549. https://doi.org/10.1016/S0141-3910(03)00051-X

Contini, M., Baccelloni, S., Massantini, R., Anelli, G., 2008. Extraction of natural antioxidants from hazelnut (*Corylus avellana* L.) shell and skin wastes by long maceration at room temperature. Food Chem. 110, 659–669. https://doi.org/10.1016/j.foodchem.2008.02.060

Çöpür, Y., Güler, C., Taşçioğlu, C., Tozluoğlu, A., 2008. Incorporation of hazelnut shell and husk in MDF production. Bioresour. Technol. 99, 7402–7406. https://doi.org/10.1016/j.biortech.2008.01.021

Cragg, S.M., Beckham, G.T., Bruce, N.C., Bugg, T.D.H., Distel, D.L., Dupree, P., Etxabe, A.G., Goodell, B.S., Jellison, J., McGeehan, J.E., McQueen-Mason, S.J., Schnorr, K., Walton, P.H., Watts, J.E.M., Zimmer, M., 2015. Lignocellulose degradation mechanisms across the tree of life. Curr. Opin. Chem. Biol. 29, 108–119. https://doi.org/10.1016/j.cbpa.2015.10.018

Cullen, D., Kersten, P.J., 2004. Enzymology and molecular biology of lignin degradation, in: Brambl, R., Marzluf, G.A. (Eds.), The Mycota III. Biochemistry and Molecular Biology. Springer Verlag, Berlin, Heidelberg, pp. 295–312. https://doi.org/10.1007/978-3-662-10367-8_13

Czubaszek, R., Wysocka-Czubaszek, A., 2018. Emissions of carbon dioxide and methane from fields fertilized with digestate from an agricultural biogas plant. Int. Agrophysics 32, 29–37. https://doi.org/10.1515/intag-2016-0087

da Luz, J.M.R., da Silva, M.D.C.S., dos Santos, L.F., Kasuya, M.C.M., 2019. Plastics polymers degradation by fungi, in: Blumenberg, M., Shaabam, M., Elgaml, A. (Eds.), Microorganisms. IntechOpen, London, UK, pp. 261–270.

da Silva, L.L., 2016. Adding value to agro-industrial wastes. Ind. Chem. 2. https://doi.org/10.4172/2469-9764.1000e103

Dahlin, J., Nelles, M., Herbes, C., 2017. Biogas digestate management:

Evaluating the attitudes and perceptions of German gardeners towards digestate-based soil amendments. Resour. Conserv. Recycl. 118, 27–38. https://doi.org/10.1016/j.resconrec.2016.11.020

Das, B., Rajkonwar, J., Jagannath, A., Raul, P.K., Deb, U., 2020. Infra-red spectra of different species of cultivated oyster mushrooms: possible tool for identifying bioactive compounds and establishing taxonomic linkage. Def. Life Sci. J. 5, 118–124. https://doi.org/10.14429/dlsj.5.15562

Das, M.P., Kumar, S., 2014. Microbial deterioration of low density polyethylene by *Aspergillus* and *Fusarium* sp. Int. J. ChemTech Res. 6, 299–305.

Dasanayaka, P.N., Wijeyaratne, S.C., 2017. Cultivation of *Schizophyllum commune* mushroom on different wood substrates. J. Trop. For. Environ. 7, 65–73. https://doi.org/10.31357/jtfe.v7i1.3023

Dashtban, M., Schraft, H., Qin, W., 2009. Fungal bioconversion of lignocellulosic residues: Opportunities & perspectives. Int. J. Biol. Sci. 5, 578–595. https://doi.org/10.7150/ijbs.5.578

Davin, L.B., Lewis, N.G., 2005. Lignin primary structures and dirigent sites. Curr. Opin. Biotechnol. 16, 407–415. https://doi.org/10.1016/j.copbio.2005.06.011

De La Rosa, J.M., Martin-Sanchez, P.M., Sanchez-Cortes, S., Hermosin, B., Knicker, H., Saiz-Jimenez, C., 2017. Structure of melanins from the fungi Ochroconis lascauxensis and Ochroconis anomala contaminating rock art in the Lascaux Cave. Sci. Rep. 7, 1–11. https://doi.org/10.1038/s41598-017-13862-7

De Laurentiis, V., Hunt, D.V.L., Rogers, C.D.F., 2016. Overcoming food security challenges within an energy/water/food nexus (EWFN) approach. Sustain. 8. https://doi.org/10.3390/su8010095

De Rosa, I.M., Kenny, J.M., Puglia, D., Santulli, C., Sarasini, F., 2010.

Morphological, thermal and mechanical characterization of okra (*Abelmoschus esculentus*) fibres as potential reinforcement in polymer composites. Compos. Sci. Technol. 70, 116–122. https://doi.org/10.1016/j.compscitech.2009.09.013

Debin, C., Ying, L., Li, Y., Wenfan, B., Yanqin, W., Changbo, Y., 2008. Culture medium for cultivating *Coprinus comatus* by straw raw material biogas residues and preparation method thereof.

Deepika, S., Jaya, M.R., 2015. Biodegradation of low density polyethylene by microorganisms from garbage soil. J. Exp. Biol. Agric. Sci. 3, 1–5.

Del Borghi, A., Moreschi, L., Gallo, M., 2020. Circular economy approach to reduce water–energy–food nexus. Curr. Opin. Environ. Sci. Heal. 13, 23–28. https://doi.org/10.1016/j.coesh.2019.10.002

Del Río, J.C., Rencoret, J., Prinsen, P., Martínez, Á.T., Gutiérrez, A., Ralph, J., 2013. Structural characterization of wheat straw lignin. Evidence for a novel monomer in grasses. Cons. Super. Investig. Científicas.

Demirbaş, E., 2003. Adsorption of cobalt(II) ions from aqueous solution onto activated carbon prepared from hazelnut shells. Adsorpt. Sci. Technol. 21, 951–963. https://doi.org/10.1260/02636170360744380

Demirbas, E., Dizge, N., Sulak, M.T., Kobya, M., 2009. Adsorption kinetics and equilibrium of copper from aqueous solutions using hazelnut shell activated carbon. Chem. Eng. J. 148, 480–487. https://doi.org/10.1016/j.cej.2008.09.027

Di Piazza, S., Benvenuti, M., Damonte, G., Cecchi, G., Mariotti, M.G., Zotti, M., 2021. Fungi and circular economy: *Pleurotus ostreatus* grown on a substrate with agricultural waste of lavender, and its promising biochemical profile. Recycling 6. https://doi.org/10.3390/recycling6020040

Dias, A.A., Freitas, G.S., Marques, G.S.M., Sampaio, A., Fraga, I.S., Rodrigues,

M.A.M., Evtuguin, D. V., Bezerra, R.M.F., 2010. Enzymatic saccharification of biologically pre-treated wheat straw with white-rot fungi. Bioresour. Technol. 101, 6045–6050. https://doi.org/10.1016/j.biortech.2010.02.110

Dibrov, P., Dzioba, J., Gosink, K.K., Häse, C.C., 2002. Chemiosmotic mechanism of antimicrobial activity of Ag+ in Vibrio cholerae. Antimicrob. Agents Chemother. 46, 2668–2670. https://doi.org/10.1128/AAC.46.8.2668-2670.2002/ASSET/94954A7F-91EE-4757-8F2B-652259076882/ASSETS/GRAPHIC/AC0820108003.JPEG

Dina, N.E., Gherman, A.M.R., Chiş, V., Sârbu, C., Wieser, A., Bauer, D., Haisch, C., 2018. Characterization of clinically relevant fungi via SERS fingerprinting assisted by novel chemometric models. Anal. Chem. https://doi.org/10.1021/acs.analchem.7b03124

Ding, F., Li, S., Lü, X.T., Dijkstra, F.A., Schaeffer, S., An, T., Pei, J., Sun, L., Wang, J., 2019. Opposite effects of nitrogen fertilization and plastic film mulching on crop N and P stoichiometry in a temperate agroecosystem. J. Plant Ecol. 12, 682–692. https://doi.org/10.1093/jpe/rtz006

Donner, M., Gohier, R., de Vries, H., 2020. A new circular business model typology for creating value from agro-waste. Sci. Total Environ. 716, 137065. https://doi.org/10.1016/j.scitotenv.2020.137065

Dwivedi, P., Vivekanand, V., Pareek, N., Sharma, A., Singh, R.P., 2011. Co-cultivation of mutant *Penicillium oxalicum* SAU E-3.510 and *Pleurotus ostreatus* for simultaneous biosynthesis of xylanase and laccase under solid-state fermentation. N. Biotechnol. 28, 616–626. https://doi.org/10.1016/j.nbt.2011.05.006

Ebringerová, A., Hromádková, Z., Heinze, T., 2005. Hemicellulose, in: Heinze, T. (Ed.), Polysaccharides I. Advances in Polymer Science. Vol 186. Springer, Berlin, Heidelberg, pp. 1–67. https://doi.org/10.1007/b136816

Edwards, H.G.M., Russell, N.C., Weinstein, R., Wynn-Williams, D.D., 1995. Fourier transform Raman spectroscopic study of fungi. J. Raman Spectrosc. 26, 911–916.

Eichorst, S.A., Kuske, C.R., 2012. Identification of cellulose-responsive bacterial and fungal communities in geographically and edaphically different soils by using stable isotope probing. Appl. Environ. Microbiol. 78, 2316–2327. https://doi.org/10.1128/AEM.07313-11

Ellen MacArthur Foundation, 2018. Cities and circular economy for food. Cowes, UK.

Esmaeili, A., Pourbabaee, A.A., Alikhani, H.A., Shabani, F., Esmaeili, E., 2013. Biodegradation of Low-Density Polyethylene (LDPE) by mixed culture of *Lysinibacillus xylanilyticus* and *Aspergillus niger* in soil. PLoS One 8. https://doi.org/10.1371/journal.pone.0071720

Esposito, T., Sansone, F., Franceschelli, S., Del Gaudio, P., Picerno, P., Aquino, R.P., Mencherini, T., 2017. Hazelnut (*Corylus avellana* L.) shells extract: Phenolic composition, antioxidant effect and cytotoxic activity on human cancer cell lines. Int. J. Mol. Sci. 18. https://doi.org/10.3390/ijms18020392

European Commission, 2020. A new circular economy action plan for a cleaner and more competitive Europe. Brussel.

European Commission, 2019. Communication from the commission: The European green deal. Brussel.

European Commission, 2012. Innovating for sustainable growth: A bioeconomy for europe. Brussel.

European Commission, 2010. Being wise with waste: the EU's approach to waste management.

Faghihzadeh, F., Anaya, N.M., Schifman, L.A., Oyanedel-Craver, V., 2016. Fourier transform infrared spectroscopy to assess molecular-level changes

in microorganisms exposed to nanoparticles. Nanotechnol. Environ. Eng. 1, 1–16. https://doi.org/10.1007/s41204-016-0001-8

Fanadzo, M., Zireva, D.T., Dube, E., Mashingaidze, A.B., 2010. Evaluation of various substrates and supplements for biological efficiency of *Pleurotus sajor-caju* and *Pleurotus ostreatus*. African J. Biotechnol. 9, 2756–2761. https://doi.org/10.5897/AJB2010.000-3100

FAOSTAT, 2019. FAOSTAT. Food and Agricultural Organization of the United Nations [WWW Document]. URL https://www.fao.org/faostat/en/#data/QCL (accessed 12.15.21).

Fazio, B., D'Andrea, C., Foti, A., Messina, E., Irrera, A., Donato, M.G., Villari, V., Micali, N., Maragò, O.M., Gucciardi, P.G., 2016. SERS detection of biomolecules at physiological pH via aggregation of gold nanorods mediated by optical forces and plasmonic heating. Sci. Rep. 6, 1–13. https://doi.org/10.1038/srep26952

Ferroukhi, R., Nagpal, D., Lopez-Peña, A., Hodges, T., Mohtar, R.H., Daher, B., Mohtar, S., Keulertz, M., 2015. Renewable energy in the water, energy & food nexus, in: IRENA. Abu Dhabi, pp. 1–125.

Floudas, D., Binder, M., Riley, R., Barry, K., Blanchette, R.A., Henrissat, B., Martínez, A.T., Otillar, R., Spatafora, J.W., Yadav, J.S., Aerts, A., Benoit, I., Boyd, A., Carlson, A., Copeland, A., Coutinho, P.M., Vries, R.P. de, Ferreira, P., Findley, K., Foster, B., Gaskell, J., Glotzer, D., Górecki, P., Heitman, J., Hesse, C., Hori, C., Igarashi, K., Jurgens, J.A., Kallen, N., Kersten, P., Kohler, A., Kües, U., Kumar, T.K.A., Kuo, A., LaButti, K., Larrondo, L.F., Lindquist, E., Ling, A., Lombard, V., Lucas, S., Lundell, T., Martin, R., McLaughlin, D.J., Morgenstern, I., Morin, E., Murat, C., Nagy, L.G., Nolan, M., Ohm, R.A., Patyshakuliyeva, A., Rokas, A., Ruiz-Dueñas, F.J., Sabat, G., Salamov, A., Samejima, M., Schmutz, J., Slot, J.C., John, F. St.,

Stenlid, J., Sun, H., Sun, S., Syed, K., Tsang, A., Wiebenga, A., Young, D., Pisabarro, A., Eastwood, D.C., Martin, F., Cullen, D., Grigoriev, I. V., Hibbett, D.S., 2012. The paleozoic origin of enzymatic from 31 fungal genomes. Science (80-.). 336, 1715–1719.

Fornito, S., Puliga, F., Leonardi, P., Di Foggia, M., Zambonelli, A., Francioso, O., 2020. Degradative ability of mushrooms cultivated on corn silage digestate. Molecules 25, 1–15. https://doi.org/10.3390/molecules25133020

Fuso, A., Risso, D., Rosso, G., Rosso, F., Manini, F., Manera, I., Caligiani, A., 2021. Potential valorization of hazelnut shells through extraction, purification and structural characterization of prebiotic compounds: A critical review. Foods 10. https://doi.org/10.3390/foods10061197

Gao, W., Zhou, L., Jiang, Q., Guan, Y., Hou, R., Hui, B., Liu, S., 2022. Reliable and realistic models for lignin content determination in poplar wood based on FT-Raman spectroscopy. Ind. Crops Prod. 182, 114884. https://doi.org/10.1016/j.indcrop.2022.114884

Garcia, D.J., You, F., 2016. The water-energy-food nexus and process systems engineering: A new focus. Comput. Chem. Eng. 91, 49–67. https://doi.org/10.1016/j.compchemeng.2016.03.003

Gardes, M., Bruns, T.D., 1993. ITS primers with enhanced specificity for basidiomycetes - application to the identification of mycorrhizae and rusts. Mol. Ecol. 2, 113–118. https://doi.org/10.1111/j.1365-294X.1993.tb00005.x

Geneau-Sbartaï, Ć., Leyris, J., Silvestre, F., Rigal, L., 2008. Sunflower cake as a natural composite: Composition and plastic properties. J. Agric. Food Chem. 56, 11198–11208. https://doi.org/10.1021/jf8011536

Geyer, R., Jambeck, J.R., Law, K.L., 2017. Production, use, and fate of all plastics ever made. Sci. Adv. 3, 3–8. https://doi.org/10.1126/sciadv.1700782

Giannini, V., Sánchez-Gil, J., García-Ramos, J. V, 2004. Modelo teórico del

mecanismo electromagnético en espectroscopia SERS. Óptica Pura y Apl. 37, 97–102.

Gierlinger, N., 2018. New insights into plant cell walls by vibrational microspectroscopy. Appl. Spectrosc. Rev. 53, 517–551. https://doi.org/10.1080/05704928.2017.1363052

Gieroba, B., Sroka-Bartnicka, A., Kazimierczak, P., Kalisz, G., Lewalska-Graczyk, A., Vivcharenko, V., Nowakowski, R., Pieta, I.S., Przekora, A., 2022. Surface chemical and morphological analysis of chitosan/1,3-β-D-glucan polysaccharide films cross-linked at 90 °C. Int. J. Mol. Sci. 23, 1–23. https://doi.org/10.3390/ijms23115953

Gioelli, F., Dinuccio, E., Balsari, P., 2011. Residual biogas potential from the storage tanks of non-separated digestate and digested liquid fraction. Bioresour. Technol. 102, 10248–10251. https://doi.org/10.1016/j.biortech.2011.08.076

Gochev, V.K., Krastanov, A.I., 2007. Fungal laccases. Bulg. J. Agric. Sci. 13, 75–83.

Gourmelon, G., 2015. Global plastic production rises, recycling lags. Vital Signs 22, 91–95.

Gow, N.A.R., Latge, J.-P., Munro, C.A., 2017. The Fungal Cell Wall: Structure, Biosynthesis, and Function. Microbiol. Spectr. 5. https://doi.org/10.1128/microbiolspec.FUNK-0035-2016

Greer, L., Dole, J.M., 2003. Aluminum foil, aluminium-painted, plastic, and degradable mulches increase yields and decrease insect-vectored viral diseases of vegetables. Horttechnology 13, 276–284. https://doi.org/10.21273/horttech.13.2.0276

Griffiths, P.R., De Haseth, J.A., 2007. Fourier transform infrared spectrometry, 2nd ed. John Wiley & Sons, New York.

Grigatti, M., Montecchio, D., Francioso, O., Ciavatta, C., 2015. Structural and thermal investigation of three agricultural biomasses following mild-NaOH pretreatment to increase anaerobic biodegradability. Waste and Biomass Valorization 6, 1135–1148. https://doi.org/10.1007/s12649-015-9423-y

Grigoriev, I. V., 2013. Fungal genomics for energy and environment, in: Horwitz, B., Mukherjee, P., Mukherjee, M., Kubicek, C. (Eds.), Genomics of Soil- and Plant-Associated Fungi. Springer, Berlin, Heidelberg, pp. 11–27. https://doi.org/10.1007/978-3-642-39339-6

Guerrini, L., Izquierdo-Lorenzo, I., Rodriguez-Oliveros, R., Sanchez-Gil, J.A., Sanchez-Cortes, S., Garcia-Ramos, J.V., Domingo, C., 2010. α,ω-Aliphatic Diamines as Molecular Linkers for Engineering Ag Nanoparticle Clusters: Tuning of the Interparticle Distance and Sensing Application. Plasmonics 5, 273–286. https://doi.org/10.1007/s11468-010-9143-x

Gulmine, J. V., Janissek, P.R., Heise, H.M., Akcelrud, L., 2002. Polyethylene characterization by FTIR. Polym. Test. 21, 557–563. https://doi.org/10.1016/S0142-9418(01)00124-6

Guney, M.S., 2013. Utilization of hazelnut husk as biomass. Sustain. Energy Technol. Assessments 4, 72–77. https://doi.org/10.1016/j.seta.2013.09.004

Guo, T., Zhang, Q., Ai, C., Liang, G., He, P., Zhou, W., 2018. Nitrogen enrichment regulates straw decomposition and its associated microbial community in a double-rice cropping system. Sci. Rep. 8, 1–12. https://doi.org/10.1038/s41598-018-20293-5

Gupta, B.S., Jelle, B.P., Gao, T., 2015. Application of ATR-FTIR spectroscopy to compare the cell materials of wood decay fungi with wood mould fungi. Int. J. Spectrosc. 2015, 1–7. https://doi.org/10.1155/2015/521938

Gupta, D.K., Rühl, M., Mishra, B., Kleofas, V., Hofrichter, M., Herzog, R.,

Pecyna, M.J., Sharma, R., Kellner, H., Hennicke, F., Thines, M., 2018. The genome sequence of the commercially cultivated mushroom *Agrocybe aegerita* reveals a conserved repertoire of fruiting-related genes and a versatile suite of biopolymer-degrading enzymes. BMC Genomics 19, 1–13. https://doi.org/10.1186/s12864-017-4430-y

Gupta, A. Das, 2017. Water-Energy-Food (WEF) nexus and sustainable development, in: Salam, P.A., Shrestha, S., Pandey, V.P., Anal, A.K. (Eds.), Water-energy-food Nexus. Principles and Practices. Wiley, Hoboken, New Jersey, pp. 223–241.

Halaburgi, V.M., Sharma, S., Sinha, M., Singh, T.P., Karegoudar, T.B., 2011. Purification and characterization of a thermostable laccase from the ascomycetes *Cladosporium cladosporioides* and its applications. Process Biochem. 46, 1146–1152. https://doi.org/10.1016/j.procbio.2011.02.002

Han, X.X., Huang, G.G., Zhao, B., Ozaki, Y., 2009. Label-free highly sensitive detection of proteins in aqueous solutions using surface-enhanced Raman scattering. Anal. Chem. 81, 3329–3333. https://doi.org/10.1021/ac900395x

Harshvardhan, K., Jha, B., 2013. Biodegradation of low-density polyethylene by marine bacteria from pelagic waters, Arabian Sea, India. Mar. Pollut. Bull. 77, 100–106. https://doi.org/10.1016/j.marpolbul.2013.10.025

Hatakka, A., Hammel, K.E., 2011. Fungal biodegradation of lignocelluloses, in: Hofrichter, M. (Ed.), Industrial Applications. The Mycota, Vol 10. Springer Verlag, Berlin, Heidelberg, pp. 319–340. https://doi.org/10.1007/978-3-642-11458-8_15

Hawksworth, D.L., Lücking, R., 2017. Fungal diversity revisited: 2.2 to 3.8 million species. Microbiol. Spectr. 5, 1–17. https://doi.org/10.1128/microbiolspec.FUNK-0052-2016.

Heinze, T., 2015. Cellulose: Structure and properties, in: Rojas, O. (Ed.),

Cellulose Chemistry and Properties: Fibers, Nanocelluloses and Advanced Materials. Springer, Cham, pp. 1–52. https://doi.org/10.1007/12_2015_319

Hidalgo, D., Martín-Marroquín, J.M., Corona, F., 2019. A multi-waste management concept as a basis towards a circular economy model. Renew. Sustain. Energy Rev. 111, 481–489. https://doi.org/10.1016/j.rser.2019.05.048

Hodge, A., Campbell, C.D., Fitter, A.H., 2001. An arbuscular mycorrhizal fungus accelerates decomposition and acquires nitrogen directly from organic material. Nature 413, 297–299. https://doi.org/10.1038/35095041

Horn, S.J., Vaaje-Kolstad, G., Westereng, B., Eijsink, V.G., 2012. Novel enzymes for the degradation of cellulose. Biotechnol. Biofuels 5, 45.

Hoşgün, E.Z., Berikten, D., Kıvanç, M., Bozan, B., 2017. Ethanol production from hazelnut shells through enzymatic saccharification and fermentation by low-temperature alkali pretreatment. Fuel 196, 280–287. https://doi.org/10.1016/j.fuel.2017.01.114

Hoşgün, E.Z., Bozan, B., 2020. Effect of different types of thermochemical pretreatment on the enzymatic hydrolysis and the composition of hazelnut shells. Waste and Biomass Valorization 11, 3739–3748. https://doi.org/10.1007/s12649-019-00711-z

Huang, X., Kocaefe, D., Kocaefe, Y., Boluk, Y., Pichette, A., 2012. Study of the degradation behavior of heat-treated jack pine (*Pinus banksiana*) under artificial sunlight irradiation. Polym. Degrad. Stab. 97, 1197–1214. https://doi.org/10.1016/j.polymdegradstab.2012.03.022

Iotti, M., Zambonelli, A., 2006. A quick and precise technique for identifying ectomycorrhizas by PCR. Mycol. Res. 110, 60–65. https://doi.org/10.1016/j.mycres.2005.09.010

Isikhuemhen, O.S., Mikiashvili, N.A., Kelkar, V., 2009. Application of solid waste from anaerobic digestion of poultry litter in *Agrocybe aegerita*

cultivation: Mushroom production, lignocellulolytic enzymes activity and substrate utilization. Biodegradation 20, 351–361. https://doi.org/10.1007/s10532-008-9226-y

Isikhuemhen, O.S., Mikiashvilli, N.A., 2009. Lignocellulolytic enzyme activity, substrate utilization, and mushroom yield by *Pleurotus ostreatus* cultivated on substrate containing anaerobic digester solids. J. Ind. Microbiol. Biotechnol. 36, 1353–1362. https://doi.org/10.1007/s10295-009-0620-1

Islam, W., Riaz, A., 2017. Yield and biological efficiency of *Pleurotus ostreatus* (Jacq. Fr.) cultivated upon various weeds and agricultural wastes. Pakistan J. Weed Sci. Res. 23, 271–279.

Janusz, G., Pawlik, A., Sulej, J., Świderska-Burek, U., Jarosz-Wilkolazka, A., Paszczyński, A., 2017. Lignin degradation: Microorganisms, enzymes involved, genomes analysis and evolution. FEMS Microbiol. Rev. 41, 941–962. https://doi.org/10.1093/femsre/fux049

Jarosz, A.M., Davelos, A.L., 1995. Effects of disease in wild plant populations and the evolution of pathogen aggressiveness. New Phytol. 129, 371–387. https://doi.org/10.1111/j.1469-8137.1995.tb04308.x

Javier-Astete, R., Jimenez-Davalos, J., Zolla, G., 2021. Determination of hemicellulose, cellulose, holocellulose and lignin content using FTIR in *Calycophyllum spruceanum* (Benth.) K. Schum. And *Guazuma crinita* Lam. PLoS One 16, 1–12. https://doi.org/10.1371/journal.pone.0256559

Jiang, L., Hassan, M.M., Ali, S., Li, H., Sheng, R., Chen, Q., 2021. Evolving trends in SERS-based techniques for food quality and safety: A review. Trends Food Sci. Technol. 112, 225–240. https://doi.org/10.1016/j.tifs.2021.04.006

Jones, J., Verma, B., Basso, B., Mohtar, R., Matlock, M., 2021. Transforming food and agriculture to circular systems: a perspective for 2050. Resour. Mag. 28,

7–9.

Jung, M.R., Horgen, F.D., Orski, S. V., Rodriguez C., V., Beers, K.L., Balazs, G.H., Jones, T.T., Work, T.M., Brignac, K.C., Royer, S.J., Hyrenbach, K.D., Jensen, B.A., Lynch, J.M., 2018. Validation of ATR FT-IR to identify polymers of plastic marine debris, including those ingested by marine organisms. Mar. Pollut. Bull. 127, 704–716. https://doi.org/10.1016/j.marpolbul.2017.12.061

Jurak, E., Patyshakuliyeva, A., De Vries, R.P., Gruppen, H., Kabel, M.A., 2015. Compost grown *Agaricus bisporus* lacks the ability to degrade and consume highly substituted xylan fragments. PLoS One 10, 1–14. https://doi.org/10.1371/journal.pone.0134169

Jurasekova, Z., Garcia-Ramos, J. V., Domingo, C., Sanchez-Cortes, S., 2006. Surface-enhanced Raman scattering of flavonoids. J. Raman Spectrosc. 37, 1239–1241. https://doi.org/10.1002/jrs.1634

Kalač, P., 2013. A review of chemical composition and nutritional value of wild-growing and cultivated mushrooms. J. Sci. Food Agric. 93, 209–218. https://doi.org/10.1002/jsfa.5960

Kalmiş, E., Sargin, S., 2004. Cultivation of two *Pleurotus* species on wheat straw substrates containing olive mill waste water. Int. Biodeterior. Biodegrad. 53, 43–47. https://doi.org/10.1016/j.ibiod.2003.08.002

Kamimura, N., Sakamoto, S., Mitsuda, N., Masai, E., Kajita, S., 2019. Advances in microbial lignin degradation and its applications. Curr. Opin. Biotechnol. 56, 179–186. https://doi.org/10.1016/j.copbio.2018.11.011

Kataki, S., Sarma, G.D., Patowary, D., Baruah, D.C., 2019. Prospects of utilization of liquid fraction of biogas digestate as substrate supplement for mushroom cultivation, in: Advances in Waste Management. Springer Singapore, pp. 445–465. https://doi.org/10.1007/978-981-13-0215-2_32

Kaya, N., Yıldız, Z., Ceylan, S., 2018. Preparation and characterisation of biochar from hazelnut shell and its adsorption properties for methylene blue dye. J. Polytech. 21, 765–776. https://doi.org/10.2339/politeknik.386963

Kazemipour, M., Ansari, M., Tajrobehkar, S., Majdzadeh, M., Kermani, H.R., 2008. Removal of lead, cadmium, zinc, and copper from industrial wastewater by carbon developed from walnut, hazelnut, almond, pistachio shell, and apricot stone. J. Hazard. Mater. 150, 322–327. https://doi.org/10.1016/j.jhazmat.2007.04.118

Khan, S., Nadir, S., Shah, Z.U., Shah, A.A., Karunarathna, S.C., Xu, J., Khan, A., Munir, S., Hasan, F., 2017. Biodegradation of polyester polyurethane by *Aspergillus tubingensis*. Environ. Pollut. 225, 469–480. https://doi.org/10.1016/j.envpol.2017.03.012

Kim, J., Lee, J., Kwon, S., Jeong, S., 2009. Preparation of biodegradable Polymer/Silver nanoparticles composite and its antibacterial efficacy. J. Nanosci. Nanotechnol. 9, 1098–1102. https://doi.org/10.1166/JNN.2009.C096

Kim, J.S., Kuk, E., Yu, K.N., Kim, J.H., Park, S.J., Lee, H.J., Kim, S.H., Park, Y.K., Park, Y.H., Hwang, C.Y., Kim, Y.K., Lee, Y.S., Jeong, D.H., Cho, M.H., 2007. Antimicrobial effects of silver nanoparticles. Nanomedicine Nanotechnology, Biol. Med. 3, 95–101. https://doi.org/10.1016/j.nano.2006.12.001

Kim, S.W., Jung, J.H., Lamsal, K., Kim, Y.S., Min, J.S., Lee, Y.S., 2012. Antifungal effects of silver nanoparticles (AgNPs) against various plant pathogenic fungi. Mycobiology 40, 53–58. https://doi.org/10.5941/MYCO.2012.40.1.053

Kneipp, K., Flemming, J., 1986. Surface enhanced Raman scattering (SERS) of nucleic acids adsrobed on colloidal silver particles. J. Mol. Struct. 145, 173–179. https://doi.org/10.1016/0022-2860(86)87041-7

Kobya, M., Demirbas, E., Öncel, M.S., Sencan, S., 2002. Adsorption kinetic

models applied to nickel ions on hazelnut shell activated carbons. Adsorpt. Sci. Technol. 20, 179–188. https://doi.org/10.1260/026361702320360595

Kracher, D., Ludwig, R., 2016. Cellobiose dehydrogenase: An essential enzyme for lignocellulose degradation in nature - A review. Die Bodenkultur J. L. Manag. Food Environ. 67, 145–163. https://doi.org/10.1515/boku-2016-0013

Król, K., Gantner, M., 2020. Morphological traits and chemical composition of hazelnut from different geographical origins: A review. Agriculture 10. https://doi.org/10.3390/agriculture10090375

Król, K., Gantner, M., Piotrowska, A., 2021. The quality characteristic and fatty acid profile of cold-pressed hazelnut oils during nine months of storage. Agronomy 11. https://doi.org/10.3390/agronomy11102045

Kubicek, C.P., 2012. Fungi and lignocellulosic biomass. John Wiley & Sons, Hoboken, New Jersey.

Kumar, A., Kumari, S., Dindhoria, K., Manyapu, V., Kumar, R., 2021. Efficient utilization and bioprocessing of agro-industrial waste, in: Rana, A., Saneja, A., Kumar, S., Lichtfouse, E. (Eds.), Sustainable Agriculture Reviews 56. Springer, Cham, pp. 1–37. https://doi.org/10.1007/978-3-030-84405-9_1

Kumla, J., Suwannarach, N., Sujarit, K., Penkhrue, W., Kakumyan, P., Jatuwong, K., Vadthanarat, S., Lumyong, S., 2020. Cultivation of mushrooms and their lignocellulolytic enzyme production through the utilization of agro-industrial waste. Molecules 25, 1–39. https://doi.org/10.3390/molecules25122811

Law, K.L., Thompson, R.C., 2014. Microplastics in the seas. Science (80-.). 345, 144–145. https://doi.org/10.1002/2014EF000240/polymer

Le Floch, A., Jourdes, M., Teissedre, P.L., 2015. Polysaccharides and lignin from oak wood used in cooperage: Composition, interest, assays: A review. Carbohydr. Res. 417, 94–102. https://doi.org/10.1016/j.carres.2015.07.003

Le Ru, E.C., Etchegoin, P.G., 2009. Principles of Surface enhanced Raman spectroscopy (and related plasmonic effects). Elsevier, Amsterdam, the Netherlands.

Lear, G., Kingsbury, J.M., Franchini, S., Gambarini, V., Maday, S.D.M., Wallbank, J.A., Weaver, L., Pantos, O., 2021. Plastics and the microbiome: impacts and solutions. Environ. Microbiomes 16, 1–19. https://doi.org/10.1186/s40793-020-00371-w

Lee, H.K., Lee, Y.H., Koh, C.S.L., Phan-Quang, G.C., Han, X., Lay, C.L., Sim, H.Y.F., Kao, Y.C., An, Q., Ling, X.Y., 2019. Designing surface-enhanced Raman scattering (SERS) platforms beyond hotspot engineering: Emerging opportunities in analyte manipulations and hybrid materials. Chem. Soc. Rev. 48, 731–756. https://doi.org/10.1039/c7cs00786h

Lemma, T., Wang, J., Arstila, K., Hytönen, V.P., Toppari, J.J., 2019. Identifying yeasts using surface enhanced Raman spectroscopy. Spectrochim. Acta - Part A Mol. Biomol. Spectrosc. 218, 299–307. https://doi.org/10.1016/j.saa.2019.04.010

Leopold, N., Lendl, B., 2003. A new method for fast preparation of highly surface-enhanced raman scattering (SERS) active silver colloids at room temperature by reduction of silver nitrate with hydroxylamine hydrochloride. J. Phys. Chem. B 107, 5723–5727. https://doi.org/10.1021/jp027460u

Lewicka, K., 2017. Activated carbons prepared from hazelnut shells, walnut shells and peanut shells for high CO2 adsorption. Polish J. Chem. Technol. 19, 38–43. https://doi.org/10.1515/pjct-2017-0025

Li, Q., Xiong, C., Huang, W., Li, X., 2017. Controlled surface fire for improving yields of *Morchella importuna*. Mycol. Prog. 16, 1057–1063. https://doi.org/10.1007/s11557-017-1350-9

Li, X.P., Li, J., Liu, H., Wang, Y.Z., 2020. A new analytical method for discrimination of species in Ganodermataceae mushrooms. Int. J. Food Prop. 23, 227–240. https://doi.org/10.1080/10942912.2020.1722159

Li, Y., Zhang, J., Li, T., Liu, H., Li, J., Wang, Y., 2017. Geographical traceability of wild *Boletus edulis* based on data fusion of FT-MIR and ICP-AES coupled with data mining methods (SVM). Spectrochim. Acta - Part A Mol. Biomol. Spectrosc. 177, 20–27. https://doi.org/10.1016/j.saa.2017.01.029

Liebminger, S., Eberl, A., Sousa, F., Heumann, S., Fischer-Colbrie, G., Cavaco-Paulo, A., Guebitz, G.M., 2007. Hydrolysis of PET and bis-(benzoyloxyethyl) terephthalate with a new polyesterase from *Penicillium citrinum*. Biocatal. Biotransformation 25, 171–177. https://doi.org/10.1080/10242420701379734

Lin, L., Xu, J., 2020. Fungal Pigments and Their Roles Associated with Human Health. J. Fungi 6, 1–37. https://doi.org/10.3390/JOF6040280

Lindahl, B.D., Tunlid, A., 2015. Ectomycorrhizal fungi - potential organic matter decomposers, yet not saprotrophs. New Phytol. 205, 1443–1447. https://doi.org/10.1111/nph.13201

Liu, M., Lu, S., Song, Y., Lei, L., Hu, J., Lv, W., Zhou, W., Cao, C., Shi, H., Yang, X., He, D., 2018. Microplastic and mesoplastic pollution in farmland soils in suburbs of Shanghai, China. Environ. Pollut. 242, 855–862. https://doi.org/10.1016/j.envpol.2018.07.051

Liu, Q., Ma, H., Zhang, Y., Dong, C., 2018. Artificial cultivation of true morels: current state, issues and perspectives. Crit. Rev. Biotechnol. 38, 259–271. https://doi.org/10.1080/07388551.2017.1333082

Lombard, V., Golaconda Ramulu, H., Drula, E., Coutinho, P.M., Henrissat, B., 2014. The carbohydrate-active enzymes database (CAZy) in 2013. Nucleic Acids Res. 42, 490–495. https://doi.org/10.1093/nar/gkt1178

López-Mondéjar, R., Zühlke, D., Becher, D., Riedel, K., Baldrian, P., 2016. Cellulose and hemicellulose decomposition by forest soil bacteria proceeds by the action of structurally variable enzymatic systems. Sci. Rep. 6, 1–12. https://doi.org/10.1038/srep25279

Lu, X., Ding, S., 2010. Effect of Cu^{2+}, Mn^{2+} and aromatic compounds on the production of laccase isoforms by *Coprinus comatus*. Mycoscience 51, 68–74. https://doi.org/10.1007/s10267-009-0002-6

Lu, Y., Lu, Y.C., Hu, H.Q., Xie, F.J., Wei, X.Y., Fan, X., 2017. Structural characterization of lignin and its degradation products with spectroscopic methods. J. Spectrosc. 2017. https://doi.org/10.1155/2017/8951658

Lupoi, J.S., Singh, S., Parthasarathi, R., Simmons, B.A., Henry, R.J., 2015. Recent innovations in analytical methods for the qualitative and quantitative assessment of lignin. Renew. Sustain. Energy Rev. 49, 871–906. https://doi.org/10.1016/j.rser.2015.04.091

Ma, G., Yang, W., Mariga, A.M., Fang, Y., Ma, N., Pei, F., Hu, Q., 2014. Purification, characterization and antitumor activity of polysaccharides from *Pleurotus eryngii* residue. Carbohydr. Polym. 114, 297–305. https://doi.org/10.1016/j.carbpol.2014.07.069

Ma, G., Yang, W., Zhao, L., Pei, F., Fang, D., Hu, Q., 2018. A critical review on the health promoting effects of mushrooms nutraceuticals. Food Sci. Hum. Wellness 7, 125–133. https://doi.org/10.1016/j.fshw.2018.05.002

Madeira, J.V., Contesini, F.J., Calzado, F., Rubio, M.V., Zubieta, M.P., Lopes, D.B., de Melo, R.R., 2017b. Agro-Industrial Residues and Microbial Enzymes: An Overview on the Eco-Friendly Bioconversion into High Value-Added Products, in: Biotechnology of Microbial Enzymes: Production, Biocatalysis and Industrial Applications. Elsevier Inc., pp. 475–511. https://doi.org/10.1016/B978-0-12-803725-6.00018-2

Maijala, P., Kango, N., Szijarto, N., Viikari, L., 2012. Characterization of hemicellulases from thermophilic fungi. Antonie Van Leeuwenhoek 101, 905–917. https://doi.org/10.1007/s10482-012-9706-2

Martín-Closas, L., Costa, J., Pelacho, A.M., 2017. Agronomic effects of biodegradable films on crop and field environment, in: Malinconico, M. (Ed.), Soil Degradable Bioplastics for a Sustainable Modern Agriculture. Springer Berlin Heidelberg, pp. 67–104. https://doi.org/10.1007/978-3-662-54130-2_4

Martin-Sanchez, P.M., Sanchez-Cortes, S., Lopez-Tobar, E., Jurado, V., Bastian, F., Alabouvette, C., Saiz-Jimenez, C., 2012. The nature of black stains in Lascaux Cave, France, as revealed by surface-enhanced Raman spectroscopy. J. Raman Spectrosc. 43, 464–467. https://doi.org/10.1002/jrs.3053

Martínez, Á.T., Speranza, M., Ruiz-Dueñas, F.J., Ferreira, P., Camarero, S., Guillén, F., Martínez, M.J., Gutiérrez, A., Del Río, J.C., 2005. Biodegradation of lignocellulosics: Microbial, chemical, and enzymatic aspects of the fungal attack of lignin. Int. Microbiol. 8, 195–204. https://doi.org/10.2436/im.v8i3.9526

Martinez, D., Challacombe, J., Morgenstern, I., Hibbett, D., Schmoll, M., Kubicek, C.P., Ferreira, P., Ruiz-Duenas, F.J., Martinez, A.T., Kersten, P., Hammel, K.E., Vanden Wymelenberg, A., Gaskell, J., Lindquist, E., Sabat, G., BonDurant, S.S., Larrondo, L.F., Canessa, P., Vicuna, R., Yadav, J., Doddapaneni, H., Subramanian, V., Pisabarro, A.G., Lavín, J.L., Oguiza, J.A., Master, E., Henrissat, B., Coutinho, P.M., Harris, P., Magnuson, J.K., Baker, S.E., Bruno, K., Kenealy, W., Hoegger, P.J., Kües, U., Ramaiya, P., Lucas, S., Salamov, A., Shapiro, H., Tu, H., Chee, C.L., Misra, M., Xie, G., Teter, S., Yaver, D., James, T., Mokrejs, M., Pospisek, M., Grigoriev, I. V.,

Brettin, T., Rokhsar, D., Berka, R., Cullen, D., 2009. Genome, transcriptome, and secretome analysis of wood decay fungus *Postia placenta* supports unique mechanisms of lignocellulose conversion. Proc. Natl. Acad. Sci. U. S. A. 106, 1954–1959. https://doi.org/10.1073/pnas.0809575106

Masaphy, S., 2010. Biotechnology of morel mushrooms: Successful fruiting body formation and development in a soilless system. Biotechnol. Lett. 32, 1523–1527. https://doi.org/10.1007/s10529-010-0328-3

Meenu, M., Xu, B., 2019. Application of vibrational spectroscopy for classification, authentication and quality analysis of mushroom: A concise review. Food Chem. 289, 545–557. https://doi.org/10.1016/j.foodchem.2019.03.091

Mehta, V., Gupta, J.K., Kaushal, S.C., 1990. Cultivation of *Pleurotus florida* mushroom on rice straw and biogas production from the spent straw. World J. Microbiol. Biotechnol. 6, 366–370. https://doi.org/10.1007/BF01202116

Melanouri, E.M., Dedousi, M., Diamantopoulou, P., 2022. Cultivating *Pleurotus ostreatus* and *Pleurotus eryngii* mushroom strains on agro-industrial residues in solid-state fermentation. Part II: Effect on productivity and quality of carposomes. Carbon Resour. Convers. 5, 52–60. https://doi.org/10.1016/j.crcon.2021.12.005

Menardo, S., Gioelli, F., Balsari, P., 2011. The methane yield of digestate: Effect of organic loading rate, hydraulic retention time, and plant feeding. Bioresour. Technol. 102, 2348–2351. https://doi.org/10.1016/j.biortech.2010.10.094

Midilli, A., Dogru, M., R. Howarth, C., Ayhan, T., 2001. Hydrogen production from hazelnut shell by applying air-blown downdraft gasification technique. Int. J. Hydrogen Energy 26, 29–37. https://doi.org/10.1016/S0360-

3199(00)00049-5

Midilli, A., Rzayev, P., Olgun, H., Ayhan, T., 2000. Solar hydrogen production from hazelnut shells. Int. J. Hydrogen Energy 25, 723–732. https://doi.org/10.1016/S0360-3199(99)00097-X

Mirończuk-Chodakowska, I., Witkowska, A.M., 2020. Evaluation of polish wild mushrooms as beta-glucan sources. Int. J. Environ. Res. Public Health 17, 1–17. https://doi.org/10.3390/ijerph17197299

Mohaček-Grošev, V., Božac, R., Puppels, G.J., 2001. Vibrational spectroscopic characterization of wild growing mushrooms and toadstools. Spectrochim. Acta - Part A Mol. Biomol. Spectrosc. 57, 2815–2829. https://doi.org/10.1016/S1386-1425(01)00584-4

Mohd Hanafi, F.H., Rezania, S., Mat Taib, S., Md Din, M.F., Yamauchi, M., Sakamoto, M., Hara, H., Park, J., Ebrahimi, S.S., 2018. Environmentally sustainable applications of agro-based spent mushroom substrate (SMS): an overview. J. Mater. Cycles Waste Manag. 20, 1383–1396. https://doi.org/10.1007/s10163-018-0739-0

Mohebby, B., 2005. Attenuated total reflection infrared spectroscopy of white-rot decayed beech wood. Int. Biodeterior. Biodegrad. 55, 247–251. https://doi.org/10.1016/j.ibiod.2005.01.003

Möller, K., Müller, T., 2012. Effects of anaerobic digestion on digestate nutrient availability and crop growth: A review. Eng. Life Sci. 12, 242–257. https://doi.org/10.1002/elsc.201100085

Monlau, F., Sambusiti, C., Ficara, E., Aboulkas, A., Barakat, A., Carrère, H., 2015. New opportunities for agricultural digestate valorization: Current situation and perspectives. Energy Environ. Sci. 8, 2600–2621. https://doi.org/10.1039/c5ee01633a

Moreira, L.R.S., Filho, E.X.F., 2008. An overview of mannan structure and

mannan-degrading enzyme systems. Appl. Microbiol. Biotechnol. 79, 165–178. https://doi.org/10.1007/s00253-008-1423-4

Moskovits, M., 1985. Surface-enhanced spectroscopy. Rev. Mod. Phys. 57, 783–826.

Moskovits, M., Suh, J.S., 1984. Surface selection rules for surface-enhanced Raman spectroscopy: calculations and application to the surface-enhanced Raman spectrum of phthalazine on silver. J. Phys. Chem. 88, 5526–5530. https://doi.org/10.1021/j150667a013

Motteu, N., Goemaere, B., Bladt, S., Packeu, A., 2022. Implementation of MALDI-TOF Mass Spectrometry to Identify Fungi From the Indoor Environment as an Added Value to the Classical Morphology-Based Identification Tool. Front. Allergy 3, 1–8. https://doi.org/10.3389/falgy.2022.826148

Mucha, A.P., Dragisa, S., Dror, I., Garuti, M., van Hullebusch, E.D., Repinc, S.K., Muňoz, J., Rodriguez-Perez, S., Stres, B., Ustak, S., 2019. Re-use of digestate and recovery techniques, in: Fermoso, F.G., Van Hullebusch, E., Collins, G., Roussel, J., Mucha, A.P., Esposito, G. (Eds.), Trace Elements in Anaerobic Biotechnologies. IWA Publishing, pp. 181–213. https://doi.org/10.2166/9781789060225

Muhonja, C.N., Makonde, H., Magoma, G., Imbuga, M., 2018. Biodegradability of polyethylene by bacteria and fungi from Dandora dumpsite Nairobi-Kenya. PLoS One 13, 1–17. https://doi.org/10.1371/journal.pone.0198446

Munir, E., Harefa, R.S.M., Priyani, N., Suryanto, D., 2018. Plastic degrading fungi *Trichoderma viride* and *Aspergillus nomius* isolated from local landfill soil in Medan. IOP Conf. Ser. Earth Environ. Sci. 126. https://doi.org/10.1088/1755-1315/126/1/012145

Mustafa, A.M., Poulsen, T.G., Sheng, K., 2016. Fungal pretreatment of rice straw

with *Pleurotus ostreatus* and *Trichoderma reesei* to enhance methane production under solid-state anaerobic digestion. Appl. Energy 180, 661–671. https://doi.org/10.1016/j.apenergy.2016.07.135

Nandni, S., Mishra, S., 2018. Crop room studies in relation to yield potential of *Lentinula edodes* strains on wheat straw . J. Hill Agric. 9, 124. https://doi.org/10.5958/2230-7338.2018.00023.x

Neng, J., Zhang, Q., Sun, P., 2020. Application of surface-enhanced Raman spectroscopy in fast detection of toxic and harmful substances in food. Biosens. Bioelectron. 167, 112480. https://doi.org/10.1016/j.bios.2020.112480

Newman, T.E., Derbyshire, M.C., 2020. The evolutionary and molecular features of broad host-range necrotrophy in plant pathogenic fungi. Front. Plant Sci. 11. https://doi.org/10.3389/fpls.2020.591733

O'Gorman, A., Downey, G., Gowen, A.A., Barry-Ryan, C., Frias, J.M., 2010. Use of fourier transform infrared spectroscopy and chemometric data analysis to evaluate damage and age in mushrooms (*Agaricus bisporus*) grown in Ireland. J. Agric. Food Chem. 58, 7770–7776. https://doi.org/10.1021/jf101123a

Oei, P., 2016. Mushroom cultivation IV: Appropriate technology for mushroom growers. ECO Consult Foundation, Amsterdam, the Netherlands.

Oei, P., 2003. Mushroom cultivation: appropriate technology for mushroom growers, 3rd ed, Mushroom cultivation: appropriate technology for mushroom growers. Backhuys Publishers, Leiden, Netherlands.

Ojha, N., Pradhan, N., Singh, S., Barla, A., Shrivastava, A., Khatua, P., Rai, V., Bose, S., 2017. Evaluation of HDPE and LDPE degradation by fungus, implemented by statistical optimization. Sci. Rep. 7, 1–13. https://doi.org/10.1038/srep39515

Olaniyi, O.O., Bankefa, E.O., Folasade, I.O., Familoni, T.V., 2015. Nutrient

enrichment of mannanase-treated cassava peels and corn cob. Res. J. Microbiol. 10, 533–541. https://doi.org/10.3923/jm.2015.533.541

Otto, C., van den Tweel, T.J.J., de Mul, F.F.M., Greve, J., 1986. Surface-enhanced Raman spectroscopy of DNA bases. J. Raman Spectrosc. 17, 289–298. https://doi.org/10.1002/JRS.1250170311

Özçelik, E., Pekşen, A., 2007. Hazelnut husk as a substrate for the cultivation of shiitake mushroom (*Lentinula edodes*). Bioresour. Technol. 98, 2652–2658. https://doi.org/10.1016/j.biortech.2006.09.020

Panáček, A., Kolář, M., Večeřová, R., Prucek, R., Soukupová, J., Kryštof, V., Hamal, P., Zbořil, R., Kvítek, L., 2009. Antifungal activity of silver nanoparticles against *Candida* spp. Biomaterials 30, 6333–6340. https://doi.org/10.1016/J.BIOMATERIALS.2009.07.065

Pandey, K.K., Pitman, A.J., 2003. FTIR studies of the changes in wood chemistry following decay by brown-rot and white-rot fungi. Int. Biodeterior. Biodegrad. 52, 151–160. https://doi.org/10.1016/S0964-8305(03)00052-0

Paolini, V., Petracchini, F., Segreto, M., Tomassetti, L., Naja, N., Cecinato, A., 2018. Environmental impact of biogas: A short review of current knowledge. J. Environ. Sci. Heal. - Part A Toxic/Hazardous Subst. Environ. Eng. 53, 899–906. https://doi.org/10.1080/10934529.2018.1459076

Pehlivan, E., Altun, T., Cetin, S., Iqbal Bhanger, M., 2009. Lead sorption by waste biomass of hazelnut and almond shell. J. Hazard. Mater. 167, 1203–1208. https://doi.org/10.1016/j.jhazmat.2009.01.126

Pekşen, A., Küçükomuzlu, B., 2004. Yield potential and quality of some *Pleurotus* species grown in substrates containing hazelnut husk. Pakistan J. Biol. Sci. 7, 768–771.

Peng, W., Lü, F., Hao, L., Zhang, H., Shao, L., He, P., 2020. Digestate management for high-solid anaerobic digestion of organic wastes: A

review. Bioresour. Technol. 297, 122485. https://doi.org/10.1016/j.biortech.2019.122485

Perera, T.W.N.K., Attanayake, R.N., Paranagama, P.A., 2020. Polyethylene degradation capability of *Schizophyllum commune*, in: Proceedings of the 1st International Conference on Frontiers in Chemical Technology. Institute of Chemistry Ceylon, Colombo, Sri Lanka, p. 17.

Pérez-Armada, L., Rivas, S., González, B., Moure, A., 2019. Extraction of phenolic compounds from hazelnut shells by green processes. J. Food Eng. 255, 1–8. https://doi.org/10.1016/j.jfoodeng.2019.03.008

Petersen, M., Yu, Z., Lu, X., 2021. Application of Raman spectroscopic methods in food safety: A review. Biosensors 11, 1–22. https://doi.org/10.3390/bios11060187

Pettersen, R.C., 1984. The chemical composition of wood, in: The Chemistry of Solid Wood. American Chemical Society, New York, NY, USA, pp. 57–126. https://doi.org/10.1038/116610a0

Pinho, G.P., Matoso, J.R.M., Silvério, F.O., Mota, W.C., Lopes, P.S.N., Ribeiro, L.M., 2014. A new spectrophotometric method for determining the enzymatic activity of endo-β-mannanase in seeds. J. Braz. Chem. Soc. 25, 1246–1252. https://doi.org/10.5935/0103-5053.20140102

Plácido, J., Capareda, S., 2015. Ligninolytic enzymes: A biotechnological alternative for bioethanol production. Bioresour. Bioprocess. 2, 23. https://doi.org/10.1186/s40643-015-0049-5

Pleszczyńska, M., Wiater, A., Siwulski, M., Szczodrak, J., 2013. Successful large-scale production of fruiting bodies of *Laetiporus sulphureus* (Bull.: Fr.) Murrill on an artificial substrate. World J. Microbiol. Biotechnol. 29, 753–758. https://doi.org/10.1007/s11274-012-1230-z

Popescu, C.M., Popescu, M.C., Vasile, C., 2010. Structural changes in

biodegraded lime wood. Carbohydr. Polym. 79, 362–372. https://doi.org/10.1016/j.carbpol.2009.08.015

Prusinkiewicz, M.A., Farazkhorasani, F., Dynes, J.J., Wang, J., Gough, K.M., Kaminskyj, S.G.W., 2012. Proof-of-principle for SERS imaging of *Aspergillus nidulans* hyphae using in vivo synthesis of gold nanoparticles. Analyst 137, 4934–4942. https://doi.org/10.1039/c2an35620a

Puliga, F., Leonardi, P., Minutella, F., Zambonelli, A., Francioso, O., 2022a. Valorization of Hazelnut Shells as Growing Substrate for Edible and Medicinal Mushrooms. Horticulturae 8. https://doi.org/10.3390/horticulturae8030214

Puliga, F., Zuffi, V., Zambonelli, A., Francioso, O., Sanchez-Cortes, S., 2022b. Application of surface-enhanced Raman scattering (SERS) for mushroom characterization. Chem. Biol. Technol. Agric. Under review.

Qin, X., Li, Yüze, Han, Y., Hu, Y., Li, Yajun, Wen, X., Liao, Y., Siddique, K.H.M., 2018. Ridge-furrow mulching with black plastic film improves maize yield more than white plastic film in dry areas with adequate accumulated temperature. Agric. For. Meteorol. 262, 206–214. https://doi.org/10.1016/j.agrformet.2018.07.018

Raaman, N., Rajitha, N., Jayshree, A., Jegadeesh, R., 2012. Biodegradation of plastic by *Aspergillus* spp. isolated from polythene polluted sites around Chennai. J. Acad. Ind. Res. 1, 313–316.

Ragaert, K., Delva, L., Van Geem, K., 2017. Mechanical and chemical recycling of solid plastic waste. Waste Manag. 69, 24–58. https://doi.org/10.1016/j.wasman.2017.07.044

Raghavendra, V.B., Uzma, M., Govindappa, M., Vasantha, R.A., Lokesh, S., 2016. Screening and identification of polyurethane (PU) and low density polyethylene (LDPE) degrading soil fungi isolated from municipal solid

waste. Int J Curr Res 8, 34753–34761.

Ragusa, A., Svelato, A., Santacroce, C., Catalano, P., Notarstefano, V., Carnevali, O., Papa, F., Rongioletti, M.C.A., Baiocco, F., Draghi, S., D'Amore, E., Rinaldo, D., Matta, M., Giorgini, E., 2021. Plasticenta: First evidence of microplastics in human placenta. Environ. Int. 146, 106274. https://doi.org/10.1016/j.envint.2020.106274

Rahman, M.R., Hamdan, S., Lai, J.C.H., Jawaid, M., Yusof, F.A. bin M., 2017. Physico-mechanical, thermal and morphological properties of furfuryl alcohol/2-ethylhexyl methacrylate/halloysite nanoclay wood polymer nanocomposites (WPNCs). Heliyon 3, e00342. https://doi.org/10.1016/j.heliyon.2017.e00342

Raja, H.A., Miller, A.N., Pearce, C.J., Oberlies, N.H., 2017. Fungal identification using molecular tools: A primer for the natural products research community. J. Nat. Prod. 80, 756–770. https://doi.org/10.1021/acs.jnatprod.6b01085

Rajandas, H., Parimannan, S., Sathasivam, K., Ravichandran, M., Su Yin, L., 2012. A novel FTIR-ATR spectroscopy based technique for the estimation of low-density polyethylene biodegradation. Polym. Test. 31, 1094–1099. https://doi.org/10.1016/j.polymertesting.2012.07.015

Rajarathnam, S., Wankhede, D.B., Patwardhan, M.V., 1979. Some chemical and biochemical changes in straw constituents during growth of *Pleurotus flabellatus* (Berk & Br) Sacc. Eur. J. Appl. Microbiol. Biotechnol. 8, 125–134.

Ramirez-Perez, J.C., A. Reis, T., Olivera, C.L.P., Rizzutto, M.A., 2022. Impact of silver nanoparticles size on SERS for detection and identification of filamentous fungi. Spectrochim. Acta - Part A Mol. Biomol. Spectrosc. 272, 120980. https://doi.org/10.1016/j.saa.2022.120980

Rasul, G., 2016. Managing the food, water, and energy nexus for achieving the

sustainable development goals in South Asia. Environ. Dev. 18, 14–25. https://doi.org/10.1016/j.envdev.2015.12.001

Ravindran, R., Hassan, S.S., Williams, G.A., Jaiswal, A.K., 2018. A review on bioconversion of agro-industrial wastes to industrially important enzymes. Bioengineering 5, 1–20. https://doi.org/10.3390/bioengineering5040093

Read, D.J., Leake, J.R., Perez-Moreno, J., 2005. Erratum: Mycorrhizal fungi as drivers of ecosystem processes in heathland and boreal forest biomes. Can. J. Bot. 83, 1073. https://doi.org/10.1139/b05-912

Read, D.J., Leake, J.R., Perez-Moreno, J., 2004. Mycorrhizal fungi as drivers of ecosystem processes in heathland and boreal forest biomes. Can. J. Bot. 82, 1243–1263. https://doi.org/10.1139/B04-123

Read, D.J., Perez-Moreno, J., 2003. Mycorrhizas and nutrient cycling in ecosystems - A journey towards relevance? New Phytol. 157, 475–492. https://doi.org/10.1046/j.1469-8137.2003.00704.x

Reinhard, S., Verhagen, J., Wolters, W., Ruben, R., 2017. Water-food-energy nexus; A quick scan, Wageningen Economic Research. Wageningen.

Restrepo-Flórez, J.M., Bassi, A., Thompson, M.R., 2014. Microbial degradation and deterioration of polyethylene - A review. Int. Biodeterior. Biodegrad. 88, 83–90. https://doi.org/10.1016/j.ibiod.2013.12.014

Rhodes, C.J., 2018. Plastic pollution and potential solutions. Sci. Prog. 101, 207–260. https://doi.org/10.3184/003685018X15294876706211

Rhodes, C.J., 2014. Mycoremediation (bioremediation with fungi) - growing mushrooms to clean the earth. Chem. Speciat. Bioavailab. 26, 196–198. https://doi.org/10.3184/095422914X14047407349335

Rico-García, D., Ruiz-Rubio, L., Pérez-Alvarez, L., Hernández-Olmos, S.L., Guerrero-Ramírez, G.L., Vilas-Vilela, J.L., 2020. Lignin-based hydrogels: Synthesis and applications. Polymers (Basel). 12, 1–23.

https://doi.org/10.3390/polym12010081

Rineau, F., Shah, F., Smits, M.M., Persson, P., Johansson, T., Carleer, R., Troein, C., Tunlid, A., 2013. Carbon availability triggers the decomposition of plant litter and assimilation of nitrogen by an ectomycorrhizal fungus. ISME J. 7, 2010–2022. https://doi.org/10.1038/ismej.2013.91

Rinker, D.L., 2002. Handling and using "spent" mushroom substrate around the world, in: Sánchez, J.E., Huerta, G., Montiel, E. (Eds.), Mushroom Biology and Mushroom Products: Proceedings of the Fourth International Conference on Mushroom Biology and Mushroom Products. Universidad Autonoma del Estado de Morelos, Cuernavaca, Morelos, Mexico, pp. 43–60.

Ritota, M., Manzi, P., 2019. *Pleurotus* spp. cultivation on different agri-food by-products: Example of biotechnological application. Sustainability 11. https://doi.org/10.3390/su11185049

Ritz, K., Crawford, J.W., 1999. Colony development in nutritionally heterogeneous environments, in: Gow, N.A.R., Robson, G.D., Gadd, G.M. (Eds.), The Fungal Colony. Cambridge University Press, Cambridge, UK, pp. 49–74.

Rivas, L., Murza, A., Sánchez-Cortés, S., García-Ramos, J. V., 2000. Interaction of Antimalarial Drug Quinacrine with Nucleic Acids of Variable Sequence Studied by Spectroscopic Methods. J. Biomol. Struct. Dyn. 18, 371–383. https://doi.org/10.1080/07391102.2000.10506674

Rivas, S., Moure, A., Parajó, J.C., 2020. Pretreatment of hazelnut shells as a key strategy for the solubilization and valorization of hemicelluloses into bioactive compounds. Agronomy 10. https://doi.org/10.3390/agronomy10060760

Ronkvist, Å.M., Xie, W., Lu, W., Gross, R.A., 2009. Cutinase-Catalyzed

hydrolysis of poly(ethylene terephthalate). Macromolecules 42, 5128–5138. https://doi.org/10.1021/ma9005318

Roy, P.K., Hakkarainen, M., Varma, I.K., Albertsson, A.C., 2011. Degradable polyethylene: Fantasy or reality. Environ. Sci. Technol. 45, 4217–4227. https://doi.org/10.1021/es104042f

Royse, D.J., Baars, J., Tan, Q., 2017. Current overview of mushroom production in the world, in: Zied, D.C., Pardo-Giménez, A. (Eds.), Edible and Medicinal Mushrooms: Technology and Applications. John Wiley & Sons Ltd., Chichester, UK, pp. 5–13. https://doi.org/10.1002/9781119149446.ch2

Royse, D.J., Rhodes, T.W., Ohga, S., Sanchez, J.E., 2004. Yield, mushroom size and time to production of *Pleurotus cornucopiae* (oyster mushroom) grown on switch grass substrate spawned and supplemented at various rates. Bioresour. Technol. 91, 85–91. https://doi.org/10.1016/S0960-8524(03)00151-2

Sadh, P.K., Duhan, S., Duhan, J.S., 2018. Agro-industrial wastes and their utilization using solid state fermentation: a review. Bioresour. Bioprocess. 5, 1–15. https://doi.org/10.1186/s40643-017-0187-z

Saeed, M., Ayaşan, T., Alagawany, M., El-Hack, M.E.A., Abdel-Latif, M.A., Patra, A.K., 2019. The role of β-Mannanase (Hemicell) in improving poultry productivity, health and environment. Rev. Bras. Cienc. Avic. 21. https://doi.org/10.1590/1806-9061-2019-1001

Saini, J.K., Saini, R., Tewari, L., 2015. Lignocellulosic agriculture wastes as biomass feedstocks for second-generation bioethanol production: concepts and recent developments. 3 Biotech 5, 337–353. https://doi.org/10.1007/s13205-014-0246-5

Sajith, S., Priji, P., Sreedevi, S., Benjamin, S., 2016. An overview on fungal cellulases with an industrial perspective. J. Nutr. Food Sci. 6, 1–13. https://doi.org/10.4172/2155-9600.1000461

Sakhalkar, S., Mishra, R.L., 2013. Screening and identification of soil fungi with potential of plastic degrading ability. Indian J. Appl. Res. 3, 3.

Salam, P.A., Pandey, V.P., Shrestha, S., Anal, A.K., 2017. The need for the nexus approach, in: Salam, P. Abdul, Shrestha, Sangam, Pandey, Vishnu Prasad, Anal, Anil Kumar (Eds.), Water-energy-food Nexus. Principles and Practices. Wiley, Hoboken, New Jersey, pp. 3–10.

Sánchez, C., 2020. Fungal potential for the degradation of petroleum-based polymers: An overview of macro- and microplastics biodegradation. Biotechnol. Adv. 40, 107501. https://doi.org/10.1016/j.biotechadv.2019.107501

Sánchez, C., 2009. Lignocellulosic residues: Biodegradation and bioconversion by fungi. Biotechnol. Adv. 27, 185–194. https://doi.org/10.1016/j.biotechadv.2008.11.001

Sangale, M.K., Shahnawaz, M., Ade, A.B., 2019. Potential of fungi isolated from the dumping sites mangrove rhizosphere soil to degrade polythene. Sci. Rep. 9, 1–11. https://doi.org/10.1038/s41598-019-41448-y

Santacruz-Juárez, E., Buendia-Corona, R.E., Ramírez, R.E., Sánchez, C., 2021. Fungal enzymes for the degradation of polyethylene: Molecular docking simulation and biodegradation pathway proposal. J. Hazard. Mater. 411. https://doi.org/10.1016/j.jhazmat.2021.125118

Santi, G., Muzzini, V.G., Galli, E., Proietti, S., Moscatello, S., Battistelli, A., 2015a. Mycelial growth and enzymatic activities of white-rot fungi on anaerobic digestates from industrial biogas plants. Environ. Eng. Manag. J. 14, 1713–1719. https://doi.org/10.30638/eemj.2015.182

Santi, G., Proietti, S., Moscatello, S., Stefanoni, W., Battistelli, A., 2015b. Anaerobic digestion of corn silage on a commercial scale: Differential utilization of its chemical constituents and characterization of the solid

digestate. Biomass and Bioenergy 83, 17–22. https://doi.org/10.1016/j.biombioe.2015.08.018

Şencan, A., Karaboyacı, M., Kılıç, M., 2015. Determination of lead(II) sorption capacity of hazelnut shell and activated carbon obtained from hazelnut shell activated with ZnCl2. Environ. Sci. Pollut. Res. 22, 3238–3248. https://doi.org/10.1007/s11356-014-2974-9

Şenol, H., 2019. Biogas potential of hazelnut shells and hazelnut wastes in Giresun City. Biotechnol. Reports 24, e00361. https://doi.org/10.1016/j.btre.2019.e00361

Sepperumal, U., Markandan, M., Palraja, I., 2013. Micromorphological and chemical changes during biodegradation of polyethylene terephthalate (PET) by micromorphological and chemical changes during biodegradation of polyethylene terephthalate (PET) by *Penicillium* sp. J. Microbiol. Biotechnol. Res. Sch. Res. Libr. J. Microbiol. Biotech. Res 3, 47–53.

Sert, S., Çelik, A., Tirtom, V.N., 2017. Removal of arsenic(III) ions from aqueous solutions by modified hazelnut shell. Desalin. Water Treat. 75, 115–123. https://doi.org/10.5004/dwt.2017.20725

Shah, A.A., Hasan, F., Hameed, A., Ahmed, S., 2008. Biological degradation of plastics: A comprehensive review. Biotechnol. Adv. 26, 246–265. https://doi.org/10.1016/j.biotechadv.2007.12.005

Silvestri, C., Bacchetta, L., Bellincontro, A., Cristofori, V., 2021. Advances in cultivar choice, hazelnut orchard management, and nut storage to enhance product quality and safety: an overview. J. Sci. Food Agric. 101, 27–43. https://doi.org/10.1002/jsfa.10557

Sinclair, C.G., Cantero, D., 1989. Fermentation modelling, in: McNeil, B.L., Harvey, M. (Eds.), Fermentation a Practical Approach. IRL Press, New York, pp. 65–112.

Sindujaa, P., Padmapriya, M., Pramila, R., Ramesh, K. V., 2011. Bio-degradation of low density polyethylene (LDPE) by fungi isolated from marine water. Res. J. Biol. Sci. 6, 141–145.

Singh, J., Gupta, K.C., 2014. Screening and identification of low density polyethylene (LDPE) degrading soil fungi isolated from polythene polluted sites around Gwalior city (MP). Int. J. Curr. Microbiol. Appl. Sci. 3, 443–448.

Singh, S., Harms, H., Schlosser, D., 2014. Screening of ecologically diverse fungi for their potential to pretreat lignocellulosic bioenergy feedstock. Appl. Microbiol. Biotechnol. 98, 3355–3370. https://doi.org/10.1007/s00253-014-5563-4

Sista Kameshwar, A.K., Qin, W., 2018. Comparative study of genome-wide plant biomass-degrading CAZymes in white rot, brown rot and soft rot fungi. Mycology 9, 93–105. https://doi.org/10.1080/21501203.2017.1419296

Smajgl, A., Ward, J., Pluschke, L., 2016. The water–food–energy nexus – Realising a new paradigm. J. Hydrol. 533, 533–540. https://doi.org/10.1016/j.jhydrol.2015.12.033

Smith, D.E., Dent, G., 2019. Modern Raman spectroscopy: A practical approach. John Wiley & Sons.

Spina, F., Tummino, M.L., Poli, A., Prigione, V., Ilieva, V., Cocconcelli, P., Puglisi, E., Bracco, P., Zanetti, M., Varese, G.C., 2021. Low density polyethylene degradation by filamentous fungi. Environ. Pollut. 274, 116548. https://doi.org/10.1016/j.envpol.2021.116548

Stamets, P., 2000. Growing gourmet and medicinal mushrooms. Ten Speed Press, Berkeley, California.

Steinmetz, Z., Wollmann, C., Schaefer, M., Buchmann, C., David, J., Tröger, J., Muñoz, K., Frör, O., Schaumann, G.E., 2016. Plastic mulching in agriculture. Trading short-term agronomic benefits for long-term soil

degradation? Sci. Total Environ. 550, 690–705. https://doi.org/10.1016/j.scitotenv.2016.01.153

Stöckel, S., Kirchhoff, J., Neugebauer, U., Rösch, P., Popp, J., 2016. The application of Raman spectroscopy for the detection and identification of microorganisms. J. Raman Spectrosc. 47, 89–109. https://doi.org/10.1002/jrs.4844

Sugano, J., Maina, N., Wallenius, J., Hildén, K., 2021. Enhanced lignocellulolytic enzyme activities on hardwood and softwood during interspecific interactions of white-and brown-rot fungi. J. Fungi 7. https://doi.org/10.3390/jof7040265

Sumathi, T., Viswanath, B., Sri Lakshmi, A., Saigopal, D.V.R., 2016. Production of laccase by *Cochliobolus* sp. isolated from plastic dumped soils and their ability to degrade low molecular weight PVC. Biochem. Res. Int. 2016. https://doi.org/10.1155/2016/9519527

Surek, E., Buyukkileci, A.O., 2017. Production of xylooligosaccharides by autohydrolysis of hazelnut (*Corylus avellana* L.) shell. Carbohydr. Polym. 174, 565–571. https://doi.org/10.1016/j.carbpol.2017.06.109

Tachibana, K., Hashimoto, K., Yoshikawa, M., Okawa, H., 2010. Isolation and characterization of microorganisms degrading nylon 4 in the composted soil. Polym. Degrad. Stab. 95, 912–917. https://doi.org/10.1016/j.polymdegradstab.2010.03.031

Talbot, J.M., Allison, S.D., Treseder, K.K., 2008. Decomposers in disguise: Mycorrhizal fungi as regulators of soil C dynamics in ecosystems under global change. Funct. Ecol. 22, 955–963. https://doi.org/10.1111/j.1365-2435.2008.01402.x

Tamaki, Y., Mazza, G., 2011. Rapid determination of lignin content of straw using Fourier transform mid-infrared spectroscopy. J. Agric. Food Chem.

59, 504–512. https://doi.org/10.1021/jf1036678

Tan, H., Kohler, A., Miao, R., Liu, T., Zhang, Q., Zhang, B., Jiang, L., Wang, Y., Xie, L., Tang, J., Li, X., Liu, L., Grigoriev, I. V., Daum, C., LaButti, K., Lipzen, A., Kuo, A., Morin, E., Drula, E., Henrissat, B., Wang, B., Huang, Z., Gan, B., Peng, W., Martin, F.M., 2019. Multi-omic analyses of exogenous nutrient bag decomposition by the black morel *Morchella importuna* reveal sustained carbon acquisition and transferring. Environ. Microbiol. 21, 3909–3926. https://doi.org/10.1111/1462-2920.14741

Temporiti, M.E.E., Nicola, L., Nielsen, E., Tosi, S., 2022. Fungal Enzymes Involved in Plastics Biodegradation. Microorganisms 10, 1–27. https://doi.org/10.3390/microorganisms10061180

Thakur, M.P., 2020. Advances in mushroom production: key to food, nutritional and employment security: A review. Indian Phytopathol. 73, 377–395. https://doi.org/10.1007/s42360-020-00244-9

Thomma, B.P.H.J., 2003. *Alternaria* spp.: From general saprophyte to specific parasite. Mol. Plant Pathol. 4, 225–236. https://doi.org/10.1046/j.1364-3703.2003.00173.x

Thompson, R.C., Olson, Y., Mitchell, R.P., Davis, A., Rowland, S.J., John, A.W.G., McGonigle, D., Russell, A.E., 2004. Lost at Sea: Where Is All the Plastic? Science (80-.). 304, 838. https://doi.org/10.1126/science.1094559

Titapoka, S., Keawsompong, S., Haltrich, D., Nitisinprasert, S., 2008. Selection and characterization of mannanase-producing bacteria useful for the formation of prebiotic manno-oligosaccharides from copra meal. World J. Microbiol. Biotechnol. 24, 1425–1433. https://doi.org/10.1007/s11274-007-9627-9

Tribot, A., Amer, G., Abdou Alio, M., de Baynast, H., Delattre, C., Pons, A., Mathias, J.D., Callois, J.M., Vial, C., Michaud, P., Dussap, C.G., 2019.

Wood-lignin: Supply, extraction processes and use as bio-based material. Eur. Polym. J. 112, 228–240. https://doi.org/10.1016/j.eurpolymj.2019.01.007

Trinci, A.P.J., 1971. Influence of the width of the peripheral growth zone on the radial growth rate of fungal colonies on solid media. J. Gen. Microbiol. 67, 325–344. https://doi.org/10.1099/00221287-67-3-325

Tryfinopoulou, P., Chourdaki, A., Nychas, G.J.E., Panagou, E.Z., 2020. Competitive yeast action against *Aspergillus carbonarius* growth and ochratoxin A production. Int. J. Food Microbiol. 317, 108460. https://doi.org/10.1016/j.ijfoodmicro.2019.108460

Tu, C., Booker, F.L., Watson, D.M., Chen, X., Rufty, T.W., Shi, W., Hu, S., 2006. Mycorrhizal mediation of plant N acquisition and residue decomposition: Impact of mineral N inputs. Glob. Chang. Biol. 12, 793–803. https://doi.org/10.1111/j.1365-2486.2006.01149.x

Tuyen, D. V., Phuong, H.N., Cone, J.W., Baars, J.J.P., Sonnenberg, A.S.M., Hendriks, W.H., 2013. Effect of fungal treatments of fibrous agricultural by-products on chemical composition and in vitro rumen fermentation and methane production. Bioresour. Technol. 129, 256–263. https://doi.org/10.1016/j.biortech.2012.10.128

Udayasimha, L., Vijayalakshmi, Y.C., 2012. Sustainable waste management by growing mushroom (*Pleurotus florida*) on anaerobically digested waste and agro residues. Int. J. Eng. Res. Technol. 1, 1–8.

UNESCO, 2015. The United Nations world water development report 2015: Water for a sustainable world. Paris.

United Nations, 2019. World population prospects 2019: Highlights. New York, NY, USA.

United Nations, 2015. Transforming our world: the 2030 agenda for sustainable development. New York.

Uzuner, S., Sharma Shivappa, R.R., Cekmecelioglu, D., 2017. Bioconversion of alkali pretreated hazelnut shells to fermentable sugars for generation of high value products. Waste and Biomass Valorization 8, 407–416. https://doi.org/10.1007/s12649-016-9607-0

Valverde, M.E., Hernández-Pérez, T., Paredes-Lopez, O., 2015. Edible mushrooms: Improving human health and promoting quality life. Int. J. Microbiol. 2015. https://doi.org/10.1155/2015/376387

Vedder, J.C., Van den Munckhof-Vedder, M., 2020. Modern mushroom growing 2020 harvesting. P.J.C. Vedder, United States.

Venturella, G., Ferraro, V., Cirlincione, F., Gargano, M.L., 2021. Medicinal mushrooms: Bioactive compounds, use, and clinical trials. Int. J. Mol. Sci. 22, 1–31. https://doi.org/10.3390/ijms22020634

Vieira, F.R., de Andrade, M.C.N., 2016. Optimization of substrate preparation for oyster mushroom (*Pleurotus ostreatus*) cultivation by studying different raw materials and substrate preparation conditions (composting: phases I and II). World J. Microbiol. Biotechnol. 32. https://doi.org/10.1007/s11274-016-2152-y

Vinciguerra, V., Spina, S., Luna, M., Petrucci, G., Romagnoli, M., 2011. Structural analysis of lignin in chestnut wood by pyrolysis-gas chromatography/mass spectrometry. J. Anal. Appl. Pyrolysis 92, 273–279. https://doi.org/10.1016/j.jaap.2011.06.009

Vivelo, S., Bhatnagar, J.M., 2019. An evolutionary signal to fungal succession during plant litter decay. FEMS Microbiol. Ecol. 95, 1–11. https://doi.org/10.1093/femsec/fiz145

von Arx, J.A., 1970. The genera of fungi sporulating in pure culture. Verlag von J. Cramer, Lehere, Germany.

Walsh, B.P., Murray, S.N., O'Sullivan, D.T.J., 2015. The water energy nexus, an

ISO50001 water case study and the need for a water value system. Water Resour. Ind. 10, 15–28. https://doi.org/10.1016/j.wri.2015.02.001

Wang, F., Gao, J., Zhai, W., Liu, D., Zhou, Z., Wang, P., 2020. The influence of polyethylene microplastics on pesticide residue and degradation in the aquatic environment. J. Hazard. Mater. 394, 122517. https://doi.org/10.1016/j.jhazmat.2020.122517

Wang, K., Pu, H., Sun, D.W., 2018. Emerging spectroscopic and spectral imaging techniques for the rapid detection of microorganisms: An overview. Compr. Rev. Food Sci. Food Saf. 17, 256–273. https://doi.org/10.1111/1541-4337.12323

Wang, L., Li, J.Q., Zhang, J., Li, Z.M., Liu, H.G., Wang, Y.Z., 2020. Traditional uses, chemical components and pharmacological activities of the genus: Ganoderma P. Karst.: A review. RSC Adv. 10, 42084–42097. https://doi.org/10.1039/d0ra07219b

Wang, Z., Li, M., Flury, M., Schaeffer, S.M., Chang, Y., Tao, Z., Jia, Z., Li, S., Ding, F., Wang, J., 2021. Agronomic performance of polyethylene and biodegradable plastic film mulches in a maize cropping system in a humid continental climate. Sci. Total Environ. 786, 147460. https://doi.org/10.1016/j.scitotenv.2021.147460

Wasser, S., 2002. Medicinal mushrooms as a source of antitumor and immunomodulating polysaccharides. Appl. Microbiol. Biotechnol. 60, 258–274. https://doi.org/10.1007/s00253-002-1076-7

Weitz, N., Strambo, C., Kemp-Benedict, E., Nilsson, M., 2017. Closing the governance gaps in the water-energy-food nexus: Insights from integrative governance. Glob. Environ. Chang. 45, 165–173. https://doi.org/10.1016/j.gloenvcha.2017.06.006

White, T.J., Bruns, T., Lee, S., Taylor, J.L., 1990. Amplification and direct

sequencing of fungal ribosomal RNA genes for phylogenetics, in: Innis, M.A., Gelfand, D.H., Sninsky, J.J., White, T.J. (Eds.), PCR Protocols: A Guide to Methods and Applications. Academic Press, San Diego, pp. 315–322. https://doi.org/https:// doi.org/10.1016/b978-0-12-372180-8.50042-1

Windsor, F.M., Durance, I., Horton, A.A., Thompson, R.C., Tyler, C.R., Ormerod, S.J., 2019. A catchment-scale perspective of plastic pollution. Glob. Chang. Biol. 25, 1207–1221. https://doi.org/10.1111/gcb.14572

Witkowska, E., Jagielski, T., Kamińska, A., Kowalska, A., Hryncewicz-Gwóźdź, A., Waluk, J., 2016. Detection and identification of human fungal pathogens using surface-enhanced Raman spectroscopy and principal component analysis. Anal. Methods 8, 8427–8434. https://doi.org/10.1039/c6ay02957d

Woiciechowski, A.L., Vandenberghe, L.P. de S., Karp, S.G., Letti, L.A.J., Carvalho, J.C. de, Medeiros, A.B.P., Spier, M.R., Faraco, V., Soccol, V.T., Soccol, C.R., 2013. The pretreatment step in lignocellulosic biomass conversion: Current systems and new biological systems, in: Franco, V. (Ed.), Lignocellulose Conversion: Enzymatic and Microbial Tools for Bioethanol Production. Springer Verlag, Berlin, Heidelberg, pp. 1–199. https://doi.org/10.1007/978-3-642-37861-4

Wong, D.W.S., 2009. Structure and action mechanism of ligninolytic enzymes. Appl. Biochem. Biotechnol. 157, 174–209. https://doi.org/10.1007/s12010-008-8279-z

Wu, B., Hussain, M., Zhang, W., Stadler, M., Liu, X., Xiang, M., 2019. Current insights into fungal species diversity and perspective on naming the environmental DNA sequences of fungi. Mycology 10, 127–140. https://doi.org/10.1080/21501203.2019.1614106

Xia, Z.K., Ma, Q.H., Li, S.Y., Zhang, D.Q., Cong, L., Tian, Y.L., Yang, R.Y., 2016. The antifungal effect of silver nanoparticles on *Trichosporon asahii*. J.

Microbiol. Immunol. Infect. 49, 182–188. https://doi.org/10.1016/J.JMII.2014.04.013

Yeoman, C.J., Han, Y., Dodd, D., Schroeder, C.M., Mackie, R.I., Cann, I.K.O., 2010. Thermostable enzymes as biocatalysts in the biofuel industry, in: Laskin, A.I., Sariaslani, S., Gadd, G.M. (Eds.), Advances in Applied Microbiology. Elsevier, pp. 1–55. https://doi.org/10.1016/S0065-2164(10)70001-0

Yildiz, S., Yildiz, Ü.C., Gezer, E.D., Temiz, A., 2002. Some lignocellulosic wastes used as raw material in cultivation of the *Pleurotus ostreatus* culture mushroom. Process Biochem. 38, 301–306. https://doi.org/10.1016/S0032-9592(02)00040-7

Yilgor, N., Dogu, D., Moore, R., Terzi, E., Kartal, S.N., 2013. Evaluation of fungal deterioration in *Liquidambar orientalis* mill. Heartwood by FT-IR and light microscopy. BioResources 8, 2805–2826. https://doi.org/10.15376/biores.8.2.2805-2826

Yillia, P.T., 2016. Water-Energy-Food nexus: framing the opportunities, challenges and synergies for implementing the SDGs. Osterr. Wasser- und Abfallwirtschaft 68, 86–98. https://doi.org/10.1007/s00506-016-0297-4

Yin, C.F., Xu, Y., Zhou, N.Y., 2020. Biodegradation of polyethylene mulching films by a co-culture of *Acinetobacter* sp. strain NyZ450 and *Bacillus* sp. strain NyZ451 isolated from *Tenebrio molitor* larvae. Int. Biodeterior. Biodegrad. 155, 105089. https://doi.org/10.1016/j.ibiod.2020.105089

Yuan, B., Lu, M., Eskridge, K.M., Hanna, M.A., 2018a. Valorization of hazelnut shells into natural antioxidants by ultrasound-assisted extraction: Process optimization and phenolic composition identification. J. Food Process Eng. 41, 1–13. https://doi.org/10.1111/jfpe.12692

Yuan, B., Lu, M., Eskridge, K.M., Isom, L.D., Hanna, M.A., 2018b. Extraction,

identification, and quantification of antioxidant phenolics from hazelnut (*Corylus avellana* L.) shells. Food Chem. 244, 7–15. https://doi.org/10.1016/j.foodchem.2017.09.116

Yüksel, S., Schwenkbier, L., Pollok, S., Weber, K., Cialla-May, D., Popp, J., 2015. Label-free detection of *Phytophthora ramorum* using surface-enhanced Raman spectroscopy. Analyst 140, 7254–7262. https://doi.org/10.1039/c5an01156f

Yusidah, I., Istifadah, N., 2018. The abilities of spent mushroom substrate to suppress basal rot disease (*Fusarium oxysporum* f.sp *cepae*) in shallot. Int. J. Biosci. 13, 440–448.

Zahra, S., Abbas, S.S., Mahsa, M.T., Mohsen, N., 2010. Biodegradation of low-density polyethylene (LDPE) by isolated fungi in solid waste medium. Waste Manag. 30, 396–401. https://doi.org/10.1016/j.wasman.2009.09.027

Zambonelli, A., Iotti, M., Puliga, F., Hall, I.R., 2021. Enhancing white truffle (*Tuber magnatum* Picco and *T. borchii* Vittad.) cultivation through biotechnology innovation, in: Al-Khayri, J.M., Jain, S.M., Johnson, D.V. (Eds.), Advances in Plant Breeding Strategies: Vegetable Crops. Springer, Cham, pp. 505–532. https://doi.org/https://doi.org/10.1007/978-3-030-66969-0_14

Zanasi, G., Rubira, R.J.G., Francioso, O., Cañamares, M.V., Constantino, C.J.L., Sanchez-Cortes, S., 2021. Sensing atrazine herbicide degradation products through their interactions with humic substances by surface-enhanced raman scattering. Chemosensors 9. https://doi.org/10.3390/chemosensors9060148

Zaukuu, J.L.Z., Benes, E., Bázár, G., Kovács, Z., Fodor, M., 2022. Agricultural potentials of molecular spectroscopy and advances for food authentication: An overview. Processes 10, 1–42. https://doi.org/10.3390/pr10020214

Zervakis, G.I., Bekiaris, G., Tarantilis, P.A., Pappas, C.S., 2012. Rapid strain classification and taxa delimitation within the edible mushroom genus *Pleurotus* through the use of diffuse reflectance infrared Fourier transform (DRIFT) spectroscopy. Fungal Biol. 116, 715–728. https://doi.org/10.1016/j.funbio.2012.04.006

Zhang, G.S., Liu, Y.F., 2018. The distribution of microplastics in soil aggregate fractions in southwestern China. Sci. Total Environ. 642, 12–20. https://doi.org/10.1016/j.scitotenv.2018.06.004

Zhang, H., Peng, J., Zhang, Y.R., Liu, Q., Pan, L.Q., Tu, K., 2020. Discrimination of volatiles of shiitakes (*Lentinula edodes*) produced during drying process by electronic nose. Int. J. Food Eng. 16, 1–13. https://doi.org/10.1515/ijfe-2019-0233

Zhang, Y., Zhao, S., Zheng, J., He, L., 2017. Surface-enhanced Raman spectroscopy (SERS) combined techniques for high-performance detection and characterization. TrAC - Trends Anal. Chem. 90, 1–13. https://doi.org/10.1016/j.trac.2017.02.006

Zhang, Y.H.P., Himmel, M.E., Mielenz, J.R., 2006. Outlook for cellulase improvement: Screening and selection strategies. Biotechnol. Adv. 24, 452–481. https://doi.org/10.1016/j.biotechadv.2006.03.003

Zhou, J.L., Song, S., Huang, Z.X., Yang, L., Jiao, A.G., Liu, Y., Wang, S.X., 2019. Cultivation of *Pleurotus ostreatus*, a potential candidate for biogas residues degradation. BioResources 13, 5432–5449. https://doi.org/10.15376/biores.13.3.5432-5449

Zhou, L.M., Li, F.M., Jin, S.L., Song, Y., 2009. How two ridges and the furrow mulched with plastic film affect soil water, soil temperature and yield of maize on the semiarid Loess Plateau of China. F. Crop. Res. 113, 41–47. https://doi.org/10.1016/j.fcr.2009.04.005

Zhou, X., Broadbelt, L.J., Vinu, R., 2016. Mechanistic understanding of thermochemical conversion of polymers and lignocellulosic biomass, in: Advances in Chemical Engineering. Elsevier Inc., pp. 95–198. https://doi.org/10.1016/bs.ache.2016.09.002

Zivanovic, S., Busher, R.W., Kim, K.S., 2000. Textural changes in mushrooms (*Agaricus bisporus*) associated with tissue ultrastructure and composition. J. Food Sci. 65, 1404–1408. https://doi.org/10.1111/j.1365-2621.2000.tb10621.x